Thesis submitted for the degree of

“Doctor Philosophiæ”

SISSA Neuroscience Area

November 2018

INVESTIGATION OF MECHANOTRANSDUCTION BY MEANS OF OPTICAL TWEEZERS

Candidate

FABIO FALLERONI

Supervisor:

VINCENT TORRE

Co-supervisor:

DAN COJOC

SISSA, Via Bonomea 265, TRIESTE, ITALY

This page was intentionally left blank

Table of Contents

LIST OF PUBLICATIONS 5

SUMMARY 6

INTRODUCTION 8

Mechanotransduction 9

Mechanosensitive channels (MSCs) 11
Mammalian mechanosentive channels 13
Mechanical activated $Ca2^{+}$ signaling 17
MSCs and cytoskeletal remodeling coupling 18

Methods to study the mechanotransduction 19

References 23

RESULTS 34

Cell mechanotransduction with piconewton forces applied by optical tweezers 34

Neuronal Mechanotransduction: 46

from force to cytoskeleton contractility 46
Abstract 46
Introduction 46
Material and methods 48
Hippocampal cell culture 48
Ng108-15 cell culture 49
Calcium experiments 49
Cell Transfection 49
Live cell imaging experiments 49
Results 50
Growth cone and soma response to mechanical indentation 50
Mechanical indentation induces actin network remodelling 51
Ca^{2+} signaling evoked by mechanical stimulation 53
RhoA GTPase activation mechanically induced 54
Piezo1 expression in Hippocampal culture 55
Conclusion 56
References 58

Integrating Optical Tweezers with Patch-Clamp Electrophysiology 60
Abstract 60
Introduction 60
Material and methods 61
Hippocampal cell culture 61
Ng108-15 cell culture 62
Mechanical cell stimulation and current recording experimental approach 62
The combined patch-clamp -- optical tweezers setup 63
Experimental results and discussion 65
Conclusion 67
References 69

DISCUSSION 71

References 78

LIST OF PUBLICATIONS

The work described in this thesis was carried out at the International School for Advanced Studies, Trieste, between November 20014 and November 2018, under the supervision of Professor Vincent Torre and Dan Cojoc.

Peer reviewed publication:

- **Cell mechanotransduction with piconewton forces applied by optical tweezers**

FABIO FALLERONI, DAN COJOC AND VINCENT TORRE

Papers in preparations:

- **Neuronal Mechanotransduction: from force to cytoskeleton contractility**

FABIO FALLERONI, YUNZHEN LI, DAN COJOC AND VINCENT TORRE

- **Integrating optical tweezers stimulation with patch-clamp electrophysiology for mechanotransduction studies in neurons**

FABIO FALLERONI, ULISSE BOCCHERO, YUNZHEN LI, VINCENT TORRE, AND DAN COJOC

SUMMARY

In living cells and organisms there is a myriad of biomolecules that are able to activate specific cellular pathways, but in mechanotransduction the same physical stimulus - that is the force - modulates a broad range of cellular function. This is due to the fact that cells in a physiological environment are exposed to a series of mechanical stresses caused mainly by tension, compression and shear stress. Cells, independently from the phylogenetic branch, from arkea to eukarya, react to the mechanical stimulations by triggering responses ranging from cytoskeletal rearrangement to epigenetic remodeling and lineage specification.

In mammals, the mechanical forces are mainly transduced by specialized sensory neurons, providing the basis of the touch, hearing and proprioception. Recent studies suggest that also other kind of non-specialized neurons, such as the olfactory neurons, and possibly all the cells of the body are able to transduce the mechanical stress.

The main aim of this thesis is to study the neuronal mechanotransduction pathway at pN range, a physical level that cells experience *in vivo*. In order to exert controlled mechanical stimulations in the pN range, we established a new method using an optical tweezers with a polystyrene microbead in an oscillatory optical trap. In this way it is possible to touch the cell in the vertical direction and to analyze cellular responses to forces in the range of 5–20 pN.

In the **first paper** we have demonstrated that weak mechanical forces in the range of 5-20 pN, can produce membrane nano-indentation and intracellular Ca^{2+} transients in mouse neuroblastoma NG 108-15 cells dependent on the strength stimuli and frequency. One of the quickest way a cell responds to the force is the opening of transmembrane ion channels, referred as mechanosensitive channels (MSCs) that allow an ionic flux, with highly selected permeability within few microseconds. By confirming the possible existence of MCS channels in the NG108-15 we have found a relatively high background expression of the mechanosensitive channel Piezo1. Through the utilization of the specific MCSs inhibitor, GSMTX-4, we have demonstrated that Ca^{2+} response is strictly dependent on the opening of MCSs.

In the **second work**, we have investigated in a more detailed way the neuronal mechanotransduction pathway using rat hippocampal neurons. We have noticed that the forces applied at the level of hippocampal growth-cone behave as a repulsive stimulus, inducing both the retraction and turning. The same forces repeatedly applied to the soma evoke its shrinkage. In order to see how actin filaments reorganize themselves inside the neuron during mechanical indentation we transfected hippocampal neurons with LifeAct-mCherry. We found that the mechanical indentation lead to a rapid re-organization of the actin cytoskeleton. In particular, in response to mechanical stress the actin network gradually disappears in the indentation area, followed by a retraction of few microns of the actin network. We have also observed that hippocampal neurons display intracellular Ca^{2+} elevation in response to mechanical indentation. Interestingly, we found that OT indentation activates the small G protein RhoA potentially leading to a reorganization of the cytoskeleton that we previously observed. Finally, immunochemistry shows that Piezo1 channels are expressed over the entire membrane of hippocampal neurons.

In the **third work** we have demonstrated the integration of the patch-clamp electrophysiology with a pulsed optical tweezers, showing preliminarily that piconewton forces applied vertically on the cell membrane induce detectable inward ion currents.

All the results obtained in this thesis altogether, show that mechanical signaling operates for very weak forces and outline the molecular events underlying this exquisite mechanosensitivity.

Introduction

Mechanotransduction

Mechanotransduction is defined as the ability of living cells to respond to a wide range of mechanical forces and convert them into biochemical and/or intracellular signal. This ability is fundamental among all cells, from bacteria to multi-cellular animals and plants, in order to sense and respond to mechanical stimuli in their external and internal environment.

In mammals, detection of mechanical forces is mainly performed by the sensory neurons of the dorsal root ganglia (DRG), trigeminal ganglia and nodose ganglia. These neurons have free or encapsulated sensory nerve endings that detect both innocuous and noxious mechanical stimuli for sensing touch (e.g. Meissner, Pacinian, Merkel and Ruffini in the skin)[1-3] or monitor stretch from muscle (e.g. Golgi tendon organs and neuromuscular spindles), vessels and visceral organs for proprioception, baroception and interception. Here, the local mechanical deformation is directly converted into electrochemical signal causing changes or variations in membrane potentials, transmitting information from periphery to central nervous structures[4,5]. Moreover, in the auditory system, the mechanical forces generated by sound waves are transduced by the hair cells in the inner ear trough depolarization and neurotransmitter release onto the acoustic sensory afferent nerve endings[6].

Recent studies suggest that also other kinds of non-specialized neurons, such as the olfactory neurons[7] and possibly all the cells of the body are able to transduce the mechanical stimulations[8-10]. In fact, mechanical stresses experienced by cells take place all the time in a physiological environment, and this is due to tension, compression and bending phenomena. The mechanical forces are able to activate different molecular pathways and various cell responses, ranging from local and global cytoskeletal rearrangement to epigenetic remodeling[11-13].

For instance, the frictional force due to unidirectional fluid shear stress (FSS) *in vitro* promotes the endothelial cells elongation and alignment along the direction of the flow and suppresses proliferation[11,12] (Figure 1A). Other evidences in vitro show how mechanical cues can directly affect differentiation of stem cells in a variety of lineages, such as mesenchymal stem cells and neuronal stem cells (NCSs)[14-16]. In particular, NSCs isolated directly from the subventricular zone (SVZ) preferably differentiate into neurons on soft substrate (0.1-1kPa), whereas substrate of increased stiffness (>5kPa) favor the differentiation into glia lineage

(Figure 1B). Recent works showed that also mouse hippocampal neurons and mixed embryonic cortical culture exhibit variable neuronal differentiation on substrates of variable stiffness[17,18].

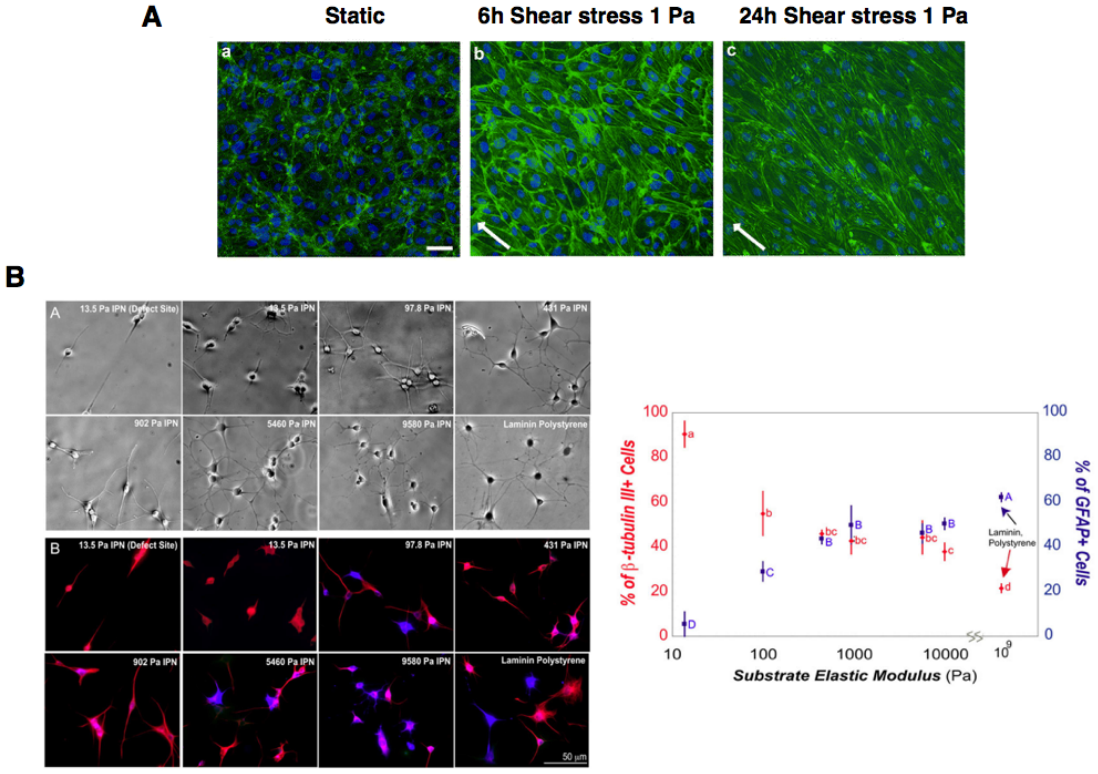

Figure 1. Example of cellular effects meditated by mechanical cues
A) Vascular endothelial cells' (HUVECs) morphological response to fluid shear stress. Epifluorescence images showing representative HUVEC monolayers stained for actin cytoskeleton (green) and nucleus (blue). The HUVECs under static conditions display morphology with no defined orientation. Although, cell elongation and alignment along the direction of flow are observed under shear stress conditions. Figure adapted from ref. [19].
B) Effect of matrix stiffness on the differentiation of NSC. Phase-contrast images (upper panel) and immunostaining (lower panel) of NSCs. Fluorescent markers: neuronal marker *β*-tubulin III (*red*) and astrocytes marker GFAP (*blue*). Right panel: percentage of cells that stained positive for *β*-tubulin III (*red*) and for GFAP (*blue*). Figure adapted from ref.[16].

In addition, the mechanical forces have been recently identified as important key players which can influence axonal growth and development[20]. For instance, the neuronal growth cones (GCs) are structures located at the tips of neurite that guide axons to their targets during development. Recently, it has been proposed that, in addition to biochemical cues, GCs are susceptible to mechanical stimuli[20-22].

Other groups have been demonstrated that substrate stiffness and tension — similar to a second messenger — can influence both for axonal development and branching[23,24]. Interestingly, it has also shown that that mechanical cues influence the shape of neuronal somata[25]. Overall, these results suggest that mechanotransduction is not only present in specialized neurons, but it may play an important role in different kind of neuronal and non-neuronal cells.

At the molecular level the list of cellular components that can be affected by mechanical forces includes different kinds of elements: mechanosensitive channels (MSCs), cell adhesion molecules such as intergrins[26] and cadherins[27], G-protein coupled receptors[28,29], signaling proteins such as focal adhesion kinase (FAK)[30], talin, vinculin and also the nucleus[31]. One of the fastest cellular response to mechanical forces is based on force-induced conformational changes in MSCs.

Mechanosensitive channels (MSCs)

The MSCs are able to rapidly convert physio-mechanical stimuli into electrochemical signals with a flux of ions across the membrane within tens of microseconds. Currently, there are two models which describe the gating of MSCs by mechanical force: the force-from-lipid concept (bilayer model) and the force-from-filament concept (tether model)[4,32] (Figure 2). In the bilayer model, the tension in the lipid bilayer alone is sufficient to gate directly the MSCs expanding the channel's central pore[33]. The changes in the trans-bilayer tension profile, can be caused either by membrane curvature or/and protein-lipid bilayer hydrophobic mismatch. This model is supported by the fact that bacterial mechanosensitive channels, such as the MscL and MscS, retain their mechanosensitivity when reconstituted in artificial membranes, excluding the need of other structures, such as force transmitters[34,35].

In contrast, in the tethered model the force is transmitted to the MSCs trough auxiliary proteins. In this case the channels can be tethered to the extracellular cellular matrix (ECM) and/or cytoskeleton and surrounding cells. This model was originally proposed for the gating of MSCs in hair cells. The mechano-receptive structure of the hair cells consists of multiple cylindrical process, called stereocilia, laterally interconnected each other with tip links, mainly composed by

cadherin-23 and protocadherin-15[36]. The deflection in the stereocilia, due to the auditory stimulus, causes tension in the tether links, which connect tips of neighboring stereocilia opening the MSCs[6]. Until now, it is not clear whether tethers directly link channel domains or whether they are associated with other proteins that modulate membrane forces around a MSCs. Since in the eukaryotic cells membranes are often interconnected by tethers with various structures, the force-from-filament model was thought as a unique mechanism for the gating of eukaryotic MSCs.

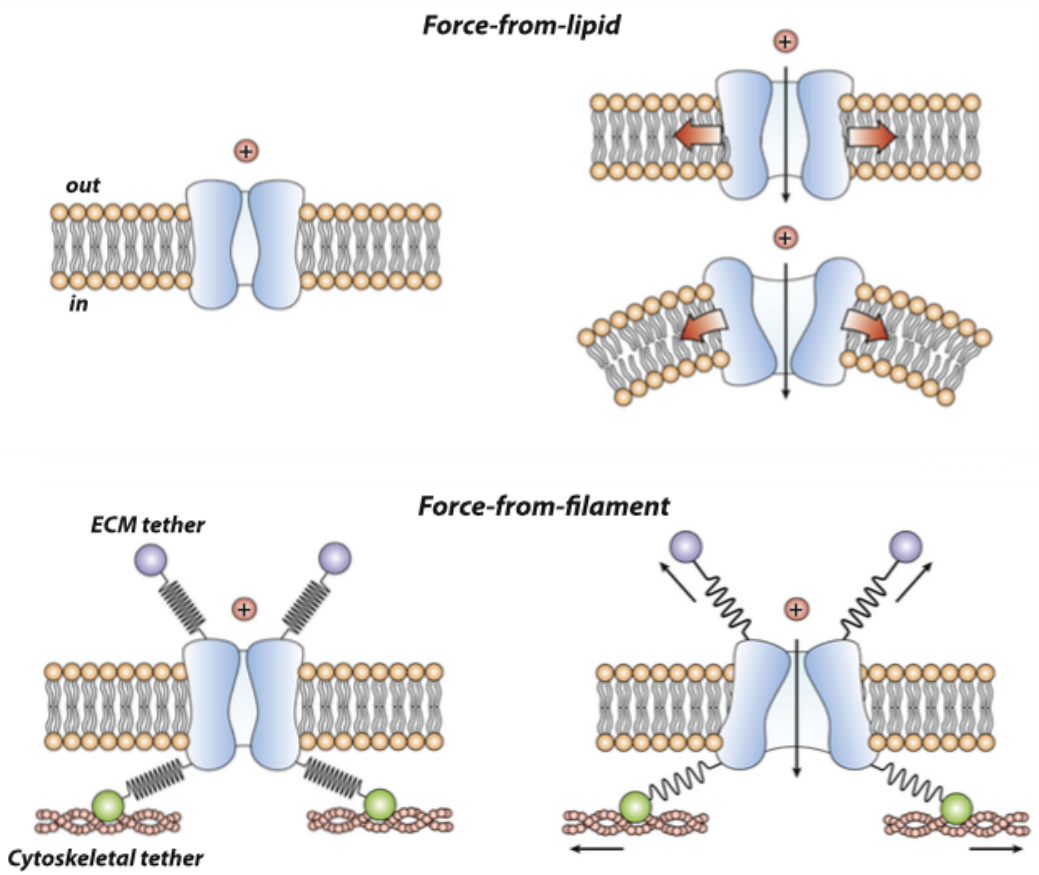

Figure 2. Schematic representation of model activation of MS channels MS channel activation by the force-from-lipids concept either by membrane tension or local membrane curvature (upper panel). MS channel activation by the force-from-filament (lower panel). Figure adapted from ref. [36].

Although, many evidences show that the force from lipids can activate not only prokaryotic MSC[37], but also eukaryotic MSCs[38,39], recently led to the proposal of a possible unifying principle of mechanotransduction based on the bilayer model [40]. The main hypothesis is that the forces from lipids can gate MSCs independently from their accessory tethered protein. One confirmation is that

removing the tether structures by engineered mutations into protocadherin-15 or cadherin-23, does alter, although does not eliminate completely the mechanosensitive currents in hair cells[39]. Interestingly, it has also been shown that removing the auxiliary structures of the MSCs through engineered mutation in the *C. Elegans* touch receptor neurons, produces either limited or no effects in the mechanically gated current. These results altogether suggest that the tether could serve as regulatory component to attenuate or amplify the mechanical force directly pulling either the channel or the lipid bilayer around the channel [41,42].

Mammalian mechanosentive channels

In the past twenty years a lot of work has been done to identify mammalian MCSs in the mechanotransduction machinery. To date, only few classes of ion channels have been implicated in mammalians mechanosensing, including: DEG/ENaC, Two-pore domain K+ channels (K2Ps), TRP channels and Piezo channels (Figure 3).

The *Acid sensing ion channels*, a proton-gated subgroup of the degenerin-epithelial NA+ channel family of cation channel (DEG/ENaC) have been identified as candidate mechanosensitive channel in mammals. The members of the DEG/ENaC share a common topology consisting of two transmembrane helices, a large extracellular domain and intracellular N- and C-terminal domains. The ASICs have a high permeability to Na^+, relative to Ca^{2+} and are voltage-independent[98]. These channels were initially implicated in mechanotransduction because of their phylogenetic homologues with the MEC-4 and MEC-10 channels in *C. Elegans* that are essential for the tactile detection[43]. It has been demonstrated that at least three members of ASIC family (AISC1, ASIC2, and ASIC3) are expressed in the free peripheral nerve ending and soma of DRG neurons, TG neurons and nodose ganglia as well in specialized mechanosensor structures (e.g. Meissner and Merkel corpuscles) suggesting a role in the peripheral mechanotransduction. However, several studies using combinations of ASIC1,2,3 knock-out showed aberrant mechanical response [44,45] suggesting that these channels are involved in the mechanosensation only as regulatory component.

The *Two-pore domain K+ channels* (K2Ps) such as TREK-1 (K2p2.1) and TRAAK (K2p4.1), have been demonstrated to be directly activated by membrane

tension and curvature in mammalian cells[46,47], supporting the existence of force-from-lipids model also in eukaryotic cells. The K2P channels show a structure with four transmembrane helices, two pore-forming regions per chain and an extracellular cap domain. TREK-1 and TRAKK channels have high level of expression in somatosensory neurons, such as DRG and TG neurons. Interestingly, the TREK-1 channel is highly expressed in the central nervous system, including hippocampus, prefrontal cortex, hypothalamus and interneurons of caudate nucleus and putamen[48]. It has been proposed that they may serve a role in controlling the excitability of sensory neurons generating hyperpolarization signals.

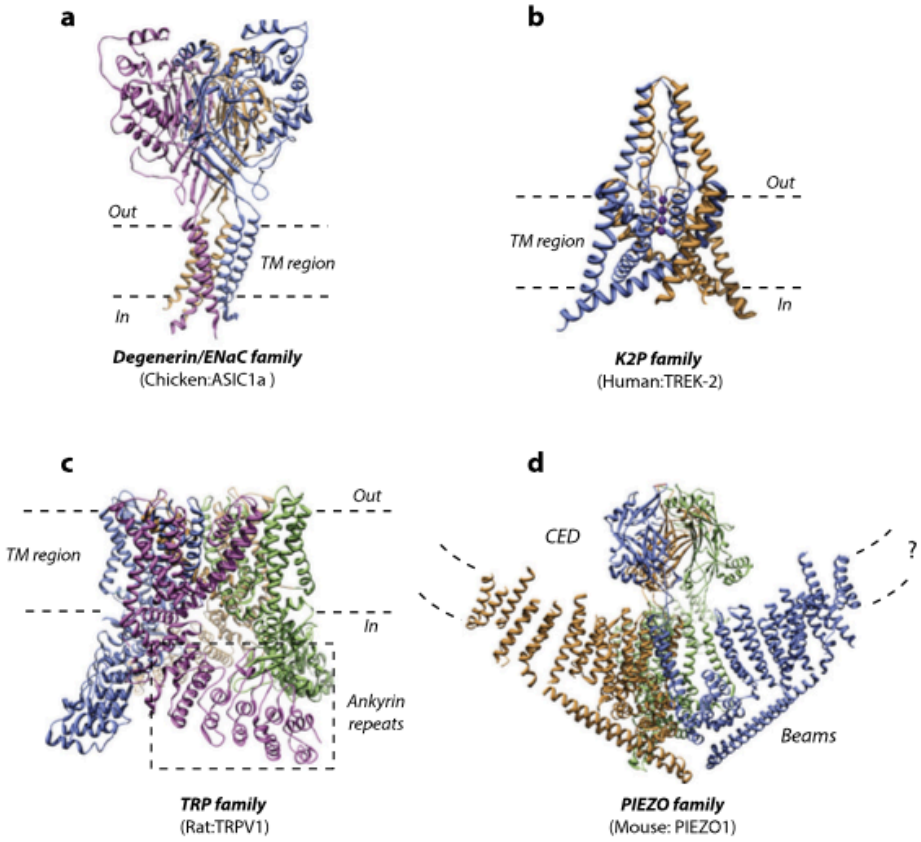

Figure 3. Structures of eukaryotic MSCs channels
A) The trimeric structure of the chicken ASIC channel. B) Human TREK-2 channel, a member of the K2P family which forms dimers. C) Structure of Rat TRPV1 showing tetrameric assembly and the classic pore helix and pore loop seen in tetrameric K_p channels. D) Mouse Piezo1 channel. Adapted from ref.[37].

While TRAKK expression is believed to be restricted to the nervous system[48] the TREK-1 channel shows relatively large expression in muscle cells, epithelial cells, kidney, lung and adrenocortical cells.

Transient receptor potential (TRP) channels have also been proposed as candidates for mechanosensitive ion channels. In mammals, the TRP superfamily is subdivided into six subfamilies based on structural homology: TRPC (canonical), TRPV (vanilloid), TRPA (ankyrin), TRPM (melastatin), TRPP (polycystin) and TRPML (mucolipin)[49]. The TRP channels are non-selective Ca^{2+} permeable cation channels, with the selectivity ratio PCa^{2+}/Na^{+} that varies between the different family members. The TRP channels are tetramers, where each monomer contains 6 transmembrane domains and a pore loop domain between TM5 and TM6.

In mammalian sensory neurons the TRP channels are best known for sensing thermal information and mediating neurogenic inflammation, and few of them have been implicated in mechanical force detection, but their role in mechanotransduction is still less clear. In mammals, the TRPV4 is expressed in sensory neurons which are responsive to systemic osmotic pressure, inner-ear hair cells, Merkel cells as well as kidney, liver and heart cells. The TRPV4 has been reported as sensitive to fluid shear stress, osmotic force induced cell swelling and stretch[50,51]. The TRPA1 channel is expressed in nociceptive neurons as well as in hair cells. It was suggested to form the main mechanotransduction channel of the inner ear assessed on expression pattern[52,53], however, no hearing deficits were observed in TRPA1 knockdown mice[54]. Within the TRPC family, TRPC 1 and TRPC6 channels are also demonstrated be involved in mechanosensory transduction[55]. These channels are widely expressed in the primary sensory neurons, smooth muscles, endothelium, salivary gland and liver. Both channels were reported to be activated directly by membrane stretch and curvature.

In addition, also the TRPM subfamily, in particular TRPM3, 4 and 7 have been reported to be involved in mechanotransduction.

Recently, it has been identified a novel class of mammalian mechanosensitive channels, called *Piezo*, by screening siRNA against candidate channels for efficacy in inhibiting endogenous mechanically-gated ionic current in the Neuro2a mouse neuroblastoma cell line[56]. Despite the relatively recent discovery the Piezo channels are extensively studied emerging as key player in the mechanotransduction pathways in a broad range of cells. Piezo channels resulted inherent mechanically-activated by various from physical stimulation

including cell indentation, membrane stretch, substrate stiffness, flow induced-shear stress and osmotic stress with high sensitivity[57,58]. For instance, the Piezo channels reconstituted into liposome were found to induce a mechanically gated ion current in pressure-clamp experiments. This demonstrates that the channel can detect changes in membrane tension and curvature in the absence of other cellular components. However other components including cytoskeleton, ECM and the interaction with other protein, such as PKD and STOML3, have been shown to modulate the activation of Piezo channels[42,59].

Activation of Piezo channels generates cationic non-selective current. In particular, the opening of piezo channels leads to Ca^{2+} entry into the cell, either triggering intracellular Ca^{2+} signaling pathways[60] or causing membrane depolarization.

Mechanosensitive Piezo ion channels are evolutionarily conserved proteins. Their existence has been reported in vertebrates, plants, nematodes, insects, and amoebae. Transmembrane prediction indicate that the channels are large integral proteins with 24-39 transmembrane domains. High resolution structures of the mouse Piezo1 protein revealed a trimeric three-bladed, propeller-shaped structure with a central pore-forming module, C-terminal extracellular domain (CED), inner helix (IH), and intracellular C-terminal domain (CTD)[61]. Mammals have two Piezo members, Piezo1 and Piezo2, that are broadly expressed in a wide range of cells[62]. Piezo2 is widely expressed in sensory dorsal root ganglia, trigeminal ganglia, nodose ganglia as well as in Merkel cells[63] and has been mainly linked in the sensation of touch, pain and proprioception. Deletion of Piezo2 in sensory DRG neurons and Merkel cells led to a dramatic reduction of mechanically activated currents[64]. In contrast, initial studies have identified Piezo1 as sensor of mechanical forces in non-specialized cells such as endothelial cells, chondrocytes, odontoblasts. Piezo1 is involved in shear stress sensing in blood vessels endothelial cell and it is implicated in the development and physiological function of circulatory system, including the proper formation of blood vessels. A confirmation of that is the embryonic lethality of Piezo1-knockout mice[65]. Recently it is emerging the role of Piezo1 at the level of central nervous system. For instance, it has been found that Piezo1 is responsible for astrogenesis from neuronal stem cells, since inhibition of channel activity by

pharmacological or siRNA- mediated knockdown suppresses neurogenesis and enhances astrogenesis[66].

Mechanically activated $Ca2^+$ signaling

Since the MSCs are mostly cation permeable, the mobilization of Ca^{2+} in particular may be responsible for activating associated with the transduction pathway. As confirmation of that, mechanical deformations due to tensile strain, fluid flow, compression and vibration induced an early increase in [Ca^{2+}] in different kind of cells[67-71]. A rapid rise in Ca^{2+} intracellular ion concentrations can depolarize the membrane, open voltage gate-dependent channels, or the ions themselves can function as secondary messengers giving to MSCs the ability to convert local mechanical events to diffuse cellular signals.

The extracellular Ca^{2+} concentration is about 1.8-2.2 mM and of this, only about 50% of it is calcium free ionized, whereas the intracellular Ca^{2+} concentration ranges from 0.5-5 mM. Although, only about 100 nM is free calcium in resting condition, the excess is stored in intracellular compartments, such as endoplasmatic reticulum, Golgi apparatus, mitochondria or bound to cytosolic proteins. Plasma membrane channels permeable to Ca^{2+} include voltage-gated, receptor-gated as well as mechanosensitive channels. The initial intracellular influx of Ca^{2+} trough transmembrane channels can induce a further release of Ca^{2+} through a process referred as Ca^{2+}-induced Ca^{2+} release (CICR). In excitable cells, such as neurons, the CICR triggers net Ca^{2+} release from the ER trough ryanodine receptors (RyRs)[72], producing a diffuse propagation of the intracellular calcium signal. Studies on epithelia cells demonstrate that fluid shear stress triggers ryanodine receptors trough Ca^{2+}-induced Ca^{2+} release mechanism[70]. Furthermore, the depletion of Ca^{2+} from the endoplasmatic reticulum can lead to inflowing calcium current with the activation of "Store-Operated Channels" (SOCs). Ca^{2+} entry through the SOCs, activated by the depletion of the intracellular calcium stores, is also known as capacitive calcium entry (CCE). In several studies, two molecules, Orai1 and STIM1[73], and the TRPC channels[74] have been identified as key players in the store-operated calcium influx mechanism.

The cytoplasmatic calcium variations are spatially and timely limited by a series of intracellular calcium-binding proteins. This protein can simply sequester Ca^{2+},

but most of them are involved in the Ca^{2+}-regulated signaling pathways. Until now, more than 300 of them have been described and most of all are characterized by a structural motive, called EF-hand including molecules such as the calmodulin, calcineurin, calbindin and calpain. The calmodulin shows a third structure with two globular domains, each of them containing two EF-hand type Ca^{2+} binding site. Upon binding four Ca^{2+} ions, calmodulin undergoes large conformational changes, which exposes hydrophobic regions and thereby enables them to interact and stimulate the activity of multiple enzymes. One principal downstream effector of calmodulin is the CAMKII. Several studies suggests CAMKII could be the key mediator between calcium influxes and cytoskeletal dynamics. For instance, CAMKII can regulate cytoskeletal reorganization and contractility by activating RhoA/ROCK signaling. Ca^{2+} can also alter actin dynamics independently from CAMKII; interestingly the RhoA has shown to be directly activated by calcium trough the calcium-sensitive tyrosine kinase pyk2[75]. CAMKII can also activates the MLCK, that in turns phosphorylates the regulatory light chains of myosin II isoform, triggering actomyosin-based contraction.

MSCs and cytoskeletal remodeling coupling

The main mammalian Rho GTPases are RhoA, Rac1 and Cdc42. The Rho GTPase have been reported to regulate many cellular processes including actin cytoskeleton remodeling, transcription, cell growth and proliferation, cell motility, morphology, as well as lineage specification[76-79]. Recent evidence suggest that a cross-talk may exist between Ca^{2+} mechanically activated signaling and Rho GTPase signaling [60,80-82]. In the mechanotransduction context, recent data suggest that RhoA is a central downstream effector since is activated by mechanical stress in various kind of cells [60,83-86]. For example, Zao *et al.* have demonstrated that the RhoA activity increases when fibroblasts are mechanically pulled by magnetic tweezers[87]. RhoA primarily acts upon the regulatory protein Rho-associated, the protein kinase ROCK. The ROCK activation promotes myosin II activity by elevating the phosphorylation of the regulatory myosin light chain MLC that promotes the assembly of myosin II into bipolar filaments and enhances the ATPase activity of myosin II, increasing the contractile force generated by myosin II on actin filaments. ROCK also phosphorylates and

activates another kinase, the LIM kinase, which in turn phosphorylates and inhibits the actin-severing protein cofilin, increasing the stability of actin filaments. Together these effects highlight RhoA GTPase as a central regulator of cytoskeleton contractility.

Interestingly, the inhibition of RhoA or its downstream effectors, such as Rho-associated kinase (ROCK) reduces the mechanically induced differentiation of human mesenchymal stem cells and it appears that stiffer tissue inhibits neurogenesis through a Ca^{2+} mediated pathway with increased activity of RhoA and contractility, as dominant-negative RhoA prevents stiffness-induced neurogenic suppression, both *in vitro* and *in vivo*[95], confirming the hypothesis of a direct coupling between MSCs and Rho GTPase pathway.

Methods to study the mechanotransduction

Several methods have been developed to apply mechanical forces to living cells. These strategies are mainly based on membrane deformation, leading potentially to the mechanotransduction pathway (for a review see ref.[94]).

One method is fluid shear stress, where a fluid flux is applied on the apical surface of the cell, through a flow chamber that typically results in parabolic laminar flow profile. Common shear stress levels range from 1 to 20 dyn/cm2 (01.-2Pa). Shear stress has been extensively used to study the mechano response in endothelial cells, since it replicates the laminar blood flow.

Other studies have employed cell stretch method. This is generally achieved by culturing the cells on elastic substrate (mainly silicone) and then applying a fixed strain to the substrate, obtaining an elongation of the substrate in both one (axial stretch) or two directions (biaxial stretch). Strain percentage range commonly from >1% to >30% of the initial substrate length.

Another method to induce mechanical stresses is the use of hypotonic or hypertonic extracellular solutions resulting in cell swelling or cell shrinkage, respectively. Both methods result in membrane stretch and this is due to altered membrane tension.

Another strategy is the utilization of chemical compounds that modify the plasmatic membrane composition. Neutral amphipathic compounds[88], such as free fatty acids, preferably insert in the outer leaflet of the membrane and induce a ball-shaped curvature (cremation); conversely positively charged amphipathic

such as the tetracaine, insert in the inner leaflet of the bilayer and cause the cell to form cup shapes.

All the above approaches, in particular shear stress or substrate stretch stress, continue to pioneer the field of mechanotransduction; although, they apply forces at multiple points on a cell, which hide the identification of the mechanoreceptors involved in the process.

In order to overcome this apparent limit, other techniques have been used to apply local mechanical stress on a given region of the cell. Focal deformation of the plasma membrane can be achieved by motor driven pressure, in which an electrically driven mechanical probe, such as pipette or microneedles, produces indentation in μm range[89]. Patch clamp technique has been used to apply positive or negative pressure[8], inducing curvature in the patch membrane. with pressure in the ranges of 0.1-1000 Pa.

Table 2. Instruments used in studies on cellular mechanics and their force ranges.

System	Force range	Newtons	Application
AFM cantilever	nN~μN	10^{-9}~10^{-6}	Cell indentation [32] Cell detachment [50] Ligand binding force measurement [131]
Electromagnetic tweezers	10 pN~nN	10^{-11}~10^{-9}	Cell deformation in local area in rigid cell [42,43] 3D orthogonal coordinative force application [44]
Optical tweezers	1~200 pN	10^{-12}~10^{-10}	Cell deformation in local area in soft cell [39] Initial binding force measurement [50] Visualizing the mechanical activation of Src [41] DNA deformation [36] Bio-material deformation [38,132]

Figure 4. Experimental tools in mechanobiology and their force ranges.
Figure adapted from Ref. [92]

Other techniques involved are capable to apply very weak forces mainly in the range from 1 pN to hundreds of nN in a more controlled way. These include AFM,

optical tweezers and magnetic tweezers (Figure 4). In the AFM a flexible cantilever is moved with a vertical (Z) actuator to indent the tip into the surface of cell membrane.

During the indentation process, the deflection of the cantilever is measured by using an optical system. The cantilever displacement can be converted into force using the Hooke law ($F = -k \cdot x$, where k is the cantilever spring constant and x is the displacement). In these experiments the lowest force that can be exerted is limited by the thermal noise of the AFM cantilever, which is in liquid around 20 pN, limiting the accuracy of the indentation measurement. In order to overcome these limitations, most of AFM experiments are routinely carried out from 0.1 to 100 nN[90,91].

Also, the magnetic tweezers[94] technique is able to produce weak forces in the range from 0.1 to 10 nN. Here, a ferromagnetic bead is used in a non-uniform magnetic field to apply linear forces to cells. The microbeads are usually coated with ECM protein to allow the attachment to cell membrane; then, a needle-like magnetic tip is positioned within few μm of the targeted microbeads, producing a pulling effect. The applied magnetic field generates a force on the bead, which is proportional to the field gradient that is strongly dependent on the nanoscale placement of the probe.

Finally, OT can be employed to characterize cell mechanics at very weak forces. Indeed, the optical tweezers can typically generate forces from 1 to 200 pN, which are dramatically smaller than the applied forces of the previous techniques. In the OT dielectric object, such as a μm-sized polystyrene or glass bead, is trapped stably focusing a laser to a diffraction-limited spot with a high numerical aperture microscope objective. Near the focus of light, the optical trap behaves as linear spring, exerting a force on trapped object linearly proportional to its displacement ($F = -k \cdot x$ where k is the OT stiffness and x is the displacement). The displacement is commonly detected using a the back focal plane interferometry in which the interference pattern between the incident light and that forward-scattered by the trapped objective is imaged onto a quadrant photodiode, enabling 3D tracking with high spatial (0.1-2 nm) and time resolution (10^{-4} s)[93].

In the mechanotransduction context the optical tweezers have been proposed to pull tether membranes[96], surface receptors or to stretch actin stress fibers[97]. In

this thesis, we have developed an oscillatory optical tweezers to apply piconewton forces perpendicularly indenting the cell membrane.

References

1) Lumpkin, Ellen A., and Michael J. Caterina. “Mechanisms of Sensory Transduction in the Skin.” *Nature*, vol. 445, no. 7130, Feb. 2007, pp. 858–65. *Crossref*, doi:10.1038/nature05662.
2) Maksimovic, Srdjan, et al. “Epidermal Merkel Cells Are Mechanosensory Cells That Tune Mammalian Touch Receptors.” *Nature*, vol. 509, no. 7502, May 2014, pp. 617–21. *Crossref*, doi:10.1038/nature13250.
3) Quindlen, Julia C., et al. “A Multiphysics Model of the Pacinian Corpuscle.” *Integrative Biology*, vol. 8, no. 11, 2016, pp. 1111–25. *Crossref*, doi:10.1039/C6IB00157B.
4) Brierley, Stuart M. “Molecular Basis of Mechanosensitivity.” *Autonomic Neuroscience*, vol. 153, no. 1–2, Feb. 2010, pp. 58–68. *Crossref*, doi:10.1016/j.autneu.2009.07.017.
5) Delmas, Patrick, and Bertrand Coste. “Mechano-Gated Ion Channels in Sensory Systems.” *Cell*, vol. 155, no. 2, Oct. 2013, pp. 278–84. *Crossref*, doi:10.1016/j.cell.2013.09.026.
6) Gillespie, Peter G., and Ulrich Müller. “Mechanotransduction by Hair Cells: Models, Molecules, and Mechanisms.” *Cell*, vol. 139, no. 1, Oct. 2009, pp. 33–44. *PubMed*, doi:10.1016/j.cell.2009.09.010.
7) Grosmaitre, Xavier, et al. “Dual Functions of Mammalian Olfactory Sensory Neurons as Odor Detectors and Mechanical Sensors.” *Nature Neuroscience*, vol. 10, no. 3, Mar. 2007, pp. 348–54. *Crossref*, doi:10.1038/nn1856.
8) Charras, Guillaume T., et al. “Estimating the Sensitivity of Mechanosensitive Ion Channels to Membrane Strain and Tension.” *Biophysical Journal*, vol. 87, no. 4, Oct. 2004, pp. 2870–84. *Crossref*, doi:10.1529/biophysj.104.040436.
9) Ekpenyong, Andrew E., et al. “Mechanotransduction in Neutrophil Activation and Deactivation.” *Biochimica et Biophysica Acta (BBA) - Molecular Cell Research*, vol. 1853, no. 11, Nov. 2015, pp. 3105–16. *Crossref*, doi:10.1016/j.bbamcr.2015.07.015.

10) Endlich, N., et al. “Podocytes Respond to Mechanical Stress in Vitro.” *Journal of the American Society of Nephrology: JASN*, vol. 12, no. 3, Mar. 2001, pp. 413–22.

11) Braddock, Martin, et al. “Fluid Shear Stress Modulation of Gene Expression in Endothelial Cells.” *News in Physiological Sciences: An International Journal of Physiology Produced Jointly by the International Union of Physiological Sciences and the American Physiological Society*, vol. 13, Oct. 1998, pp. 241–46.

12) Chiquet, Matthias, et al. “Gene Regulation by Mechanotransduction in Fibroblasts.” *Applied Physiology, Nutrition, and Metabolism*, vol. 32, no. 5, Oct. 2007, pp. 967–73. *Crossref*, doi:10.1139/H07-053.

13) Yim, Evelyn KF, and Michael P. Sheetz. “Force-Dependent Cell Signaling in Stem Cell Differentiation.” *Stem Cell Research & Therapy*, vol. 3, no. 5, 2012, p. 41. *Crossref*, doi:10.1186/scrt132.

14) Engler, Adam J., et al. “Matrix Elasticity Directs Stem Cell Lineage Specification.” *Cell*, vol. 126, no. 4, Aug. 2006, pp. 677–89. *Crossref*, doi:10.1016/j.cell.2006.06.044.

15) Leipzig, Nic D., and Molly S. Shoichet. “The Effect of Substrate Stiffness on Adult Neural Stem Cell Behavior.” *Biomaterials*, vol. 30, no. 36, Dec. 2009, pp. 6867–78. *Crossref*, doi:10.1016/j.biomaterials.2009.09.002.

16) Saha, Krishanu, et al. “Substrate Modulus Directs Neural Stem Cell Behavior.” *Biophysical Journal*, vol. 95, no. 9, Nov. 2008, pp. 4426–38. *Crossref*, doi:10.1529/biophysj.108.132217.

17) Georges, Penelope C., et al. “Matrices with Compliance Comparable to That of Brain Tissue Select Neuronal over Glial Growth in Mixed Cortical Cultures.” *Biophysical Journal*, vol. 90, no. 8, Apr. 2006, pp. 3012–18. *Crossref*, doi:10.1529/biophysj.105.073114.

18) Kostic, A., et al. “RPTP Is Required for Rigidity-Dependent Inhibition of Extension and Differentiation of Hippocampal Neurons.” *Journal of Cell Science*, vol. 120, no. 21, Oct. 2007, pp. 3895–904. *Crossref*, doi:10.1242/jcs.009852.

19) Sathanoori, Ramasri, et al. “P2Y2 Receptor Modulates Shear Stress-Induced Cell Alignment and Actin Stress Fibers in Human Umbilical Vein

Endothelial Cells." *Cellular and Molecular Life Sciences*, vol. 74, no. 4, Feb. 2017, pp. 731–46. *Crossref*, doi:10.1007/s00018-016-2365-0.

20) Albuschies, Jörg, and Viola Vogel. "The Role of Filopodia in the Recognition of Nanotopographies." *Scientific Reports*, vol. 3, no. 1, Dec. 2013. *Crossref*, doi:10.1038/srep01658.

21) Xiong, Ying, et al. "Topography and Nanomechanics of Live Neuronal Growth Cones Analyzed by Atomic Force Microscopy." *Biophysical Journal*, vol. 96, no. 12, June 2009, pp. 5060–72. *Crossref*, doi:10.1016/j.bpj.2009.03.032.

22) Franze, Kristian, et al. "Neurite Branch Retraction Is Caused by a Threshold-Dependent Mechanical Impact." *Biophysical Journal*, vol. 97, no. 7, Oct. 2009, pp. 1883–90. *Crossref*, doi:10.1016/j.bpj.2009.07.033.

23) Anava, Sarit, et al. "The Regulative Role of Neurite Mechanical Tension in Network Development." *Biophysical Journal*, vol. 96, no. 4, Feb. 2009, pp. 1661–70. *Crossref*, doi:10.1016/j.bpj.2008.10.058.

24) Heidemann, S. R., and R. E. Buxbaum. "Mechanical Tension as a Regulator of Axonal Development." *Neurotoxicology*, vol. 15, no. 1, 1994, pp. 95–107.

25) Hanein, Y., et al. "Neuronal Soma Migration Is Determined by Neurite Tension." *Neuroscience*, vol. 172, Jan. 2011, pp. 572–79. *Crossref*, doi:10.1016/j.neuroscience.2010.10.022.

26) Ross, Tyler D., et al. "Integrins in Mechanotransduction." *Current Opinion in Cell Biology*, vol. 25, no. 5, Oct. 2013, pp. 613–18. *Crossref*, doi:10.1016/j.ceb.2013.05.006.

27) Leckband, D. E., and J. de Rooij. "Cadherin Adhesion and Mechanotransduction." *Annual Review of Cell and Developmental Biology*, vol. 30, no. 1, Oct. 2014, pp. 291–315. *Crossref*, doi:10.1146/annurev-cellbio-100913-013212.

28) Chachisvilis, M., et al. "G Protein-Coupled Receptors Sense Fluid Shear Stress in Endothelial Cells." *Proceedings of the National Academy of Sciences*, vol. 103, no. 42, Oct. 2006, pp. 15463–68. *Crossref*, doi:10.1073/pnas.0607224103.

29) Makino, Ayako, et al. "G Protein-Coupled Receptors Serve as Mechanosensors for Fluid Shear Stress in Neutrophils." *American Journal*

of Physiology-Cell Physiology, vol. 290, no. 6, June 2006, pp. C1633–39. *Crossref*, doi:10.1152/ajpcell.00576.2005.

30) Zebda, Noureddine, et al. "Focal Adhesion Kinase Regulation of Mechanotransduction and Its Impact on Endothelial Cell Functions." *Microvascular Research*, vol. 83, no. 1, Jan. 2012, pp. 71–81. *Crossref*, doi:10.1016/j.mvr.2011.06.007.

31) Orr, A. Wayne, et al. "Mechanisms of Mechanotransduction." *Developmental Cell*, vol. 10, no. 1, Jan. 2006, pp. 11–20. *Crossref*, doi:10.1016/j.devcel.2005.12.006.

32) Delmas, Patrick, and Bertrand Coste. "Mechano-Gated Ion Channels in Sensory Systems." *Cell*, vol. 155, no. 2, Oct. 2013, pp. 278–84. *Crossref*, doi:10.1016/j.cell.2013.09.026.

33) Delmas, Patrick, and Bertrand Coste. "Mechano-Gated Ion Channels in Sensory Systems." *Cell*, vol. 155, no. 2, Oct. 2013, pp. 278–84. *Crossref*, doi:10.1016/j.cell.2013.09.026.

34) Häse, C. C., et al. "Purification and Functional Reconstitution of the Recombinant Large Mechanosensitive Ion Channel (MscL) of Escherichia Coli." *The Journal of Biological Chemistry*, vol. 270, no. 31, Aug. 1995, pp. 18329–34.

35) Sukharev, Sergei. "Purification of the Small Mechanosensitive Channel of Escherichia Coli (MscS): The Subunit Structure, Conduction, and Gating Characteristicsin Liposomes." *Biophysical Journal*, vol. 83, no. 1, July 2002, pp. 290–98. *Crossref*, doi:10.1016/S0006-3495(02)75169-2.

36) Martinac, B., and C. D. Cox. "Mechanosensory Transduction: Focus on Ion Channels ☆." *Reference Module in Life Sciences*, Elsevier, 2017. *Crossref*, doi:10.1016/B978-0-12-809633-8.08094-8.

37) Martinac, B., and C. D. Cox. "Mechanosensory Transduction: Focus on Ion Channels ☆." *Reference Module in Life Sciences*, Elsevier, 2017. *Crossref*, doi:10.1016/B978-0-12-809633-8.08094-8.

38) Martinac, B., and C. D. Cox. "Mechanosensory Transduction: Focus on Ion Channels ☆." *Reference Module in Life Sciences*, Elsevier, 2017. *Crossref*, doi:10.1016/B978-0-12-809633-8.08094-8.

39) Hamill, Owen P., and Boris Martinac. “Molecular Basis of Mechanotransduction in Living Cells.” *Physiological Reviews*, vol. 81, no. 2, Apr. 2001, pp. 685–740. *Crossref*, doi:10.1152/physrev.2001.81.2.685.

40) Kung, Ching. “A Possible Unifying Principle for Mechanosensation.” *Nature*, vol. 436, no. 7051, Aug. 2005, pp. 647–54. *Crossref*, doi:10.1038/nature03896.

41) Anishkin, A., and C. Kung. “Stiffened Lipid Platforms at Molecular Force Foci.” *Proceedings of the National Academy of Sciences*, vol. 110, no. 13, Mar. 2013, pp. 4886–92. *Crossref*, doi:10.1073/pnas.1302018110

42) Gaub, Benjamin M., and Daniel J. Müller. “Mechanical Stimulation of Piezo1 Receptors Depends on Extracellular Matrix Proteins and Directionality of Force.” *Nano Letters*, vol. 17, no. 3, Mar. 2017, pp. 2064–72. *Crossref*, doi:10.1021/acs.nanolett.7b00177.

43) O’Hagan, Robert, et al. “The MEC-4 DEG/ENaC Channel of Caenorhabditis Elegans Touch Receptor Neurons Transduces Mechanical Signals.” *Nature Neuroscience*, vol. 8, no. 1, Jan. 2005, pp. 43–50. *Crossref*, doi:10.1038/nn1362.

44) Mogil, J. S. “Transgenic Expression of a Dominant-Negative ASIC3 Subunit Leads to Increased Sensitivity to Mechanical and Inflammatory Stimuli.” *Journal of Neuroscience*, vol. 25, no. 43, Oct. 2005, pp. 9893–901. *Crossref*, doi:10.1523/JNEUROSCI.2019-05.2005.

45) Mogil, J. S. “Transgenic Expression of a Dominant-Negative ASIC3 Subunit Leads to Increased Sensitivity to Mechanical and Inflammatory Stimuli.” *Journal of Neuroscience*, vol. 25, no. 43, Oct. 2005, pp. 9893–901. *Crossref*, doi:10.1523/JNEUROSCI.2019-05.2005.

46) Brohawn, Stephen G., et al. “Mechanosensitivity Is Mediated Directly by the Lipid Membrane in TRAAK and TREK1 K^+ Channels.” *Proceedings of the National Academy of Sciences*, vol. 111, no. 9, Mar. 2014, pp. 3614–19. *Crossref*, doi:10.1073/pnas.1320768111.

47) Brohawn, Stephen G., et al. “Mechanosensitivity Is Mediated Directly by the Lipid Membrane in TRAAK and TREK1 K^+ Channels.” *Proceedings of the National Academy of Sciences*, vol. 111, no. 9, Mar. 2014, pp. 3614–19. *Crossref*, doi:10.1073/pnas.1320768111.

48) Honoré, Eric. “The Neuronal Background K2P Channels: Focus on TREK1.” *Nature Reviews Neuroscience*, vol. 8, no. 4, Apr. 2007, pp. 251–61. *Crossref*, doi:10.1038/nrn2117.

49) Clapham, David E., et al. “The Trp Ion Channel Family.” *Nature Reviews Neuroscience*, vol. 2, no. 6, June 2001, pp. 387–96. *Crossref*, doi:10.1038/35077544.

50) Köhler, Ralf, and Joachim Hoyer. “Role of TRPV4 in the Mechanotransduction of Shear Stress in Endothelial Cells.” *TRP Ion Channel Function in Sensory Transduction and Cellular Signaling Cascades*, edited by Wolfgang B. Liedtke and Stefan Heller, CRC Press/Taylor & Francis, 2007. *PubMed*, http://www.ncbi.nlm.nih.gov/books/NBK5250/.

51) Mizuno, Atsuko, et al. “Impaired Osmotic Sensation in Mice Lacking TRPV4.” *American Journal of Physiology-Cell Physiology*, vol. 285, no. 1, July 2003, pp. C96–101. *Crossref*, doi:10.1152/ajpcell.00559.2002.

52) TRPA1 Contributes to Specific Mechanically Activated Currents and Sensory Neuron Mechanical Hypersensitivity: TRPA1 and Mechanical Hypersensitivity.” *The Journal of Physiology*, vol. 589, no. 14, July 2011, pp. 3575–93. *Crossref*, doi:10.1113/jphysiol.2011.206789.

53) Corey, David P., et al. “TRPA1 Is a Candidate for the Mechanosensitive Transduction Channel of Vertebrate Hair Cells.” *Nature*, vol. 432, no. 7018, Dec. 2004, pp. 723–30. *Crossref*, doi:10.1038/nature03066.

54) Kwan, Kelvin Y., et al. “TRPA1 Contributes to Cold, Mechanical, and Chemical Nociception but Is Not Essential for Hair-Cell Transduction.” *Neuron*, vol. 50, no. 2, Apr. 2006, pp. 277–89. *Crossref*, doi:10.1016/j.neuron.2006.03.042.

55) Maroto, Rosario, et al. “TRPC1 Forms the Stretch-Activated Cation Channel in Vertebrate Cells.” *Nature Cell Biology*, vol. 7, no. 2, Feb. 2005, pp. 179–85. *Crossref*, doi:10.1038/ncb1218.

56) Coste, Bertrand, Bailong Xiao, et al. “Piezo Proteins Are Pore-Forming Subunits of Mechanically Activated Channels.” *Nature*, vol. 483, no. 7388, Mar. 2012, pp. 176–81. *Crossref*, doi:10.1038/nature10812.

57) Lewis, Amanda H., and Jörg Grandl. “Mechanical Sensitivity of Piezo1 Ion Channels Can Be Tuned by Cellular Membrane Tension.” *ELife*, vol. 4, Dec. 2015. *Crossref*, doi:10.7554/eLife.12088.

58) Wu, Jason, Amanda H. Lewis, et al. “Touch, Tension, and Transduction – The Function and Regulation of Piezo Ion Channels.” *Trends in Biochemical Sciences*, vol. 42, no. 1, Jan. 2017, pp. 57–71. *Crossref*, doi:10.1016/j.tibs.2016.09.004.

59) Nourse, Jamison L., and Medha M. Pathak. “How Cells Channel Their Stress: Interplay between Piezo1 and the Cytoskeleton.” *Seminars in Cell & Developmental Biology*, vol. 71, Nov. 2017, pp. 3–12. *Crossref*, doi:10.1016/j.semcdb.2017.06.018.

60) Pardo-Pastor, Carlos, et al. “Piezo2 Channel Regulates RhoA and Actin Cytoskeleton to Promote Cell Mechanobiological Responses.” *Proceedings of the National Academy of Sciences*, vol. 115, no. 8, Feb. 2018, pp. 1925–30. *Crossref*, doi:10.1073/pnas.1718177115.

61) Coste, Bertrand, Swetha E. Murthy, et al. “Piezo1 Ion Channel Pore Properties Are Dictated by C-Terminal Region.” *Nature Communications*, vol. 6, no. 1, Dec. 2015. *Crossref*, doi:10.1038/ncomms8223.

62) Coste, B., et al. “Piezo1 and Piezo2 Are Essential Components of Distinct Mechanically Activated Cation Channels.” *Science*, vol. 330, no. 6000, Oct. 2010, pp. 55–60. *Crossref*, doi:10.1126/science.1193270.

63) Ikeda, Ryo, and Jianguo G. Gu. “Piezo2 Channel Conductance and Localization Domains in Merkel Cells of Rat Whisker Hair Follicles.” *Neuroscience Letters*, vol. 583, Nov. 2014, pp. 210–15. *Crossref*, doi:10.1016/j.neulet.2014.05.055.

64) Woo, Seung-Hyun, et al. “Piezo2 Is Required for Merkel-Cell Mechanotransduction.” *Nature*, vol. 509, no. 7502, May 2014, pp. 622–26. *Crossref*, doi:10.1038/nature13251.

65) Ranade, S. S., et al. “Piezo1, a Mechanically Activated Ion Channel, Is Required for Vascular Development in Mice.” *Proceedings of the National Academy of Sciences*, vol. 111, no. 28, July 2014, pp. 10347–52. *Crossref*, doi:10.1073/pnas.1409233111.

66) Pathak, Medha M., et al. “Stretch-Activated Ion Channel Piezo1 Directs Lineage Choice in Human Neural Stem Cells.” *Proceedings of the National*

Academy of Sciences, vol. 111, no. 45, Nov. 2014, pp. 16148–53. *Crossref*, doi:10.1073/pnas.1409802111.

67) Horner, Vanessa L., and Mariana F. Wolfner. "Mechanical Stimulation by Osmotic and Hydrostatic Pressure Activates Drosophila Oocytes in Vitro in a Calcium-Dependent Manner." *Developmental Biology*, vol. 316, no. 1, Apr. 2008, pp. 100–09. *Crossref*, doi:10.1016/j.ydbio.2008.01.014.

68) Murata, Naohiko, et al. "Ca2+ Influx and ATP Release Mediated by Mechanical Stretch in Human Lung Fibroblasts." *Biochemical and Biophysical Research Communications*, vol. 453, no. 1, Oct. 2014, pp. 101–05. *Crossref*, doi:10.1016/j.bbrc.2014.09.063.

69) Han, Sang-Kuy, et al. "Mechanically Induced Calcium Signaling in Chondrocytes in Situ." *Journal of Orthopaedic Research*, vol. 30, no. 3, Mar. 2012, pp. 475–81. *Crossref*, doi:10.1002/jor.21536.

70) Liu, Bo, et al. "Two Distinct Phases of Calcium Signalling under Flow." *Cardiovascular Research*, vol. 91, no. 1, July 2011, pp. 124–33. *Crossref*, doi:10.1093/cvr/cvr033.

71) Charles, A. C., et al. "Intercellular Signaling in Glial Cells: Calcium Waves and Oscillations in Response to Mechanical Stimulation and Glutamate." *Neuron*, vol. 6, no. 6, June 1991, pp. 983–92.

72) Kuba, K. "Ca(2+)-Induced Ca2+ Release in Neurones." *The Japanese Journal of Physiology*, vol. 44, no. 6, 1994, pp. 613–50.

73) Potier, Marie, et al. "Evidence for STIM1- and Orai1-Dependent Store-Operated Calcium Influx through I_{CRAC} in Vascular Smooth Muscle Cells: Role in Proliferation and Migration." *The FASEB Journal*, vol. 23, no. 8, Aug. 2009, pp. 2425–37. *Crossref*, doi:10.1096/fj.09-131128.

74) Cheng, Kwong Tai, et al. "Contribution and Regulation of TRPC Channels in Store-Operated Ca2+ Entry." *Current Topics in Membranes*, vol. 71, Elsevier, 2013, pp. 149–79. *Crossref*, doi:10.1016/B978-0-12-407870-3.00007-X.

75) Ying, Zhekang, et al. "PYK2/PDZ-RhoGEF Links Ca^{2+} Signaling to RhoA." *Arteriosclerosis, Thrombosis, and Vascular Biology*, vol. 29, no. 10, Oct. 2009, pp. 1657–63. *Crossref*, doi:10.1161/ATVBAHA.109.190892.

76) Etienne-Manneville, Sandrine, and Alan Hall. “Rho GTPases in Cell Biology.” *Nature*, vol. 420, no. 6916, Dec. 2002, pp. 629–35. *Crossref*, doi:10.1038/nature01148.

77) Keung, Albert J., et al. “Rho GTPases Mediate the Mechanosensitive Lineage Commitment of Neural Stem Cells.” *STEM CELLS*, vol. 29, no. 11, Nov. 2011, pp. 1886–97. *Crossref*, doi:10.1002/stem.746.

78) Olson, M., et al. “An Essential Role for Rho, Rac, and Cdc42 GTPases in Cell Cycle Progression through G1.” *Science*, vol. 269, no. 5228, Sept. 1995, pp. 1270–72. *Crossref*, doi:10.1126/science.7652575.

79) Sit, S. T., and E. Manser. “Rho GTPases and Their Role in Organizing the Actin Cytoskeleton.” *Journal of Cell Science*, vol. 124, no. 5, Mar. 2011, pp. 679–83. *Crossref*, doi:10.1242/jcs.064964.

80) Martinac, B. “Mechanosensitive Ion Channels: Molecules of Mechanotransduction.” *Journal of Cell Science*, vol. 117, no. 12, May 2004, pp. 2449–60. *Crossref*, doi:10.1242/jcs.01232.

81) Ingber, Donald E. “Cellular Mechanotransduction: Putting All the Pieces Together Again.” *The FASEB Journal*, vol. 20, no. 7, May 2006, pp. 811–27. *Crossref*, doi:10.1096/fj.05-5424rev.

82) Luis Alonso, José, et al. “Cellular Mechanotransduction.” *AIMS Biophysics*, vol. 3, no. 1, 2016, pp. 50–62. *Crossref*, doi:10.3934/biophy.2016.1.50.

83) McBeath, Rowena, et al. “Cell Shape, Cytoskeletal Tension, and RhoA Regulate Stem Cell Lineage Commitment.” *Developmental Cell*, vol. 6, no. 4, Apr. 2004, pp. 483–95. *Crossref*, doi:10.1016/S1534-5807(04)00075-9.

84) Wojciak-Stothard, Beata, and Anne J. Ridley. “Shear Stress–Induced Endothelial Cell Polarization Is Mediated by Rho and Rac but Not Cdc42 or PI 3-Kinases.” *The Journal of Cell Biology*, vol. 161, no. 2, Apr. 2003, pp. 429–39. *Crossref*, doi:10.1083/jcb.200210135.

85) Xu, Baiyao, et al. “RhoA/ROCK, Cytoskeletal Dynamics, and Focal Adhesion Kinase Are Required for Mechanical Stretch-Induced Tenogenic Differentiation of Human Mesenchymal Stem Cells.” *Journal of Cellular Physiology*, vol. 227, no. 6, June 2012, pp. 2722–29. *Crossref*, doi:10.1002/jcp.23016.

86) Yuan, Ying, et al. “The Role of the RhoA/ROCK Signaling Pathway in Mechanical Strain-Induced Scleral Myofibroblast Differentiation.” *Investigative Opthalmology & Visual Science*, vol. 59, no. 8, July 2018, p. 3619. *Crossref*, doi:10.1167/iovs.17-23580.

87) Zhao, X. H., et al. “Force Activates Smooth Muscle -Actin Promoter Activity through the Rho Signaling Pathway.” *Journal of Cell Science*, vol. 120, no. 10, May 2007, pp. 1801–09. *Crossref*, doi:10.1242/jcs.001586.

88) Martinac, Boris, et al. “Mechanosensitive Ion Channels of E. Coli Activated by Amphipaths.” *Nature*, vol. 348, no. 6298, Nov. 1990, pp. 261–63. *Crossref*, doi:10.1038/348261a0.

89) Hao, Jizhe, and Patrick Delmas. “Recording of Mechanosensitive Currents Using Piezoelectrically Driven Mechanostimulator.” *Nature Protocols*, vol. 6, no. 7, July 2011, pp. 979–90. *Crossref*, doi:10.1038/nprot.2011.343.

90) Eghiaian, Frédéric, and Iwan A. T. Schaap. “Structural and Dynamic Characterization of Biochemical Processes by Atomic Force Microscopy.” *Single Molecule Enzymology*, edited by Gregory I. Mashanov and Christopher Batters, vol. 778, Humana Press, 2011, pp. 71–95. *Crossref*, doi:10.1007/978-1-61779-261-8_6.

91) Falleroni, Fabio, et al. “Cell Mechanotransduction With Piconewton Forces Applied by Optical Tweezers.” *Frontiers in Cellular Neuroscience*, vol. 12, May 2018. *Crossref*, doi:10.3389/fncel.2018.00130.

92) Fong-Chin, S., Chia_Ching W. and Shu, C.” Review: Roles of Microenviroment and mechanical forces in cell and tissue remodeling”. Journal of medical and biological engineering, 31(4): 233-244

93) Neuman, Keir C., and Steven M. Block. “Optical Trapping.” *The Review of Scientific Instruments*, vol. 75, no. 9, Sept. 2004, pp. 2787–809. *PubMed*, doi:10.1063/1.1785844.

94) Huang, Hayden, et al. “Cell Mechanics and Mechanotransduction: Pathways, Probes, and Physiology.” *American Journal of Physiology-Cell Physiology*, vol. 287, no. 1, July 2004, pp. C1–11. *Crossref*, doi:10.1152/ajpcell.00559.2003.

95) Keung, Albert J., et al. “Rho GTPases Mediate the Mechanosensitive Lineage Commitment of Neural Stem Cells.” *STEM CELLS*, vol. 29, no. 11, Nov. 2011, pp. 1886–97. *Crossref*, doi:10.1002/stem.746.

96)Brownell, William E., et al. “Cell Membrane Tethers Generate Mechanical Force in Response to Electrical Stimulation.” *Biophysical Journal*, vol. 99, no. 3, Aug. 2010, pp. 845–52. *PubMed*, doi:10.1016/j.bpj.2010.05.025.

97)K. Hayakawa, H. Tatsumi, and M. Sokabe, "Actin stress fibers transmit and focus force to activate mechanosensitive channels," J Cell Sci **121**, 496-503 (2008).

98)Sherwood, Thomas W., et al. “Structure and Activity of the Acid-Sensing Ion Channels.” *American Journal of Physiology-Cell Physiology*, vol. 303, no. 7, Oct. 2012, pp. C699–710. *Crossref*, doi:10.1152/ajpcell.00188.2012.

Results

frontiers in Cellular Neuroscience

METHODS
published: 14 May 2018
doi: 10.3389/fncel.2018.00130

Cell Mechanotransduction With Piconewton Forces Applied by Optical Tweezers

Fabio Falleroni[1], *Vincent Torre*[1,2,3]* *and Dan Cojoc*[4]*

[1] Neuroscience Area, International School for Advanced Studies, Trieste, Italy, [2] Cixi Institute of Biomedical Engineering, Ningbo Institute of Materials Technology and Engineering, Chinese Academy of Sciences, Zhejiang, China, [3] Center of Systems Medicine, Chinese Academy of Medical Sciences, Suzhou Institute of Systems Medicine, Suzhou Industrial Park, Suzhou, China, [4] Institute of Materials, National Research Council of Italy (CNR), Trieste, Italy

Mechanical stresses are always present in the cellular environment and mechanotransduction occurs in all cells. Although many experimental approaches have been developed to investigate mechanotransduction, the physical properties of the mechanical stimulus have yet to be accurately characterized. Here, we propose a mechanical stimulation method employing an oscillatory optical trap to apply piconewton forces perpendicularly to the cell membrane, for short instants. We show that this stimulation produces membrane indentation and induces cellular calcium transients in mouse neuroblastoma NG108-15 cells dependent of the stimulus strength and the number of force pulses.

Keywords: cell mechanotransduction, calcium signaling, optical tweezers, cell indentation, piconewton forces

OPEN ACCESS

Edited by:
Carsten Schulte,
Università degli Studi di Milano, Italy

Reviewed by:
Amanda H. Lewis,
Duke University, United States
Marco Capitanio,
European Laboratory for Non-linear Spectroscopy (LENS), Italy

***Correspondence:**
Vincent Torre
torre@sissa.it
Dan Cojoc
cojoc@iom.cnr.it

Received: *21 December 2017*
Accepted: *24 April 2018*
Published: *14 May 2018*

Citation:
Falleroni F, Torre V and Cojoc D (2018) Cell Mechanotransduction With Piconewton Forces Applied by Optical Tweezers. Front. Cell. Neurosci. 12:130. doi: 10.3389/fncel.2018.00130

INTRODUCTION

Several sensory neurons transduce mechanical stimulations that provide the basis of hearing, touch, and noxious mechanical sensation (Ernstrom and Chalfie, 2002; Lumpkin et al., 2010). Mechanosensitive channels (Arnadóttir and Chalfie, 2010), however, are not found exclusively in these specialized neurons, but, rather, many other cells such as olfactory sensory neurons and possibly almost all neurons respond to an applied pressure (Connelly et al., 2015). Micropipettes/microneedles are used to pull and push cells and provide a localized mechanical stimulation (Hao and Delmas, 2011). Magnetic actuation of nanoparticles in combination with pressure-clamp electrophysiology have identified mechanically sensitive domains in mechanosensitive ionic channels (Wu et al., 2016). None of these methods, however, provide a precise and simultaneous measurement of the applied force and the indentation caused by the mechanical stimulus. The precise measurement of these two quantities is key in understanding the operation of the mechanical sensors and distinguishing between the membrane-tension model (Coste et al., 2010, 2015) and tether models (Sachs, 2015; Jin et al., 2017). In membrane-tension models, the change in membrane tension drives the opening of mechanosensitive channels, such as for Piezo 1 and 2 channels (Coste et al., 2012; Lewis and Grandl, 2015). In tether models, a link to the cytoskeleton controls channel gating, such as for the transient receptor potential (TRP) mechanosensitive channel (NOMPC) (Walker et al., 2000; Sachs, 2015; Jin et al., 2017). All of these channels have been reported to respond to membrane tension in the range of 0.1–10 mN/m (Zhang et al., 2015; Wu et al., 2017), and the pressure sensitivity of Piezo 1 and 2 mechanosensitive channels has been estimated to be in the range of some tens of mmHg (10^3–10^4) Pa (Charras et al., 2004; Coste et al., 2010; Wu et al., 2017). However, the applied force and pressure have not been measured precisely but only estimated.

It is possible to produce an indentation with nN forces to a cellular membrane by using a flexible cantilever in AFM (Gaub and Müller, 2017). In this case, the lowest force that can be exerted is limited by the thermal noise of the AFM cantilever, which in liquid is around 20 pN (Eghiaian and Schaap, 2011) limiting also the accuracy of the indentation measurement. To overcome these limitations, most of AFM experiments are routinely carried out from 0.1 to 100 nN (Lee et al., 2014; Gaub and Müller, 2017) and the indentation is performed at nN forces causing large deformations and possibly damages to the cell (Murphy et al., 2006). The force generated by growing microtubules (Dogterom and Yurke, 1997) or by f-actin–binding myosin motors (Finer et al., 1994) is in the order of 3–5 pN, therefore cells are likely to experience mechanical stimulations from just some pN up to several nN.

In order to exert controlled mechanical stimulations in the pN range, we established a method using an optical tweezers with a polystyrene microbead in an oscillatory optical trap. In this way it is possible to touch the cell in the vertical direction and to analyze cellular responses to forces in the range of 5–20 pN. By using this technique, we provide a method able to: (i) produce small (hundreds of nm) indentation of the cell membrane in the vertical direction; (ii) measure with nm precision the displacement of the microbead when the optical trap is set in contact with the cell membrane and determine precisely the applied force and the indentation produced into the cell membrane. Although the force exerted by the bead to the cell membrane is small, this stimulation is enough to trigger Ca^{2+} intracellular transients.

MATERIALS AND METHODS

Cell Culture

Mouse neuroblastoma × rat glioma hybrid (NG108-15) cells were obtained from Sigma-Aldrich. The NG108-15 cells were cultured in Dulbecco's modified Eagle's medium (ThermoFisher) supplemented with 10% fetal bovine serum (FBS). The cells were cultured in a humidified incubator with 95% O_2 and 5% CO_2 at 37°C. For subculturing, the cells were washed with PBS and detached by minimal trypsinization (0.25% trypsin-EDTA solution) followed by incubation at 37°C until the cells detached. Fresh culture medium was added, and the cells were seeded in new culture flasks in a 1:4 ratio. For the experiments, cells were plated into coverslip coated with 50 μg/ml poly-L-ornithine (Sigma-Aldrich,) in 6 well plate culture containing Neurobasal medium (ThermoFisher) and with 2% B27 supplement (ThermoFisher) for 24–28 h to induce neuronal differentiation of NG108-15 cells.

Calcium Imaging

The cells were loaded with a cell-permeable calcium dye Fluo4-AM (Life Technologies) by incubating them with 4 μM Fluo4-AM dissolved in anhydrous DMSO (Sigma-Aldrich) and Pluronic F-127 20% solution in DMSO (Life Technologies) at a ratio of 1:1 in Krebs-Ringer's solution containing 119 mM NaCl, 2.5 mM KCl, 1 mM NaH_2PO_4, 2.5 mM $CaCl_2$, 1.3 mM $MgCl_2$, 11 mM D-glucose, and 20 mM HEPES (pH 7.4) at 37°C for 45 min. After incubation the cells were washed three times for at least 15 min total to allow complete intracellular de-esterification of the dye then transferred to the stage of an Olympus IX-81 inverted microscope equipped with LED illumination (X-Cite XLED1 from Excelitas Technologies). The experiments were performed at 37°C, and images were acquired using Micromanager software with an Apo-Fluor 60x/1.4 NA objective at a sampling rate of 5 Hz for 3–10 min. To avoid saturation of the signals, the excitation light intensity was attenuated by one neutral density filter (OD = 0.5, Thorlabs). Imaging experiments were conducted with Krebs-Ringer's solution containing 119 mM NaCl, 2.5 mM KCl, 1 mM NaH_2PO_4, 2.5 mM $CaCl_2$, 1.3 mM $MgCl_2$, 11 mM D-glucose, and 20 mM HEPES (pH 7.4).

Mechanical Cell Stimulation Using the Oscillatory Optical Trap

To mechanically stimulate the cell, we used a polystyrene bead with a diameter d = 3.5-μm diameter (G. Kisker GbR,) optically manipulated in an oscillatory optical trap (OOT) (**Figure 1** and Supplementary Video 1). The main component of the OOT is the Focused Tunable Lens (EL-10-30-NIR-LD, Optotune AG), of which focal length can be precisely tuned to change the vertical position of the trapped bead (**Figure 2A**). Cell stimulation is achieved by trapping the bead above the cell and then moving it against the cell membrane (**Figure 1B**).

To rule out the effect of the laser light on the cellular calcium transients we measured the fluorescence change (DF/F). DF/F taken over the cell, was measured for the cell not exposed to laser light (5 min) as reference, followed by cell exposed to laser (5 min). An example of the fluorescence change is shown in **Figure 3A**. The amplitude Ai, is defined as the difference between the maximum and minimum values of DF/F during the experiment. The experiment in **Figure 3A** displays the maximum amplitude, A = 0.0125 ($n = 5$ experiments). This value remains however well below the minimum value of the DF/F peaks, corresponding to Calcium transitions induced by force pulses (see **Figures 5**, **6**), indicating that the IR laser beam does not perturb the cell. The mean amplitude is 0.01 ($SD = 0.0018$) and this value is used to define the peak presence: $A_p > 0.02$, where A_p is the amplitude of the peak with respect to the baseline. Similar results, showing that the laser beam does not affect the cell, have been obtained also when a bead was trapped and kept above the cell.

The axial position of the trap could be regulated within a range of 0–12 μm above the focus of the microscope lens by changing the convergence of the beam entering the pupil of the lens (**Figure 2**). Beam convergence was changed using the focal length of the Focus Tunable Lens (EL-10-30-NIR-LD, Optotune AG), $f_{FTL} = 55$–90 mm in combination with a convergent lens of fixed focal length (FL), $f_{FL} = 150$ mm. The axial position of the trap from the focus of the microscope objective (trap shift) can be calculated by geometrical optics:

$$Z_{trap} = 10^3 \left[\frac{f_{MO}^2}{\frac{f_{FL}^2}{f_{FTL}+f_{FL}-d_{LT}} + d_{MO} - f_{FL} - f_{MO}} \right] \quad (1)$$

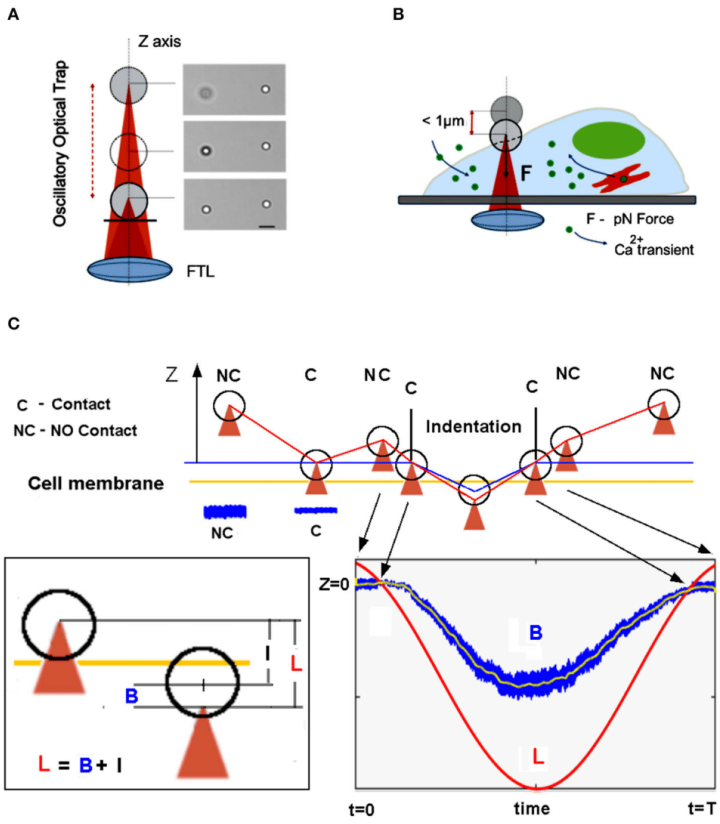

FIGURE 1 | Overview of the mechanical stimulation with piconewton forces by optical tweezers. **(A)** The Oscillatory Optical Trap (OOT), implemented with a Focused Tunable Lens (FTL), enables continuous movement of the trap along the z-axis. Right side: image of a trapped bead shifted by 4 µm up from the focal plane; the bead on the right is fixed. Scale bar 5 µm. **(B)** Scheme of the mechanical stimulation inducing calcium transient experiment. **(C)** The measurement approach: the trap is lowered until the bead touches the cell membrane, indicated by the amplitude decrease of the bead fluctuations (see blue traces NC vs. C). The trap is moved up in NC position and the oscillatory movement of the trap begins to indent the cell membrane. The bead displacement, B from the center of the trap is measured (see blue trace in the bottom right inset). The relation between trap displacement L, bead displacement B, and indentation I is shown in the left inset.

where Z_{trap} is the trap axial shift in µm; f_{MO} is the focal length of the microscope objective, $f_{MO} = 2$ [mm]; f_{FL} is the focal length of the fixed lens, $f_{FL} = 150$ [mm]; d_{MO} is the distance between the fixed lens and the microscope objective in mm, $d_{MO} = 380$ [mm]; d_{LT} is the distance between the Focused Tunable Lens (FTL) and the fixed lens (FL) in mm, $d_{LT} = 250$ [mm]; f_{FTL} is the focal length of the FTL in mm, which is a function of the intensity current, I (in mA) applied to the FTL:

$$f_{FTL} = \frac{10^3}{\Phi} = \frac{10^3}{8.3 + S \bullet I} \quad (2)$$

Φ is the power of the lens in diopters, 1 dpt = 1/m, $S = 0.0571$ dpt/mA is the FTL sensitivity (provided by the manufacturer). Introducing Equation (2) into Equation (1), one defines the axial trap shift, Z_{trap} as a function of the driving current, I. The focal length, f_{FTL} and the axial trap shift, Z_{trap} are plotted in **Figure 2B** for the driving current, I from 60 to 170 [mA]. Although f_{FTL} and Z_{trap} equations are not linear, for the limited range of I values represented in **Figure 2B**, Z_{trap} theoretical curve can be very well fitted with a line: $Z_{\text{trap}} = -0.1^*I + 17$, (Root Mean Square Error RMSE = 0.021; $R^2 = 1$). We then measured the experimental axial trap shift, ZE_{trap}, assuming the position of the trap is in the focus of the beam and using the beam reflection by the coverslip ($n = 5$ measurements). The driving current I was first set to I = 170 mA and the nanopiezo (Nano-LPS100, Mad City Labs, Inc.) stage of the microscope moved vertically until the focus of the beam was observed (minimum spot on the coverslip). The

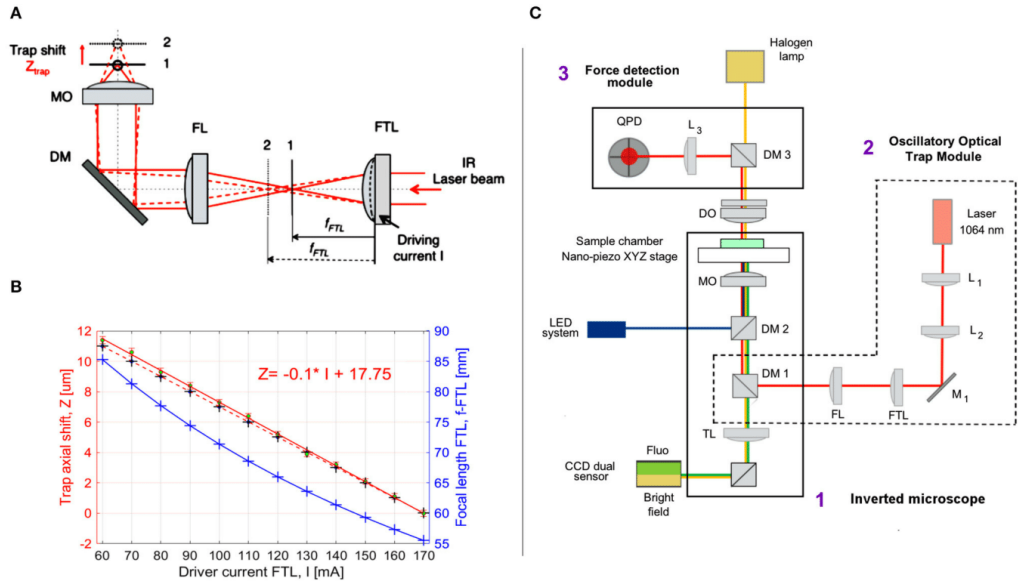

FIGURE 2 | Optical manipulation and imaging setup. **(A)** Oscillatory Optical Trap (OOT): the collimated IR laser beam is focused by FTL in a focal point between planes 1 and 2, according to the driving current I. A convergent lens with fixed focal length (FL) re-collimates the laser beam, which is directed by the dichroic mirror (DM) into the microscope objective (MO), generating an optical trap between planes 1 and 2 near the MO focus. The trap is shifted axially in the range 0–12 μm from the nominal focal plane of the MO. **(B)** The trap shift, Z_{trap}, as a function of the driving current I: $Z_{trap} = Z_{trap}(I)$. The blue crosses and curve represent the focal length of FTL as function of I; black crosses: theoretical values calculated for Z_{trap}, linearly fitted with the red dotted line. The green dots represent the average of the Z_{trap} measured values ($n = 5$) linearly fitted with the red line: $Z = -0.1044*I+17.75$. **(C)** Optical manipulation and imaging setup: 1, inverted microscope; 2, oscillatory optical trap OOT; 3, Force measurement module. Optical components: L1, L2, convergent lenses, f1 = f2 = 100 mm; M1, mirror; FTL, Focus Tunable Lens, f_{FTL} = 55–90 mm; FL, Fixed focal Lens, f = 150 mm; DM1, dichroic mirror (900 dcsp, Chroma); DM2, dichroic mirror (XF22045, Chroma); TL, Tube Lens; MO, Microscope Objective, Olympus 60X, NA 1.4, oil immersion; DO, condenser objective, 10 X, NA 0.3; DM3, Dichroic Mirror (900dcsp, Chroma); L3, convergent lens, f = 40 mm; QPD, Quadrant Photo Diode.

current was then increased in steps of 10 mA and the stage moved until the focus was found again. The measured displacement of the stage represents the experimental value of the axial trap shift, ZE_{trap} (**Figure 2B**). These values are close to the theoretical values (MSE = 0.091), with larger differences observed for bigger axial trap shift values, due to the spherical aberrations (Theofanidou et al., 2004). Nevertheless, the linear fit of the experimental values is very good:

$$Z_{trap} = -0.1044 \bullet I + 17.75 \quad (3)$$

where RMSE = 0.121, $R^2 = 0.999$, allowing to precisely control the trap position by the driving current. The coefficients p1 and p2 of the linear fit: $Z_{trap} = p1^*I + p2$ were obtained with 95% confidence: p1 = −0.1044 (−0.1067, −0.1022); p2 = 17.75 (17.48, 18.02).

For mechanical stimulation, a bead is trapped above the cell at about 2–3 um (**Figure 1C**), then lowered toward the cell membrane in small steps (dI = 1–2 mA) until the variance of the axial displacement decreases considerably (>50%). This condition defines the criterium for the contact between the bead and the cell membrane. From this point, the bead is retracted back by one step (dI = 1 mA, corresponding to dZ = 100 nm), and then the trap oscillation is started. The maximum experimental error detecting the contact is thus given by the axial step dZ = 100 nm. The displacement of the bead, B from the center of the trap is however independent of this error, whereas the indentation of the cell, defined as: I = L-B is altered because of the error defining the starting point (NC in **Figure 1C**) for the oscillation, L. Therefore, the indentation I might be overestimated by 100 nm.

Combined Stimulation and Imaging Setup

The combined stimulation and imaging setup is based on an inverted microscope (Olympus IX81) and includes three main optical paths: IR optical trapping (**Figure 2C**, red line), brightfield imaging (yellow) and fluorescence imaging (blue/green). Two custom modules were adapted to the microscope: Oscillatory Optical Trap (OOT) and Force Detection (FD) to allow cell mechanical stimulation with forces measured in the range of 5–20 pN.

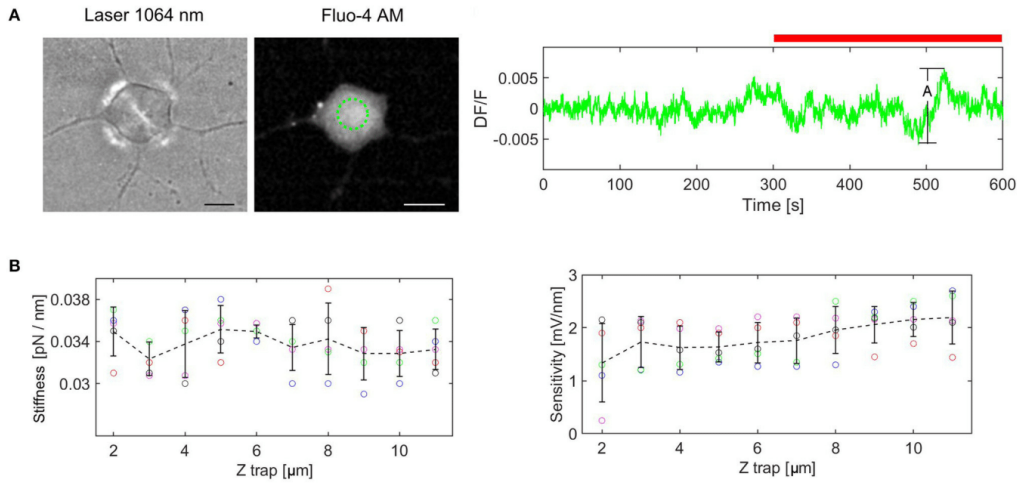

FIGURE 3 | Control experiments. **(A)** Cell exposure to IR laser. The cell is exposed to laser beam (brightfield image at the left) and fluorescence is monitored for the ROI marked in green (image in the middle). DF/F measured for 10 min (red bar indicates laser irradiation), A = $(DF/F)_{max}$, $(DF/F)_{min}$ = 0.0125. **(B)** Trap stiffness and QPD sensitivity as a function of trap height. The error bars represent standard deviation (n = 5 experiments for each height). The dotted line links the mean values for each height.

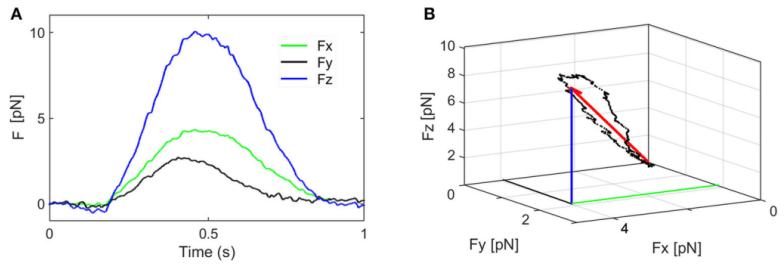

FIGURE 4 | Components of the stimulation force. **(A)** The force components Fx, Fy, Fz, and their fluctuations during one stimulation period. **(B)** The orientation of the resultant force F and the change in its amplitude and direction (the coordinates of the black dots are given by Fx, Fy, Fz).

To direct the IR trapping beam toward the microscope lens (Olympus 60X, NA 1.4 oil immersion), we inserted a dichroic mirror (DM1 in **Figure 2C**) below the wheel of the fluorescence cubes, using a custom mounting that replaced the lens magnification adaptor of the Olympus microscope. The force exerted by the bead on the cell can be measured by the FD module using the IR laser light scattered by the trapped bead (probe) (Neuman and Block, 2004). To couple the FD module with the microscope optical path, the condenser lens of the microscope was replaced with a microscope lens (Olympus 10X, NA 0.3). This allows to suitably collect the IR light scattered by the probe (trapped bead) and project the interference pattern formed at the back-pupil plane onto the Quadrant Photo Detector (PDQ80A, Thorlabs).

The light used for fluorescence excitation (X-Cite XLED1, Excelitas Technology) was launched through the epifluorescence port at the back of the microscope. We used a CCD camera (Orca-D2, Hamamatsu) with a dual sensor to record the fluorescence image and the brightfield image simultaneously. This optical configuration enabled simultaneous optical trapping, cell mechanical stimulation, bright-field and epi-fluorescence imaging, and tracking the position of the trapped bead in X, Y, and Z directions. All the components (FTL, CCD camera, and QPD) were synchronized and controlled using a custom Labview software as well as the time-lapse control of the LED system. Data from the FTL and the QPD were acquired and digitized using a data acquisition board (NI PCI-6259, National Instruments).

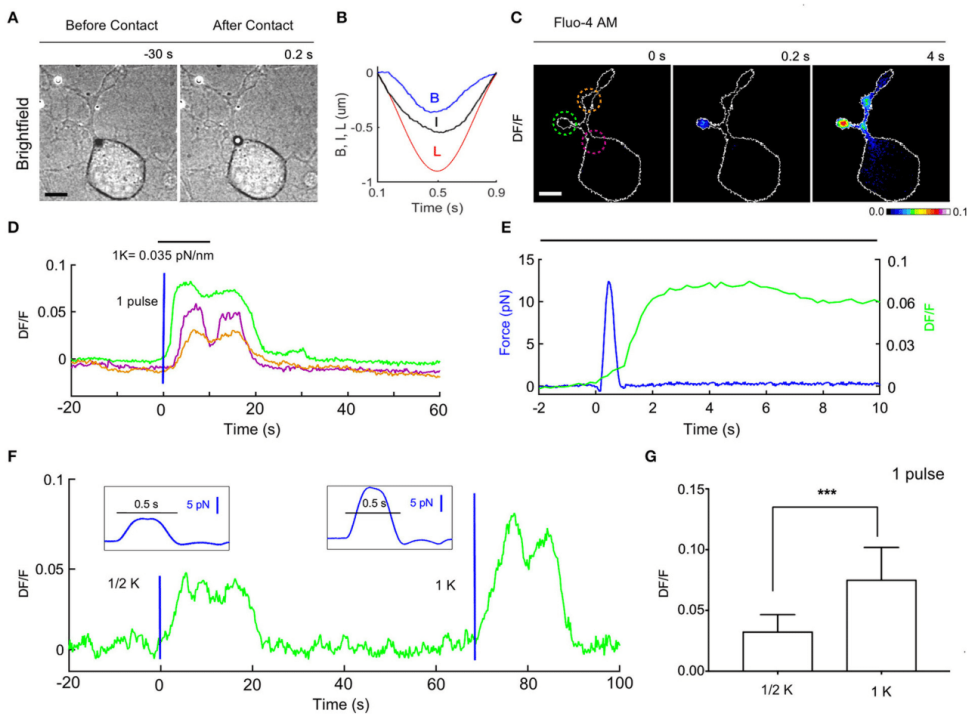

FIGURE 5 | Ca^{2+} transients evoked by calibrated mechanical stimulations in NG10-15 cells. **(A)** Trapped bead above the cell, before (left) and after (right) contact with cell, scale bar: 10 µm. **(B)** Time course of the trap (L) and bead (B) measured displacements and calculated indentation I. **(C)** Fluorescence change, DF/F images, with 3 different ROIs to determine the fluorescence change vs. time **(D)**. **(E)** Detail of the time course of the applied force (blue) and the evoked calcium transient corresponding to green ROI. **(F)** Time course of evoked calcium transient (green) for an experiment in which a weak stimulus was first applied (trap stiffness, k/2), followed by a stronger stimulus (trap stiffness, k). The blue lines indicate application of the force pulses represented in inlets. **(G)** Statistics for the maximum of DF/F (mean ± *SD*) for k/2 (mean 0.0326 ± 0.004, $n = 10$) and k (0.075 ± 0.008, $n = 12$). *t*-test: $^{***}P \leq 0.001$.

Force Measurement

The displacement, S = (X, Y, Z) of the bead from the center of the trap can be measured with 0.2 ms time resolution and 5 nm precision using the Back-Plane Interferometry (BFI) technique (Neuman and Block, 2004).

When the displacement, S, is less than 500 nm, it can be related to the force, F exerted on the bead (which is equal to the force exerted by the bead on the cell) by a proportionality factor, *k*:

$$F = F = k \bullet S \tag{4}$$

where the force components are: $F = (F_x, F_y, F_z)$ and $k = (k_x, k_y, k_z)$ is called elastic constant or trap stiffness. The value of the force components Fx, Fy, Fz, are represented in **Figure 4** for a stimulus period of 1 s. The orientation of the resultant force F and the change in its amplitude and direction are represented in **Figure 4B** and Supplementary Video 2. To keep the discussion simple, only the axial force component, Fz is considered here and the contribution of the smaller lateral forces is discussed later. To determine the trap stiffness, we recorded the bead fluctuations in the trap at a sampling frequency 5 kHz rate, for $t = 5$ s. The sampling frequency is much higher than the cutoff frequency of the constrained Brownian motion of the bead in the trap, thus allowing a correct sampling. Since the QPD signal is in Volts, this is converted in nm using the QPD sensitivity S_Z [mV/nm]. Both parameters, k_Z and S_Z, can be determined using the power spectrum density (PSD) method (Neuman and Block, 2004). The PSD is calculated by Fourier transforming the QPD signal in Volts and is fitted with a Lorenz function to determine two constants: the plateau and the corner frequency, which define S_Z and k_Z.

For a laser power of 25 mW at the sample plane, and the height of the trap, $Z_{trap} = 6$ µm from the focus of the objective, we obtained: $k_Z = 0.035$ [pN/nm] and $S_Z = 1.9$ [mV/nm]. When the height of the trap was altered, the bead remained trapped. However, since the convergence of the trapping laser changed slightly, we wondered how much this influenced the QPD signal. Therefore, we measured the trap stiffness and the

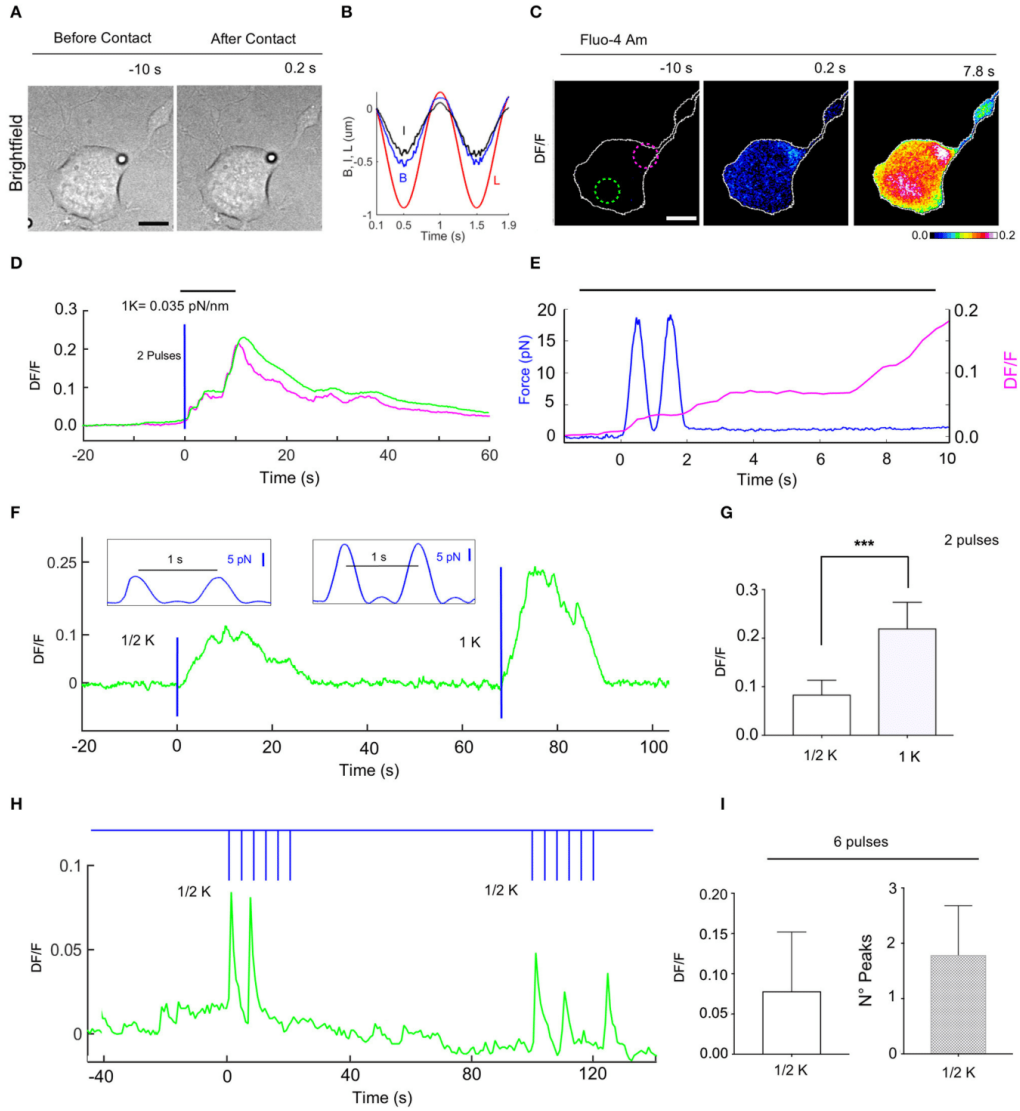

FIGURE 6 | Calcium transients evoked by repetitive mechanical stimulations of NG108-15 cells. **(A)** Trapped bead above the cell, before (left) and after contact with cell (right), scale bar: 10 μm. **(B)** Time course of the trap (L) and bead (B) measured displacements and calculated indentation I for two pulses. **(C)** Fluorescence change, DF/F images, with 2 different ROIs to determine the fluorescence change vs. time **(D)**. **(E)** Time course of the applied force (blue trace) and the evoked calcium transient (magenta) from ROI. **(F)** Time course of evoked calcium transient (green) for an experiment in which a two pulses stimulus was first applied (trap stiffness, k/2), followed by a second two pulses stimulus (trap stiffness, k = 0.035 pN/nm). The blue lines indicate application of the stimuli with the force pulses represented in inlets. **(G)** Statistics for the maximum of DF/F values for k/2 (0.083 ± 0.011, $n = 8$) and k (0.22 ± 0.018, $n = 9$). T-test: $^{***}P \leq 0.001$. **(H)** Time course of the evoked DF/F (green) and the mechanical stimulation (blue) composed of two train of 6 pulses at 0.25 Hz with k/2. **(I)** Statistics bar graph representing the mean value of DF/F induced by 6 pulses with k/2 (left, 0.078 ± 0.02, $n = 13$) and the mean value of the number of calcium peaks for each train of 6 pulses (right, 1.8 ± 0.2, $n = 14$).

detector sensitivity for different heights of the trap (from 2 to 11 μm) using a polystyrene bead (diameter d = 3.5 μm) in $n = 5$ different experiments. The results are plotted in the **Figure 3B**. The trap stiffness varies between a minimum value, kmin = 0.029 pN/nm to a maximum value, kmax = 0.039 pN/nm, with the mean value k = 0.034 pN/nm, (SD = 0.002). The sensitivity varies between 0.23 and 2.75 mV/nm, with a mean value of 1.817 mV/nm, (SD = 0.482). The sensitivity fluctuates more for Z_{trap} = 2–4 um, but it is much more stable for the region in which we are actually working (Z_{trap} = 4–8 um). Considering these results, the stiffness and sensitivity variations will generate maximum errors of 15 and 40%, respectively. If the errors are cumulative, the maximum error for force measurement would be 55%. However, for the height range we are working in the maximum error is reduced to 30%. Since the main goal of our paper is to show that calcium transients are induced by cell stimulation with forces of the order of 5–20 pN, i.e., much smaller (2–3 orders of magnitude) than the level of the forces previously reported (Lee et al., 2014; Gaub and Müller, 2017), the tolerance is acceptable in this context. Moreover, performing the calibration with the bead trapped above the cell before each indentation experiment, we could avoid this problem and regulate the stiffness to the nominal value by slightly adjusting the laser power.

Immunohistochemistry

NG108-15 cells were fixed in 4% paraformaldehyde containing 0.15% picric acid in phosphate-buffered saline (PBS), saturated with 0.1 M glycine, permeabilized with 0.1% triton X-100, saturated with 0.5% BSA (all from Sigma- Aldrich) in PBS and the incubated for 1 h with primary antibodies: anti-Piezo1 (Alomone Labs). The secondary antibody was goat anti-rabbit Alexa Fluor 488 and the incubation time was 30 min. Nuclei were stained with 2 μg/ml in PBS Hoechst 33342 (Sigma-Aldrich) for 5 min. The cells were examined using a Nikon Eclipse C1si Confocal microscope. Images were acquired with a 40x 1.4 oil-immersion objective.

Inhibition of Mechanosensitive Channels With GsMTx-4

GsMTx-4, a peptide toxin from *Grammostola spatulata* spider venom, was purchased from Tocris Bioscience and a 0.1 mM stock solution was prepared in distilled water. Working solutions were prepared by dilution in Krebs-Ringer's solution at the concentration of 8 μM. In pilot experiments, cells were treated with either GsMTx-4 or left untreated and used directly for calcium experiment. GsMTx4 is a gating modifier known for its selective inhibition of cation-permeable MCS channels belonging to the Piezo and TRP channel families.

Data and Statistical Analysis

For calcium experiment the DF/F was quantified by custom developed code Matlab (MathWorks, Inc.) and Imagej software v1.6 (National Institutes of Health). The peaks of the Ca^{2+} transients were extracted using the threshold condition: $A_p > 0.02$, where A_p is the amplitude of the peak with respect to the baseline (**Figure 3A**). All the results are presented as mean ± SD and statistically differences were determined using a t-test, as appropriate with $p < 0.05$ considered statistically significant (GraphPad Prism 7, GraphPad software, San Diego, CA).

RESULTS

Piconewton Forces Induce Cell Membrane Indentation

Cell membrane indentation is usually obtained with forces in the nN range (Gaub and Müller, 2017), much larger than intercellular forces which are in the pN range (Cojoc et al., 2007). By using an OOT with a micro-bead as the probe, we asked whether piconewton forces can induce a pressure large enough to indent the cell membrane, and how large can be this indentation. We trapped a polystyrene bead (diameter d = 3.5 μm) above a NG108-15 cell (**Figure 5A**) and adjusted the laser power so that the trap stiffness was k = 0.035 [pN/nm]. The bead was moved toward the cell membrane so to establish contact (**Figure 1C**). Following contact, the trapped bead was moved up by one step (100 nm) and then the trap was shifted down following a sinusoidal signal, L(t) with amplitude A = 1 μm and frequency f = 1 Hz. The interaction bead-cell membrane produces a displacement B(t) of the bead from the center of the trap and an indentation I(t) of the cell membrane, which are related to L(t) by the relation:

$$L(t) = B(t) + I(t) + Ct \tag{5}$$

We measured the bead displacement $B(t)$ from the center of the trap (see section Materials and Methods) and calculated $I(t) = L(t) - B(t)$-Ct (**Figure 5B**) and in the experiment illustrate in **Figure 5**. The maximum bead displacement is B_{max} = 350 nm, and the maximum indentation is I_{max} = 540. The time courses $B(t)$ and $I(t)$ show maxima at different time moments because the resistance opposed by the cell membrane to the bead pressure is different between pushing and pulling cycles. Using a trap stiffness, k_Z = 0.035 pN/nm we measured F_{max} = 12.3 pN. The pressure P produced by the vertical force is P = F/S, where S is the contact area between the bead and the cell, $S = \pi \cdot d \cdot I$. The maximum pressure P_{max} corresponds to the maximum force Fmax so that $P_{max} = F_{max}/S$ = 2.2 Pa = 0.017 mm Hg, which is 3 orders of magnitude less than the pressure exerted in the AFM stimulation using a bead of diameter d = 5 μm (Gaub and Müller, 2017). The variation of the membrane tension, produced by this pressure is: T = P*D/4, where D is the diameter of the contact circle: D = sqrt[I(d-I)] (Sachs, 2015). Using the above values, we obtain a change of tension: $\Delta T = 2.12 \cdot 10^{-3}$ mN/m. This value is about 3 orders of magnitude smaller than the values previously assumed to trigger the opening of the mechanosensitive channels (Sachs, 2015; Jin et al., 2017). Since we measure also the lateral forces, Fx, Fy, we considered also their contribution: $\Delta Txy = Fxy/\pi D \sim 1.6 \cdot 10^{-3}$ mN/m, where $Fxy = sqrt(F^2x + F^2y) \sim 6$ pN is the maximum lateral force, and D = 1.22 μm (I = 500 nm) is the contact circle diameter. The total tension change $\Delta T + \Delta Txy = 3.62 \cdot 10^{-3}$ mN/m is bigger but still much smaller than the values previously assumed to be necessary for the opening of mechanosensitive channels.

A Single Force Pulse Induces Ca^{2+} Transients in the Cell

To evaluate whether forces in the pN range evoke a biological response we analyzed possible induced Ca^{2+} transients and we loaded the NG108-15 cells with the membrane permeable Calcium dye Fluo-4 (see section Materials and Methods). Before the mechanical stimulation was applied, fluorescence images were acquired at 5 Hz for 2 min to verify whether the intracellular Ca^{2+} level was stable and then we proceeded with the mechanical stimulation using the OOT. In the experiment illustrated in **Figures 5A–E**—with a maximum force equal to 12.3 pN and indentation equal to 540 nm-we observed an increase of intracellular Ca^{2+} level immediately after the stimulation (**Figures 5C–E**). This change was first localized in the neurite near the site of the mechanical stimulation, and then diffused into the other neurites (**Figures 5C,D**). The maximum fluorescence change (DF/F = 0.08) occurred in the first region about 5 s after stimulation, and with a delay of about 8 s in the other two regions. After about 20 s Ca^{2+} returned to the basal level. Similar changes of DF/F were observed in 12 experiments (DF/F peak: mean 0.075 ± 0.008 and **Figure 5G**) out of a total of 15 stimulated NG108-15 cells.

The mechanical forces exerted in experiments with trap stiffness k = 0.035 pN/nm (e.g., **Figures 5A–E**) had maximum values in the range 10–18 pN (mean 13.8 pN ± 2.5) and induced detectable changes of intracellular Ca^{2+}. In order to establish a threshold for the mechanical stress which can induce Ca^{2+} intracellular transients, we decreased the trap stiffness k by a factor of 2, from k = 0.035 to k/2 = 0.0175 pN/nm. In this case, the maximum value of DF/F was 0.0326 ± 0.004 (n = 10), and no calcium activation was observed in 4 cells. The maximum forces were in the range 4–10 pN (mean 7.2 pN ± 1.5) which means the force applied was reduced by approximately the same factor as the trap stiffness. Considering also the values of the fluorescence change (DF/F—**Figure 5G**) our experiments show that the amplitude of Ca^{2+} transients scales with the applied force.

Our method allows a fast change of the trap stiffness, so it is possible to apply mechanical stimuli with different strengths to the same cell, as shown in **Figure 5F**.

Adaptation to Repetitive Stimulations

We then applied mechanical stimulations composed of two consecutive force pulses with 1 Hz frequency (**Figure 6**) to observe whether cells show a cumulative force-dependent response to a pulsatile regime. Using a trap stiffness k = 0.035 pN/nm the maximum of the applied force (of two pulses) was 14.1 ± 2.5 pN (n = 9), and the amplitude of evoked Ca^{2+} transients was 0.22 ± 0.018 (**Figure 6G**), which was more than twice of that observed with one force pulse (0.075 ± 0.008, **Figure 5G**). Repeating the experiments with the trap stiffness k/2, the maximum of the applied force was 6.8 ± 2 pN (n = 8), and DF/F was 0.083 ± 0.011.

In order to explore the cell adaptation, we probed the response of NG108-15 cells to repetitive low strength (k/2) force pulses of 1 s with a resting time of 4 s (Supplementary Video 3 and **Figure 6H**). In these experiments, the DF/F had an amplitude of 0.078 ± 0.02 (n = 13) with a similar time (**Figures 6H,I**). However, in this case a DF/F peak could not be detected for every force pulse, a mean of 1.8 ± 0.2 (n = 14) pulses/train of pulses being detected (**Figure 6I**).

Although these gentle mechanical stimulations did not evoke any morphological change visible under bright-field illumination, when the mechanical stimulation was prolonged (1–3 min) the NG108-15 cell shrank, retracting the compartment submitted to low level mechanical stress by some microns (Supplementary Video 4).

Expression of Piezo1 Channels in NG108-15 Cells and MCS Inhibition

To examine if MCS channels are expressed in NG108-15 cells, we verified the presence of the PIEZO1 channel by immunostaining. The mechanosensitive channel Piezo1 is robustly expressed in the NG108-15 cells (**Figure 7A**) and is a good candidate for transducing the mechanical stimulus. Then, to identify better the source of the intracellular calcium elevation we tested the peptide GsMTx-4 that inhibits the cationic mechanosensitive channels (Gnanasambandam et al., 2017), as well as the Piezo channels (Bae et al., 2011). In the NG108-15 cells, we observed that the Gsmtx-4 at the concentration of 8 μM inhibited the occurrence of Ca^{2+} transient almost completely: in the presence of GsMTx-4 the amplitude of Ca^{2+} transient DF/F was 0.006 ± 0.002 (n = 10), compared with what obversed from the untreated cells during the same experimental session 0.067 ± 0.007 (n = 8; **Figures 7B–D**).

DISCUSSION

We have developed an optical tweezers method to apply weak forces in the 5–20 pN range to the cell membrane and demonstrated that these small forces produce an indentation of the cell membrane and trigger Ca^{2+} transients in NG108-15 cells. A similar approach, but with a fixed trap and moving the piezostage, has been recently used to investigate the indentation in breast cancer cells (Coceano et al., 2015; Yousafzai et al., 2016). Our approach, using an oscillatory optical trap (OOT) allows to keep the cell in focus during the stimulation, enabling optimum brightfield, and fluorescence imaging of the cell. This unique feature is possible by using the Focused Tunable Lens (FTL), which is positioned in an optical path separated from the imaging optical path of the microscope. Another possibility to decouple sample imaging from the trapping position has been reported using spatial light modulators (Emiliani et al., 2005) but this technique is more complex, less precise, and slower than the OOT with FTL.

It is known, that when the mechanical stress is applied, an early increase in intracellular calcium is generated (Godin et al., 2007), possibly caused by the opening of mechanosensitive channels which can be followed by larger calcium waves likely due to the release of calcium from internal stores such as the endoplasmatic reticulum and/or the delayed opening of additional calcium-permeable ionic channels (Wang et al., 2005; Kim et al., 2015). We found that localized mechanical stress

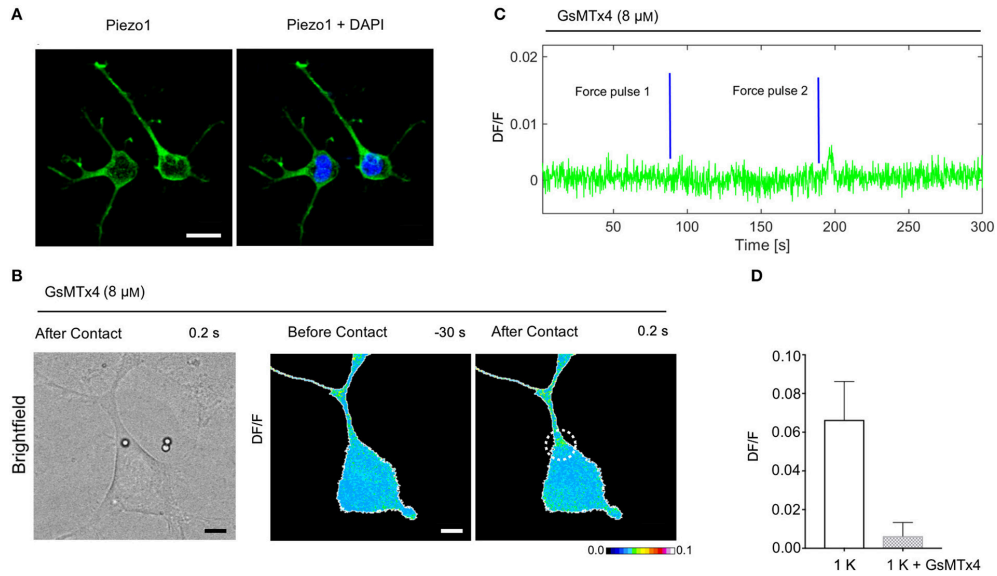

FIGURE 7 | Expression of Piezo1 channels in NG108-15 cells and the effect of Gsmtx-4 on mechanically activated Ca^{2+} transient. **(A)** NG108-15 cells at 2DIV stained for Piezo 1 (green) and Hoechst 33342 nuclear stain (blue). **(B)** Brightfield and DF/F image obtained before and after the mechanical stimulation. **(C)** Time course of the evoked calcium transient (green trace) from white ROI in **(B)**. The blue lines indicate the application of the mechanical force. **(D)** Bar graphs represent fluorescence changes of Ca^{2+} (DF/F) in untreated cells stimulated with one pulse of strength k, as control group ($n = 8$) vs. cells treated with Gsmtx-4 ($n = 10$).

induces a Ca^{2+} elevation immediately after stimulation and nearby the site where the stimulation was applied (**Figures 5C**, **6C**). Interestingly, the amplitude of the Ca^{2+} oscillations for two pulses (strength k, force 14.1 pN ± 2.5) reached 0.22 ± 0.018 vs. the amplitude corresponding to one pulse (strength k, force 13.8 pN ± 2.5) stimulation: 0.075 ± 0.008 (**Figures 5G**, **6G**). These results suggest that mechanical stimulation can modulate the calcium signal transduction pathway.

We also showed that the treatment of the NG108-15 cells with GsMTx4 to specifically inhibit mechanically activated cation channels, strongly reduced the calcium response upon the mechanical stress. This suggests that the mechanosensitive ion channels are necessary for the calcium mechanotransduction. Moreover, when low regime mechanical stimulation was prolonged (repeated trains of weak pulses, k/2) NG108-15 cells retract the compartment under the mechanical stress; these results are in agreement with the previous observation in which calcium influx trough mechanosensitive channels can induce retraction (Doyle et al., 2004) and inhibits neurite outgrowth in opposition to other influx pathways and releases from the intracellular store (Jacques-Fricke et al., 2006).

Our work has two major implications: first, we have shown how to apply mechanical stimuli under controlled conditions, the force and indentation of which are measured directly and precisely; second, in addition to mechanotransduction operating for large forces in the range of 0.1–500 nN, we have shown that very low levels of mechanical stress (5–20 pN) are able to induce a calcium intracellular response in NG108-15.

Our results suggest that the mechanotransduction pathway may be sensitive to physiologically mechanical touches, characterized by pN forces, as the one produced by a moving lamellipodium (Cojoc et al., 2007). Understanding the molecular and biophysical mechanism of how cells locally regulate the complex mechanical response may clarify how cells change shape and control their migratory behavior. Therefore, mechanical signaling among cells is important and ubiquitous but still needs to be better clarified.

AUTHOR CONTRIBUTIONS

FF, DC, and VT designed the study. FF and DC designed and implemented the experimental setup. FF performed experiments. FF and DC collected and analyzed data. FF, DC, and VT wrote the manuscript.

SUPPLEMENTARY MATERIAL

The Supplementary Material for this article can be found online at: https://www.frontiersin.org/articles/10.3389/fncel.2018.00130/full#supplementary-material

REFERENCES

Arnadóttir, J., and Chalfie, M. (2010). Eukaryotic mechanosensitive channels. *Annu. Rev. Biophys.* 39, 111–137. doi: 10.1146/annurev.biophys.37.032807.125836

Bae, C., Sachs, F., and Gottlieb, P. A. (2011). The mechanosensitive ion channel piezo1 is inhibited by the peptide GsMTx4. *Biochemistry* 50, 6295–6300. doi: 10.1021/bi200770q

Coste, B., Xiao, B., Santos, J. S., Syeda, R., Grandl, J., Spencer, K. S. et al. (2012). Piezo proteins are pore-forming subunits of mechanically activated channels. *Nature* 483, 176–181. doi: 10.1038/nature10812

Charras, G. T., Williams, B. A., Sims, S. M., and Horton, M. A. (2004). Estimating the sensitivity of mechanosensitive ion channels to membrane strain and tension. *Biophys. J.* 87, 2870–2884. doi: 10.1529/biophysj.104.040436

Coceano, G., Yousafzai, M. S., Ma, W., Ndoye, F., Venturelli, L., Hussain, I., et al. (2015). Investigation into local cell mechanics by atomic force microscopy mapping and optical tweezers vertical indentation. *Nanotechnology* 27:065102. doi: 10.1088/0957-4484/27/6/065102

Cojoc, D., Difato, F., Ferrari, E., Shahapure, R. B., Laishram, J., Righi, M., et al. (2007). Properties of the force exerted by filopodia and lamellipodia and the involvement of cytoskeletal components. *PLoS ONE* 2:e1072. doi: 10.1371/journal.pone.0001072

Connelly, T., Yu, Y., Grosmaitrea, X.,Wanga, J., Santarellia, L. C., Savigner, A., et al. (2015). G protein-coupled odorant receptors underlie mechanosensitivity in mammalian olfactory sensory neurons. *Proc. Natl. Acad. Sci. U.S.A.* 112, 590–595. doi: 10.1073/pnas.1418515112

Coste, B., Mathur, J., Schmidt, M., Earley, T. J., Ranade, S., Petrus, M. J., et al. (2010). Piezo1 and Piezo2 are essential components of distinct mechanically activated cation channels. *Science* 330, 55–60. doi: 10.1126/science.1193270

Coste, B., Murthy, S. E., Mathur, J., Schmidt, M., Mechioukhi, Y., Delams, P., et al. (2015). Piezo1 ion channel pore properties are dictated by C-terminal region. *Nat. Commun.* 6:7223. doi: 10.1038/ncomms8223

Dogterom, M., and Yurke, B. (1997). Measurement of the force-velocity relation for growing microtubules. *Science* 278, 856–860.

Doyle, A., Marganski, W., and Lee, J. (2004). Calcium transients induce spatially coordinated increases in traction force during the movement of fish keratocytes. *J. Cell Sci.* 117, 2203–2214. doi: 10.1242/jcs.01087

Eghiaian, F., and Schaap, I. A. (2011). Structural and dynamic characterization of biochemical processes by atomic force microscopy. *Methods Mol. Biol.* 778, 71–95. doi: 10.1007/978-1-61779-261-8_6

Emiliani, V., Cojoc, D., Ferrari, E., Garbin, V., Durieux, C., Coppey-Moisan, M., et al. (2005). Wave front engineering for microscopy of living cells. *Opt. Express* 13, 1395–1405. doi: 10.1364/OPEX.13.001395

Ernstrom, G. G., and Chalfie, M. (2002). Genetics of sensory mechanotransduction. *Annu. Rev. Genet.* 36, 411–453. doi: 10.1146/annurev.genet.36.061802.101708

Finer, J. T., Simmons, R. M., and Spudich, J. A. (1994). Single myosin molecule mechanics: piconewton forces and nanometre steps. *Nature* 368, 113–119. doi: 10.1038/368113a0

Gaub, B. M., and Müller, D. J. (2017). Mechanical stimulation of Piezo1 receptors depends on extracellular matrix proteins and directionlity of force. *Nanoletters* 17, 2064–2072. doi: 10.1021/acs.nanolett.7b00177

Gnanasambandam, R., Ghatak, C., Yasmann, A., Nishizawa, K., Sachs, F., Ladokhin, A. S., et al. (2017). GsMTx4: mechanism of inhibiting mechanosensitive ion channels. *Biophys. J.* 112, 31–45. doi: 10.1016/j.bpj.2016.11.013

Godin, L. M., Suzuki, S., Jacobs, C. R., Donahue, H. J., and Donahue, S. W. (2007). Mechanically induced intracellular calcium waves in osteoblasts demonstrate calcium fingerprints in bone cell mechanotransduction. *Biochem. Model Mechanobiol.* 6, 391–398. doi: 10.1007/s10237-006-0059-5

Hao, J., and Delmas, P. (2011). Recording of mechanosensitive currents using piezoelectrically driven mechanostimulator. *Nat. Protoc.* 6, 979–990. doi: 10.1038/nprot.2011.343

Jacques-Fricke, B. T., Seow, Y., Gottlieb, P. A., Sachs, F., and Gomez, T. M. (2006). Ca^{2+} influx through mechanosensitive channels inhibits neurite outgrowth in opposition to other influx pathways and release from intracellular stores. *J. Neurosci.* 26, 5656–5664. doi: 10.1523/JNEUROSCI.0675-06.2006

Jin, P., Bulkley, D., Guo, Y., Zhang, W., Guo, Z., Huynh, W., et al. (2017). Electron cryo-microscopy structure of the mechanotransduction channel NOMPC. *Nature* 547, 118–122. doi:10.1038/nature22981

Kim, T., Joo, C., Seong, J., Vafabakhsh, R., Botvinick, E., Berns, M. W., et al. (2015). Distinct mechanisms regulating mechanical force-induced Ca^{2+} signals at the plasma membrane and the ER in human MSCs. *Elife* 4:e04876. doi: 10.7554/eLife.04876.001

Lee, W., Leddy, H. A., Chen, Y., Lee, S. H., Zelenski, N. A., McNulty, A. L., et al. (2014). Sinergy between Piezo 1 and Piezo2 channels confers high-strain mechanosensitivity to articular cartilage. *Proc. Natl. Acad. Sci. U.S.A.* 111, E5114–E5122. doi: 10.1073/pnas.1414298111

Lewis, A. H., and Grandl, J. (2015). Mechanical sensitivity of Piezo1 ion channels can be tuned by cellular membrane tension *Elife* 4:e12088. doi: 10.7554/eLife.12088

Lumpkin, E. A., Marshall, K. L., and Nelson, A. M. (2010). The cell biology of touch. *J. Cell Biol.* 191, 237–248. doi: 10.1083/jcb.201006074

Murphy, M. F., Lalor, M. J., Manning, F. C., Lilley, F., Crosby, S. R., Randall, C., et al. (2006). Comparative study of the conditions required to image live human epithelial and fibroblast cells using atomic force microscopy. *Microsc. Res. Tehnol.* 69, 757–765. doi: 10.1002/jemt.20339

Neuman, K. C., and Block, S. M. (2004). Optical trapping. *Rev. Sci. Instrum.* 75, 2787–2809. doi: 10.1063/1.1785844

Sachs, F. (2015). Mechanical transduction by ion channels: a cautionary tale. *World J. Neurol.* 5, 74–87. doi: 10.5316/wjn.v5.i3.74

Theofanidou, E., Wilson, L., Hossack, W. J., and Arlt, J. (2004). Sperichal aberration correction for optical tweezers. *Opt. Commun.* 236, 145–150. doi: 10.1016/j.optcom.2004.03.009

Walker, R. G., Willingham, A. T., and Zuker, C. S. (2000). A Drosophila mechanosensory transduction channel. *Science* 287, 2229–2234. doi: 10.1126/science.287.5461.2229

Wang, Y., Botvinick, E. L., Zhao, Y., Berns, M. W., Usami, S., et al. (2005). Visualizing the mechanical activation of Src. *Nature* 434, 1040–1045. doi: 10.1038/nature03469

Wu, J., Goyal, R., and Grandl, J. (2016). Localized force application reveals mechanically sensitive domains of Piezo1. *Nat. Commun.* 7:12939. doi: 10.1038/ncomms12939

Wu, J., Lewis, A. H., and Grandl, J. (2017). Touch, tension, and transduction – the function and regulation of Piezo Ion channels. *Trends Biochem. Sci.* 42, 58–68. doi: 10.1016/j.tibs.2016.09.004

Yousafzai, M. S., Ndoye, F., Coceano, G., Niemela, J., Bonin, S., Scoles, G., et al. (2016). Substrate-dependent cell elasticity measured by optical tweezers indentation. *Opt. Lasers Eng.* 76, 27–33. doi: 10.1016/j.optlaseng.2015.02.008

Zhang, W., Cheng, L. E., Kittelmann, M., Li, J., Petkovic, M., and Cheng, T., et. al. (2015). Ankyrin repeats convey force to gate the NOMPC mechanotransduction channel. *Cell* 162, 1391–1403. doi: 10.1016/j.cell.2015.08.024

Conflict of Interest Statement: The authors declare that the research was conducted in the absence of any commercial or financial relationships that could be construed as a potential conflict of interest.

Neuronal Mechanotransduction: from force to cytoskeleton contractility

FABIO FALLERONI, YUNZHEN LI, DAN COJOC AND VINCENT TORRE

Abstract

Mechanical stresses are ubiquitous in Biology, and a variety of experimental approaches have been developed to investigate mechanotransduction. Recently, we have developed an optical tweezer method to apply forces in the 5-20 pN range and to measure the indentation produced in the cell. The role mechanical forces play in the development and maintenance of neuronal networks has been increasingly recognized and addressed. Despite significant advances, many aspects of the mechanical control of neuronal functions remain unclear. Here we show that repetitive mechanical forces, delivered with a tunable optical trap and applied to growth cones of hippocampal neurons induce retraction and turning. The same repeated forces applied to the soma evoke localized contraction events. We therefore report that mechanical indentation triggers a structural remodeling and contraction of actin cytoskeleton network. Furthermore, we have found that the mechanical stimulation allows the entry of Ca^2. Moreover, we report the activation of the small G protein RhoA, due to the mechanical indentation. The activation of Rho-GTPase, such as RhoA, and the Rho-associated kinase (ROCK) may be responsible for the cytoskeleton contractility mechanically induced. The presence of MSCs has been confirmed by Immunochemistry showing that Piezo 1 is well expressed over the entire membrane of hippocampal neurons. These results show that mechanical signaling operates in central neurons for very weak forces and outline the molecular events underlying this exquisite mechanosensitivity.

Introduction

The mechanotransduction and mechanical signaling is well studied at the level of several sensory neurons specialized in the transduction of mechanical stimuli mediating the basis of hearing, touch and proprioception[1]. However, recent studies suggest that mechanical sensation is more widespread in the nervous system and possibly is active among almost all cells and neurons. For instance,

many aspects of axonal growth and neuronal development have been examined in the context of mechanical force[2,3]. The neuronal growth cones GC are structures located at the tips of neurite that guide axon to their targets during development. Recently, it has been proposed that, in addition to biochemical cues, Growth cones (GCs) are susceptible to mechanical stimuli[4,5]. For instance, it has been demonstrated that substrate stiffness and tension can influence for axonal development and branching[6]. We have found weak mechanical forces in the range of pN, which behave as a repulsive stimulus, induce retraction and turning of the growth cones of hippocampal neurons (Figure 1). Furthermore, in accordance with previous studies, in which it has been demonstrated that the mechanical stress influences the shape of neuronal somata[7], we have found that the OT indentation applied to the soma evokes its rearrangement with a localized retraction at the site of mechanical indentation (Figure 2).

Since the structural rearrangements are mediated by the cytoskeleton, through the actomyosin network we have investigated the spatio-temporal dynamics of mechanical-induced cytoskeletal modifications, by labelling the endogenous F-actin with fluorescent LifeAct. We show that pN forces apply by indenting the plasma membrane, lead to contractility with structural modification of the actin network, both in hippocampal neurons and NG108-15 cells (Figure 3 and 4).

While increasing evidences show that the forces and the mechanical properties of neuronal environment play a key role in the homeostasis of the nervous system[8], it remains unclear how the physical forces are sensed and transduced by cells to give rise to the appropriate output. We found that hippocampal neurons display a calcium intracellular elevation, due to the mechanical stress in the pN range, confirmed by Ca^{2+} imaging with the Fluo-4 AM.

Then, we analyzed the possible molecular cascades initiated by an elevation of intracellular Ca^{2+}, that can potentially lead to a re-organization of the cytoskeleton. Several molecular cascades initiated by an elevation of intracellular calcium involve the activation of CaMKII and of small GTPases. CaMKII is one of the most abundant proteins in the post synaptic domain and plays a fundamental role in synaptic plasticity[9]. When intracellular Ca^{2+} increases, Ca^{2+} binds to calmodulin, and the activated Ca^{2+}/calmodulin binds to a CaMKII subunit, causing activation through its conformational change. The CaMKII in turn can activate the multiple pathways, including the Rho GTPases signalling. The Rho family

GTPases, including Ras homolog (RhoA), Cell division cycle 42 (Cdc42) and Ras-related C3 botulinum toxin substrate (Rac) are key players in regulating the actin cytoskeleton[10]. Interestingly, several groups reported that Rho GTPase are mechanically-activated[11]. We used a FRET sensor to verify the possible activation of RhoA following mechanical stimulation. In line with previous studies conducted in other kind of cells[12-14], we observed that RhoA shows an activation due to the mechanical indentation in the pN range in hippocampal neurons (figure 5). RhoA primarily acts upon the regulatory protein Rho-associated, ROCK, increasing the contractile force generated by myosin II on actin filaments. ROCK also phosphorylates and activates another kinase, the LIM kinase, which in turn phosphorylates and inhibits the actin-severing protein cofilin, increasing the stability of actin filaments[15]. Together these effects highlighting RhoA GTPase as a central regulator of cytoskeleton contractility. Finally, we looked for the presence of the MSC Piezo 1 by immunohistochemistry in hippocampal neurons and we found a diffuse staining in the great majority of hippocampal neurons, both in the soma and in the neurites.

Altogether, our results give an indication of how mechanical inputs are translated into biochemical signaling, explain neuronal mechano-responsiveness, provide an insight into a formerly unknown branch pruning mechanism and clearly strengthen the idea that mechanical cues are involved in neuronal physiology.

Material and methods

Hippocampal cell culture

Hippocampal neurons were dissected from Wistar rat brain (P1-P2). After decapitation the meninge-free hippocampi were incubated with 5 mg/ml trypsin (Sigma) and 0.75 mg/ml DNase I (Sigma) for 5 minutes at room temperature for the enzymatic dissociation. Then trypsin was neutralized by 1 mg/ml trypsin inhibitor (Sigma) and a mechanical dissociation was performed with a Pasteur pipette. The cell suspension was then centrifuged at 100 G for 5 min, and the pellet was re-suspended. Finally, hippocampal neurons were plated on coverslip coated with 50 µg/ml poly-L-ornithine (Sigma). The hippocampal cultures were incubated (95% O2, 5% CO2 at 37 °C) for 4-6 days in Neurobasal medium (Sigma) containing 25 µm GlutaMAX (Thermo Fisher Scientific) and B27

supplement at 2% (Sigma). Cell were used for experiment after 5-6 days in culture. All experimental procedure on animals were done in accordance with the European Communities Council Directive of November 2016 (86/609/EEC).

Ng108-15 cell culture

Mouse neuroblastoma x rat glioma hybrid (NG108-15) cells were obtained from Sigma-Aldrich. The cells were cultured as described in ref.[25].

Calcium experiments

The cells were loaded with a cell-permeable calcium dye Fluo4-AM (Life Technologies) by incubating them with 4μM Fluo4-AM in Ringer's solution (145 mM NaCl, 3 mM KCl, 1.5 mM $CaCl_2$, 1 mM $MgCl_2$, 10 mM glucose and 10 mM Hepes, pH 7.4) at 37 °C for 1 hour. After incubation, the cultures were washed and then transferred to the stage of an Olympus IX-81 inverted microscope.

Cell Transfection

Cells were transfected 24 h after the seeding with the LifeAct plasmid to visualize the actin network or with the intramolecular RhoA FRET biosensors (Murakoshi et al., 2011). The FRET probe consists of truncated RhoA, a RhoA binding domain (RBD) of an effector protein, and a pair of GFP (green) and RFP (red). The intramolecular binding of active RhoA to RBD leads to the close association of GFP with RFP. Thus, the FRET activity of the RhoA biosensor was monitored to determine RhoA activity. The cells have been transfected using Lipofectamine p3000 reagent (Invitrogen) following the manufacturer's protocol and imaged 1 day after transfection.

Live cell imaging experiments

Live cell imaging experiment have been performed on an epi-fluorescence microscope (Olympus IX-81, Olympus) equipped with LED illumination (λ = 590 nm for LifeAct-mCherry; λ = 480 nm for Fluo-4 and RhoA FRET-sensor; all purchased from Excilitas tecnology). During all imaging experiments cells were

kept at 37°C. Time-lapse images were taken using a 100X oil objective (Olympus, NA = 1.4) or an 80X oil immersion objective (Olympus, NA = 1.4). All acquisitions were done with a CCD dual sensor at 12bit (ORCA-D2, Hamamatsu).

Results

Growth cone and soma response to mechanical indentation

In order to investigate the neuronal response to mechanical indentation, hippocampal growth cones were exposed to repetitive mechanical pulses. GCs from hippocampal neurons were routinely found *in vitro*, moving vigorously. When a GC was seen active for at least 5 minutes, a polystyrene bead, trapped in the equilibrium position of the laser beam of the OT, was moved above the GC; then, a controlled mechanical stress, composed by 6 mechanical stimuli at the frequency of 1 Hz, was applied to the GC. In response to mechanical stress the

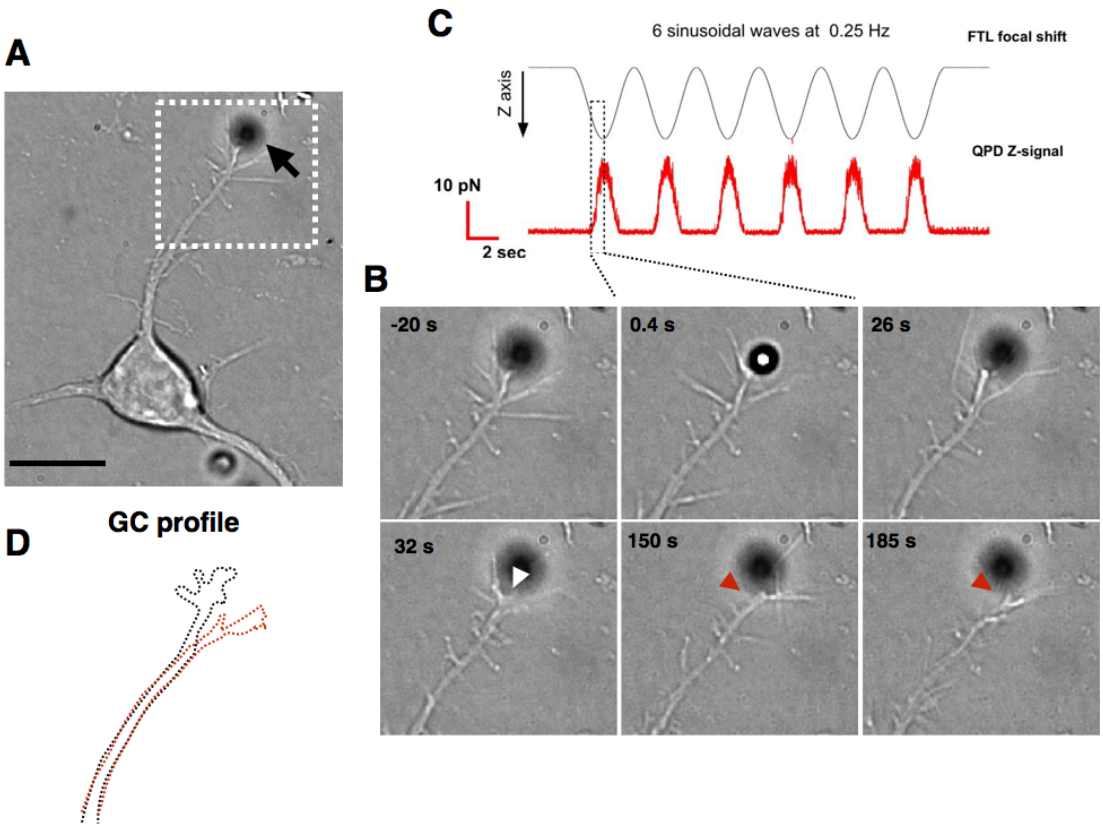

Figure 1. Response of Hippocampal GC to mechanical stimulation. A) Brightfield image of Hippocampal neuron and a trapped bead (black arrow) near the GC. B) Time course of GC response: after mechanical stress retraction (white arrow) and turning (red arrow) of GC. C) Details of mechanical stimulation. D) GC profile pre- (black) and post- (red) stimulation. Scale bar 10 μm.

GC collapsed within 20 secs. In 5 over 9 hippocampal GCs the collapse is followed by retraction (Figure 1B, white arrow) and turning (Figure 1B, red arrow). In these cases, the GC started re-growing into a new direction with an average angle of 30°.

We then analyzed the effect of the same stimulation, at the level of the hippocampal soma. Here, the physical stress results in local retraction of the cell edge with a main value of 2 μm.

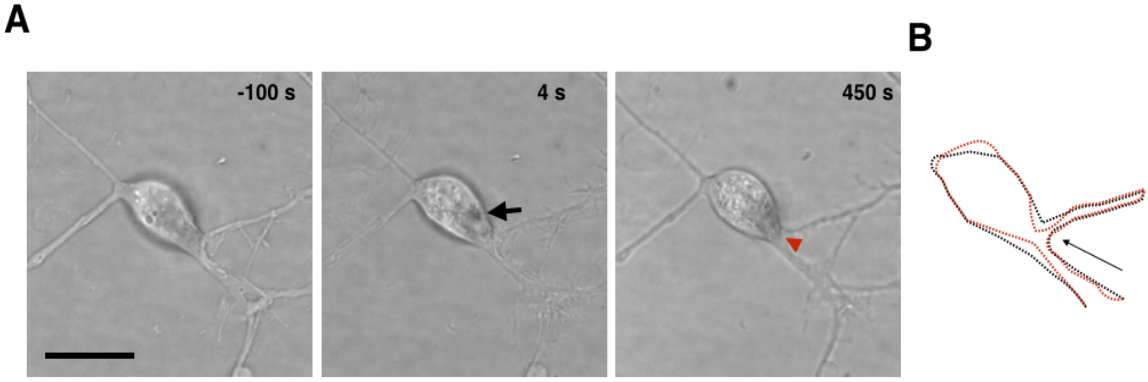

Figure 2 Response of Hippocampal soma to mechanical stimulation, composed by 6 sinusoidal wave at 1 Hz). A) Brightfield image of Hippocampal neuron and a trapped bead (black arrow) above the GC. The mechanical stress induces a localized retraction of soma (red arrow); B) Soma profile pre (black) and post (red) stimulation. Scale bar 10 μm

Mechanical indentation induces actin network remodelling

In order to see how the cytoskeletal actin network, reorganize its elves during mechanical indentation, we used both hippocampal neurons and NG108-15 cells expressing endogenous F-actin with fluorescent LifeAct. We found that the mechanical stimulation in the range of 10-20 pN leads to a rapid disruption and re-organization of the actin cytoskeleton. Firstly, we tested the actin network mechano-response at the level of the GC, using the NG108-15 cells as model for neurons. As shown in figure 3, the mechanical stress induces a rapid retraction of NG108-15 GC, with mean retraction amplitude of 4 μm (n=8). Interestingly, in 3 of 8 experiments, the retraction is followed by a retrograde flow of the actin in the adjacent cortical path (Figure 3B red arrow).

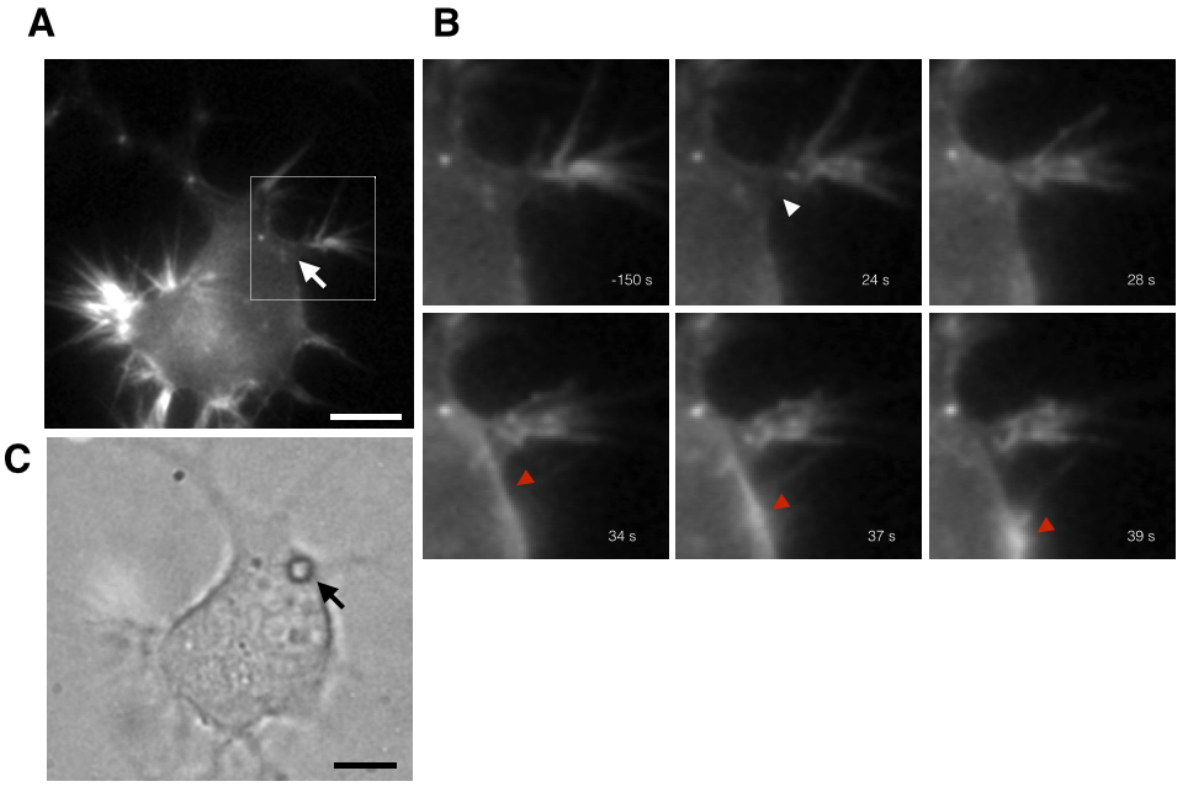

Figure 3. Response of NG108-15 GC expressing LifeAct-mcherry to mechanical indentation. A) Fluorescence image of the actin with white arrow that indicates the position of the bead and one ROI. B) Time course of actin dynamics: the actin network disappears (white arrow), then the GC retracts. After the retraction, the actin runs along the cortical paths (red arrows). C) Brightfield image of NG108-15 and trapped bead (black arrow). Scale bar 10 μm.

Next, we followed the actin dynamics in Hippocampal neurons soma. We report that the actin network gradually disappears in the indentation area during the

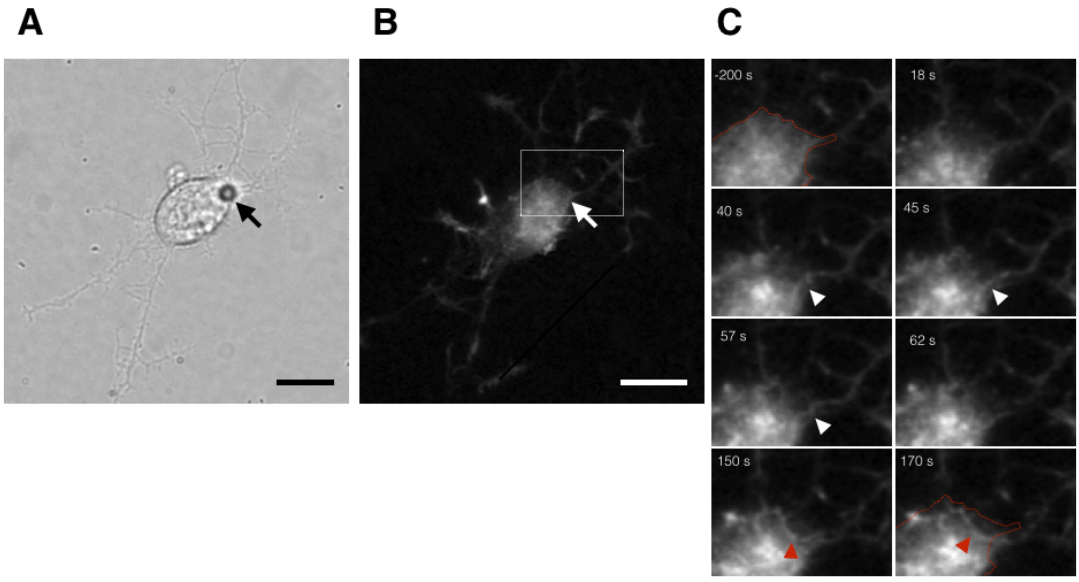

Figure 4. Response of Hippocampal soma to mechanical indentation. Cultured Hippocampal neuron expressing LifeAct-mcherry.A) and B) as A) and C) in Figure 3. C) Time course of actin dynamics upon mechanical stress; the actin network disappears (white arrow) at the site of mechanical indentation. Following the formation of new actin filament (white arrow), the soma retracts forming one actin arc (red arrow). Scale bar 10 μm

mechanical stimulation period. This event is followed by rearrangement of the actin network (Figure 4C, white arrow) and the formation of new actin arcs filaments (Figure 4C, red arrow) that reshape the edge soma morphology with an average retraction of 2 μm (n=6).

Ca^{2+} signaling evoked by mechanical stimulation

We proceed to analyze the Ca^{2+} mechano-response monitoring free intracellular calcium levels, using the calcium sensitive fluorescent dye Fluo-4. The weak mechanical stress application, composed by 1 pulse, to hippocampal soma caused a rapid rise in the intracellular Ca^{2+} concentration within 1 sec after force application. When we apply one mechanical stress the calcium elevation reaches at maximum DF/F value of 0.3% within 15 s, and then the concentration returns to the baseline in 20 sec (n=4).

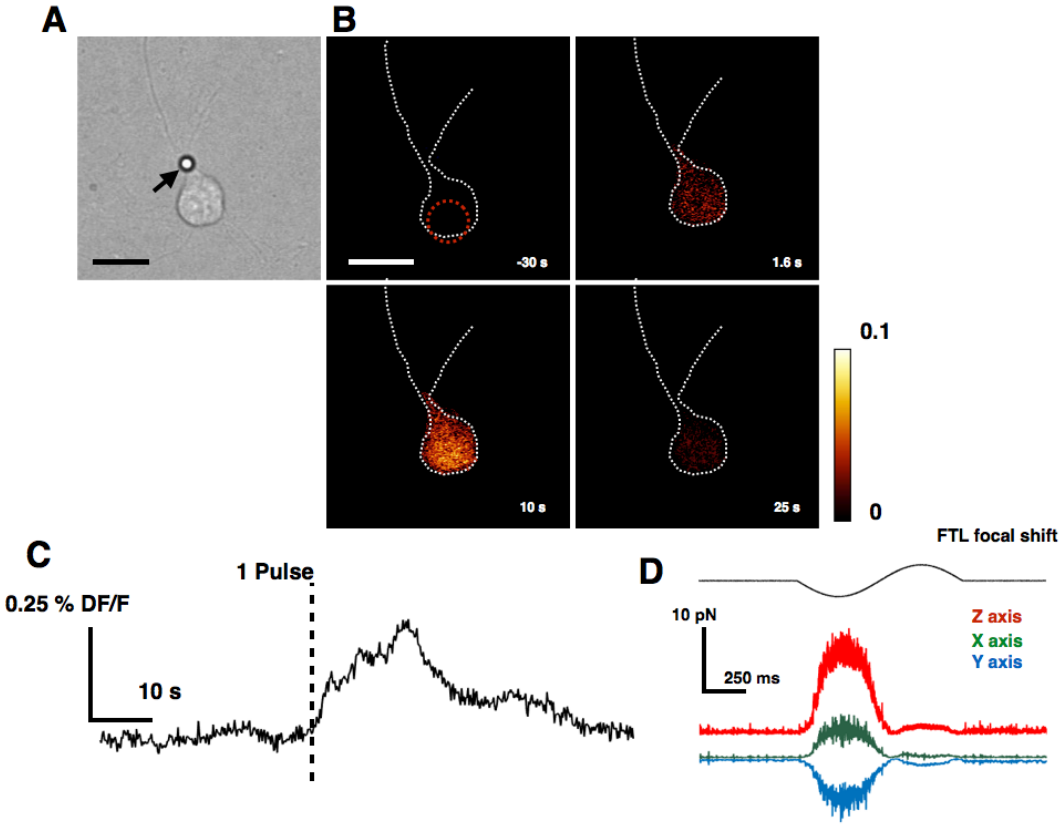

Figure 5. Calcium oscillation evoked by mechanical stimulation (1 Pulse). A) Brightfield image of hippocampal neuron and one trapped bead (black arrow). B) DF/F images of calcium concentration. C) Time course of calcium oscillation computed from the ROI (red dotted circle). D) Traces of the force components (F_z, F_x and F_y respectively in red, green and blue) during the stimulation period (upper trace: FTL focal shift). Scale bar 10 μm.

However, when we applied three consecutive mechanical pulses at frequency of 1Hz we observed a relative high and prolonged increase in the intracellular Ca^{2+} elevations with a mean DF/F peak of about 0.7%. Figure 4) In these experiments the Ca^{2+} response appears to be composed by a fast and local increase near the site of stimulation and a second component that spread toward the soma probably due the opening of voltage gated channel or release from the intracellular store, such the ER.

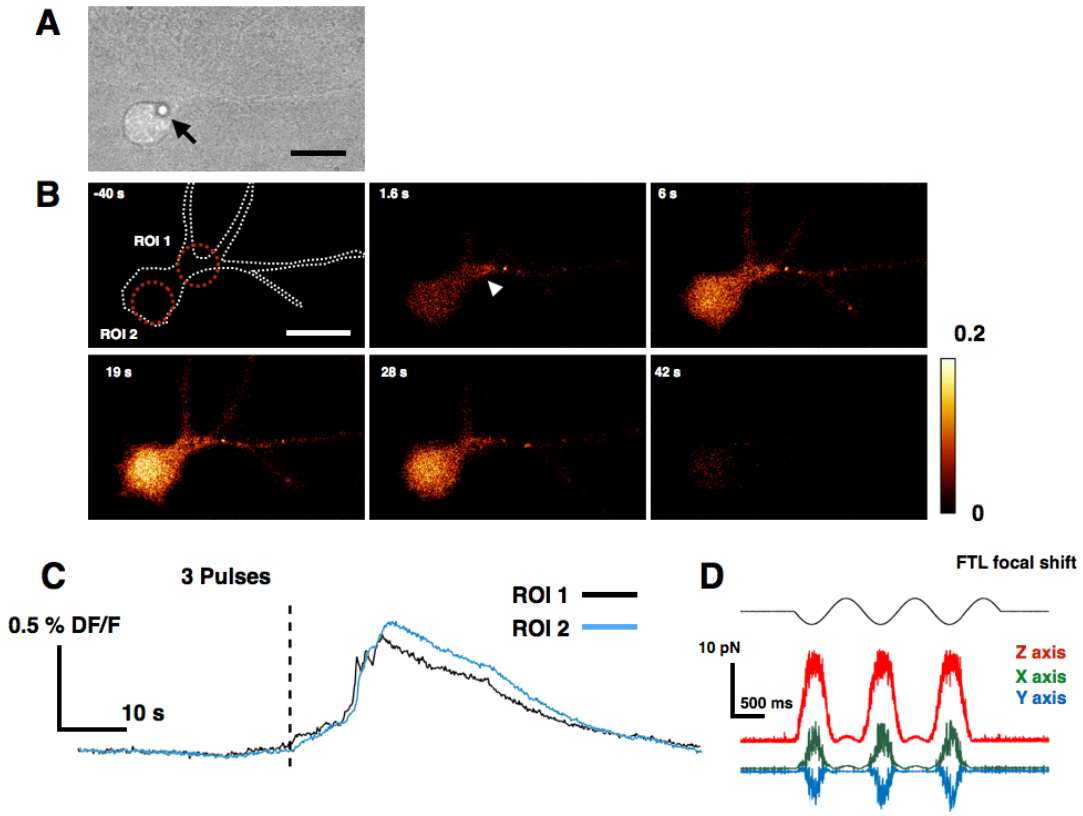

Figure 6. Calcium oscillation evoked by mechanical stimulation (3 Pulse). A) Brightfield image of Hippocampal neuron and one trapped bead (black arrow). B) DF/F images of intracellular calcium concentration. C) Time course of calcium oscillation from the two ROIs (red dotted circles). D) Traces of the force components (F_z, F_x and F_y respectively in red, green and blue) during the stimulation period (upper trace: FTL focal shift) Scale bar 10 µm.

RhoA GTPase activation mechanically induced

Next, in order to investigate the mechanism coupling mechanical stress to the cytoskeleton rearrangement, we followed the activity of a small GTPase protein RhoA, using intramolecular FRET sensor, in which two fluorophores are attached to both ends of the molecule. We found that the nano-indentation induces a rapid

activation of RhoA (Fig.3C and D). The RhoA activation reach a maximum peak in 10 secs and returns to basal level within 20 sec. These results are consistent with the findings of other groups, in which the RhoA has been shown be activated by mechanical stimulation.

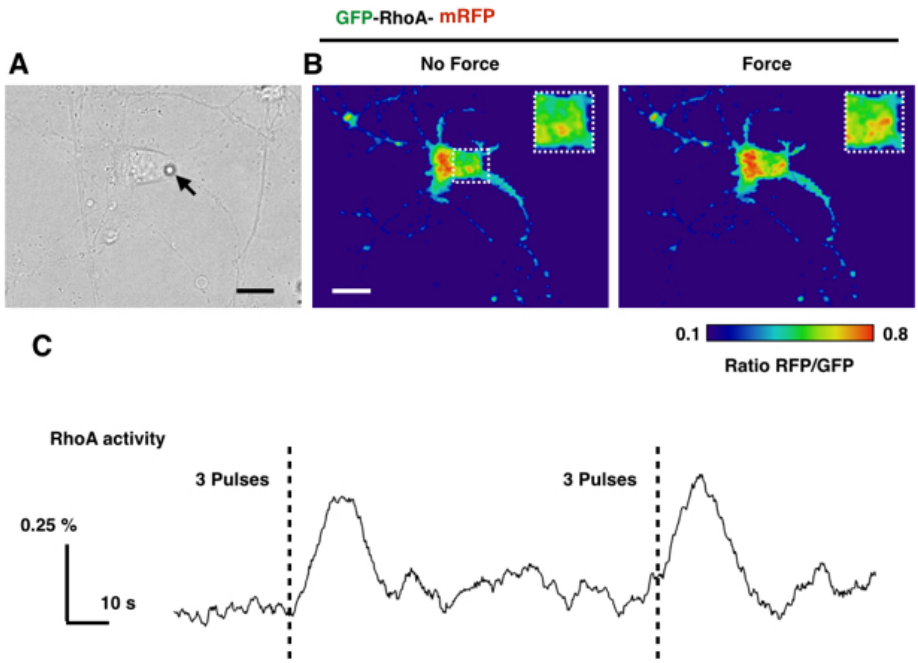

Figure 8. Effect of mechanical stimulation on the activation of RhoA detected by FRET imaging. A) Brightfield image showing a trapped bead (black arrow) above a hippocampal soma. B) Ratiometric images before and after (8 secs) stimulation with one ROI used to compute the FRET signal. C) Time course of the FRET signal. Dotted lines indicate the OT stimulation.

Piezo1 expression in Hippocampal culture

We have looked for the presence of the MSC Piezo 1 by immunohistochemistry in hippocampal neurons and we found a diffuse staining in the hippocampal cell culture. The Piezo 1 results expressed both in the soma and in the neurites (Fig.3B). Thus, Piezo 1 can be one of the master regulator for the mechanotransduction pathways in hippocampal neurons.

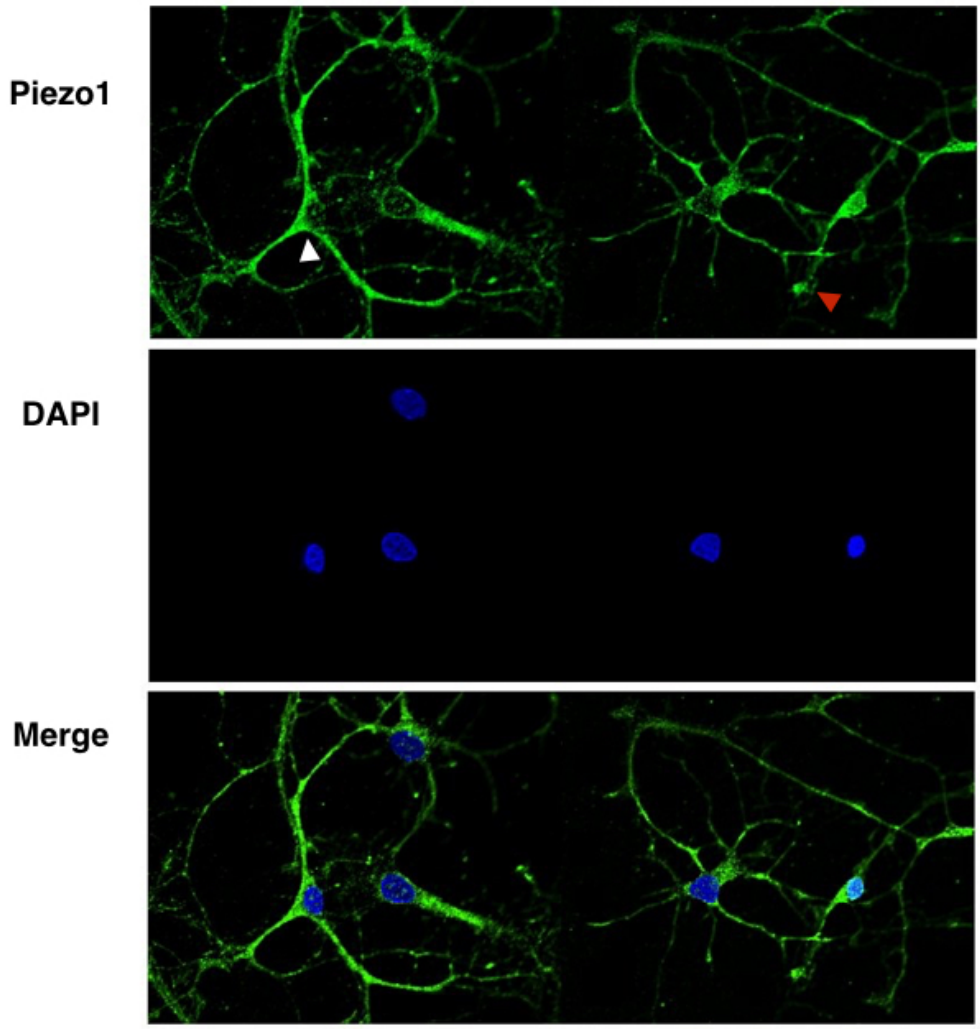

Figure7. Expression of Piezo 1 channels in Hippocampal neuron culture Neurons stained at 2 DIV with Piezo 1 antibody (green) and DAPI (blue). The Piezo1 channels are expressed both at the tip of neuronal process (red arrow) and soma (white arrow).

Conclusion

Our MS has two major conclusions: 1) mechanical signaling in hippocampal neurons is mediated by a biochemical pathway involving calcium dynamics and the activation of RhoA GTPase leading to a reorganization of the intracellular actin network within few minutes. 2) mechanical signaling, among neurons of the

central nervous system such as hippocampal neurons, occurs for weak forces – such as that exerted by a moving lamellipodium (Cojoc et al 2007) - and is likely to be ubiquitous in the whole brain.

References

1. Marshall, Kara L., and Ellen A. Lumpkin. “The Molecular Basis of Mechanosensory Transduction.” *Sensing in Nature*, edited by Carlos López-Larrea, vol. 739, Springer US, 2012, pp. 142–55. *Crossref*, doi:10.1007/978-1-4614-1704-0_9.
2. Franze, Kristian, et al. “Mechanics in Neuronal Development and Repair.” *Annual Review of Biomedical Engineering*, vol. 15, no. 1, July 2013, pp. 227–51. *Crossref*, doi:10.1146/annurev-bioeng-071811-150045.
3. Koser, David E., et al. “Mechanosensing Is Critical for Axon Growth in the Developing Brain.” *Nature Neuroscience*, vol. 19, no. 12, Dec. 2016, pp. 1592–98. *Crossref*, doi:10.1038/nn.4394.
4. Albuschies, Jörg, and Viola Vogel. “The Role of Filopodia in the Recognition of Nanotopographies.” *Scientific Reports*, vol. 3, no. 1, Dec. 2013. *Crossref*, doi:10.1038/srep01658.
5. Franze, Kristian, et al. “Neurite Branch Retraction Is Caused by a Threshold-Dependent Mechanical Impact.” *Biophysical Journal*, vol. 97, no. 7, Oct. 2009, pp. 1883–90. *Crossref*, doi:10.1016/j.bpj.2009.07.033.
6. Anava, Sarit, et al. “The Regulative Role of Neurite Mechanical Tension in Network Development.” *Biophysical Journal*, vol. 96, no. 4, Feb. 2009, pp. 1661–70. *Crossref*, doi:10.1016/j.bpj.2008.10.058.
7. Hanein, Y., et al. “Neuronal Soma Migration Is Determined by Neurite Tension.” *Neuroscience*, vol. 172, Jan. 2011, pp. 572–79. *Crossref*, doi:10.1016/j.neuroscience.2010.10.022.
8. Petridou, Nicoletta., Spiró, Zoltán and Heisenberg Carl-Philipp .” Multiscale force sensing in development” *Nature Cell Biology,* vol 19, no. 6, june 2017
9. Rangamani, Padmini, et al. “Paradoxical Signaling Regulates Structural Plasticity in Dendritic Spines.” *Proceedings of the National Academy of Sciences*, vol. 113, no. 36, Sept. 2016, pp. E5298–307. *Crossref*, doi:10.1073/pnas.1610391113.

10. Etienne-Manneville, Sandrine, and Alan Hall. “Rho GTPases in Cell Biology.” *Nature*, vol. 420, no. 6916, Dec. 2002, pp. 629–35. *Crossref*, doi:10.1038/nature01148.
11. Hoon, Jing Ling, et al. “The Regulation of Cellular Responses to Mechanical Cues by Rho GTPases.” *Cells*, vol. 5, no. 2, Apr. 2016. *PubMed*, doi:10.3390/cells5020017.
12. Haws, Hillary J., et al. “Control of Cell Mechanics by RhoA and Calcium Fluxes during Epithelial Scattering.” *Tissue Barriers*, vol. 4, no. 3, July 2016, p. e1187326. *Crossref*, doi:10.1080/21688370.2016.1187326.
13. McBeath, Rowena, et al. “Cell Shape, Cytoskeletal Tension, and RhoA Regulate Stem Cell Lineage Commitment.” *Developmental Cell*, vol. 6, no. 4, Apr. 2004, pp. 483–95. *Crossref*, doi:10.1016/S1534-5807(04)00075-9.
14. Yuan, Ying, et al. “The Role of the RhoA/ROCK Signaling Pathway in Mechanical Strain-Induced Scleral Myofibroblast Differentiation.” *Investigative Opthalmology & Visual Science*, vol. 59, no. 8, July 2018, p. 3619. *Crossref*, doi:10.1167/iovs.17-23580.
15. Julian, Linda, and Michael F. Olson. “Rho-Associated Coiled-Coil Containing Kinases (ROCK): Structure, Regulation, and Functions.” *Small GTPases*, vol. 5, no. 2, Apr. 2014, p. e29846. *Crossref*, doi:10.4161/sgtp.29846.

Integrating Optical Tweezers with Patch-Clamp Electrophysiology

FABIO FALLERONI, ULISSE BOCCHERO, YUNZHEN LI, VINCENT TORRE, AND DAN COJOC

Abstract

Neuronal activity is not solely influenced by chemical and electrical factors, mechanical stimulation can also modulate neuronal excitability and signaling. Here we have integrated mechanical stimulation of the cell membrane using a pulsing optical tweezers with patch-clamp, to measure the electric effects on neuronal cells. The forces are applied by axially displacing a trapped bead with an electrical tunable lens (ETL) and measured in Z directions by back focal plane (BFP) interferometry on a quadrant photo diode (QPD). The electrical activity of the cell is monitored in cell voltage clamp by measuring the ion currents. We demonstrate, both for primary hippocampal cells and NG108-15 cells, that stimulation with piconewton forces is enough to regulate the ion currents through the cell membrane.

Introduction

Mechanotransduction studies how cells sense physical forces and the cellular signal transduction in response to mechanical stimuli[1]. Cells perceive force through a variety of molecular sensors, of which the mechanosensitive ion channels are the most efficient and act the fastest[2]. Tension in the membrane alters the probability of channel opening and leads to an influx of ions[3]. Patch-clamp (PC) is a traditional technique to study the electrical activity of living neurons, with the goal to unravel the molecular and cellular processes that govern their signaling induced by different stimuli.

PC versatility allows measuring currents through single ion channels or whole-cell recordings, with sub millisecond temporal resolution[4]. The whole-cell variation in combination with voltage clamp allows direct electrical control of the cell transmembrane potential[5].

Recently we have developed an oscillatory optical tweezers to apply piconewton forces perpendicularly to the cell membrane and demonstrated that also these small forces can trigger cellular calcium transients[6] by fluorescence imaging. Optical tweezers have been also proposed to pull tether membranes[7] or to stretch actin stress fibers[8]. Here we demonstrate the integration of the patch-clamp with a pulsed optical tweezers, showing that piconewton forces applied vertically on the cell membrane induce detectable ion currents.

The force is applied by a trapped bead in a pulsed-oscillatory optical trap. By using a focus tunable lens (FTL), the trap position can be precisely and fast moved vertically in a range of 12 um, while the 3D position of the bead is measured by back focal plane (BPF) interferometry using a quadrant photo detector (QPD)[9].

The ability to measure the applied force and the membrane indentation during the experiment and correlate these quantities with the ionic currents passing through the cell membrane, in our approach, might be essential in understanding the function of the mechanical sensors, especially regarding the MSCs. Here, we demonstrate the capability of the system in mouse neuroblastoma NG 108-15 cells and mouse hippocampal neurons.

Material and methods

Hippocampal cell culture

Hippocampal neurons were dissected from Wistar rat brain (P1-P2). After decapitation the meninge-free hippocampi were incubated with 5 mg/ml trypsin (Sigma) and 0.75 mg/ml DNase I (Sigma) for 5 minutes at room temperature for the enzymatic dissociation.

Then trypsin was neutralized by 1 mg/ml trypsin inhibitor (Sigma) and a mechanical dissociation was performed with a Pasteur pipette. The cell suspension was then centrifuged at 100 G for 5 min, and the pellet was re-suspended.

Finally, hippocampal neurons were plated on coverslip coated with 50 µg/ml poly-L-ornithine (Sigma). The hippocampal cultures were incubated (95% O2, 5% CO2 at 37 °C) for 4-6 days in Neurobasal medium (Sigma) containing 25 µm GlutaMAX (Thermo Fisher Scientific) and B27 supplement at 2% (Sigma).

Cell were used for experiment after 5-6 days in culture. All experimental procedure on animals were done in accordance with the European Communities Council Directive of November 2016 (86/609/EEC).

Ng108-15 cell culture

Mouse neuroblastoma x rat glioma hybrid (NG108-15) cells were obtained from Sigma-Aldrich. The cells were cultured as described in Falleroni 2018[6].

Mechanical cell stimulation and current recording experimental approach

To mechanically stimulate **a** bead was trapped and positioned above the cell of interest (label 1 in Figure 1A and left image in Figure 1B) by an infrared trapping laser (1064 nm, max 5W, cw, IPG Photonics, US).
Then we used a manual micromanipulator to move vertically the patch clamp pipette in contact with the cell membrane. After reaching a seal between the membrane and the electrode of more than 1 GΩ resistance, we applied a gentle suction to break the membrane patch in order to enter in whole-cell configuration. Whole-cell currents were recorded using borosilicate glass pipette (Blaubrand, intramark micropipette, Germany) with a resistance of 2-5 M Ω filled with intracellular solution containing (in mM): 10 NaCl, 140 KCl, 1 MgCl2, 5 EGTA and 10 HEPES.
To confirm the integrity of the whole-cell configuration, we induced voltage gated Na^+ and K^+ currents by depolarizing the cell with voltage steps from -80 mV to + 80 mV (10 mV increments). Figure 1C display an example of such recording.
The negative portion of the current, at the beginning of the traces, is an inward Na^+ current, while the positive part immediately after evidenced an outward K^+ currents.
Then, we proceeded with the simultaneous cell mechanical stimulation with forces in the range of 5-20 pN and the characterization of the responses in the whole-cell configuration.
The mechanical stimulation is achieved as described in the our previous article[6].

For all experiments, the cells were bathed in an extracellular ringer solution containing in mM 140 NaCl, 2.8 KCl, 1 $MgCl_2$, 2 $CaCl_2$ and 10 HEPES and maintained at an holding potential of -80 mV.

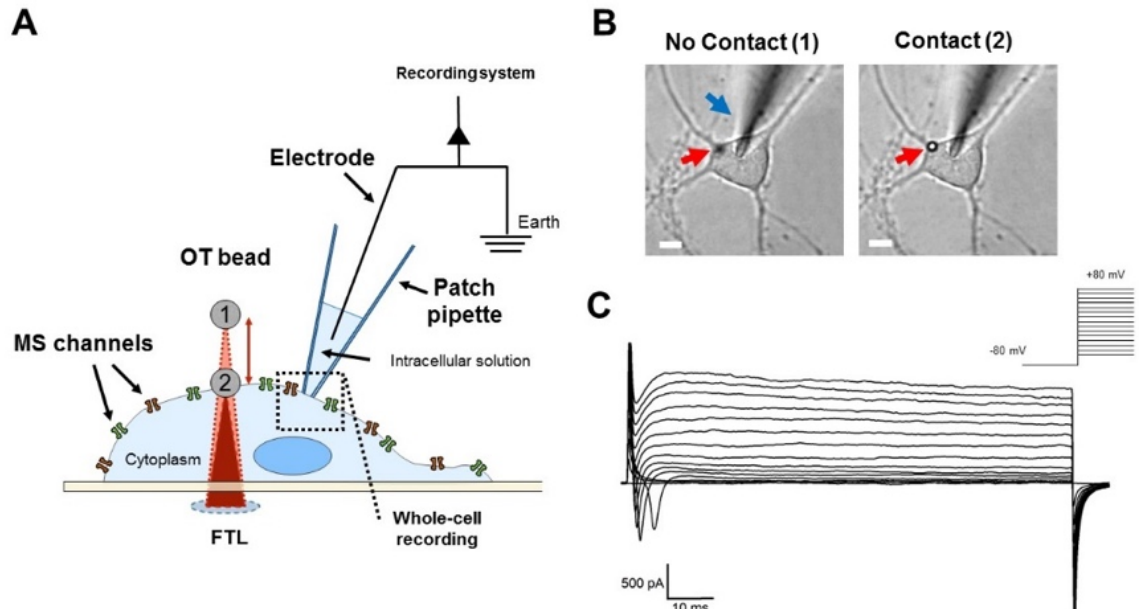

Figure 1. Schematic of the integrated patch-clamp current recording with the pulsed optical tweezers mechanical stimulation. **(A)** Scheme of the mechanical stimulation using an optically trapped (OT) bead positioned first above the cell (label 1) and then moved in contact to the cell membrane (label 2) by means of the Focused Tunable Lens (FTL) and schematic of the patch-clamp approach. **(B)** Image of a hippocampal neuron approached by the patch pipette (blue arrow) and the trapped bead (red arrows) above the cell (1) and in contact with the cell membrane (2). **(C)** Example of recorded Na^+ and K^+ currents in whole cell configuration.

The combined patch-clamp -- optical tweezers setup

The integrated patch-clamp with pulsed/oscillatory optical tweezers setup is shown in Figure 2. The system was built on an inverted microscope (IX81, Olympus), to which tree custom modules were adapted: Oscillatory optical trap (OOT), Force detection module (FD) and the Electrophysiology module (EP) (see Figure 2).The sample chamber is imaged in brightfield by the microscope lens MO (60X, NA 1.4 oil immersion, Olympus) and through the tube lens, TL on the CCD camera (Orca D2, Hamamatsu). The pulsed/oscillatory optical tweezers (OOT) was designed and built as described in our recent paper[6]. Briefly, the trapping laser is an ytterbium continuous wave fiber laser operating at 1064 nm (IPG Laser GmbH). The laser beam is directed toward a custom collimator (L1, L2 f1=f2= 100 mm) to fit the size of the FTL (fFTL= 55-90 mm) and a third

convergent lens (L3, f3=150 mm) is used to size the diameter of the beam such that it overfills the entrance pupil of the microscope lens and ensure efficient trapping.

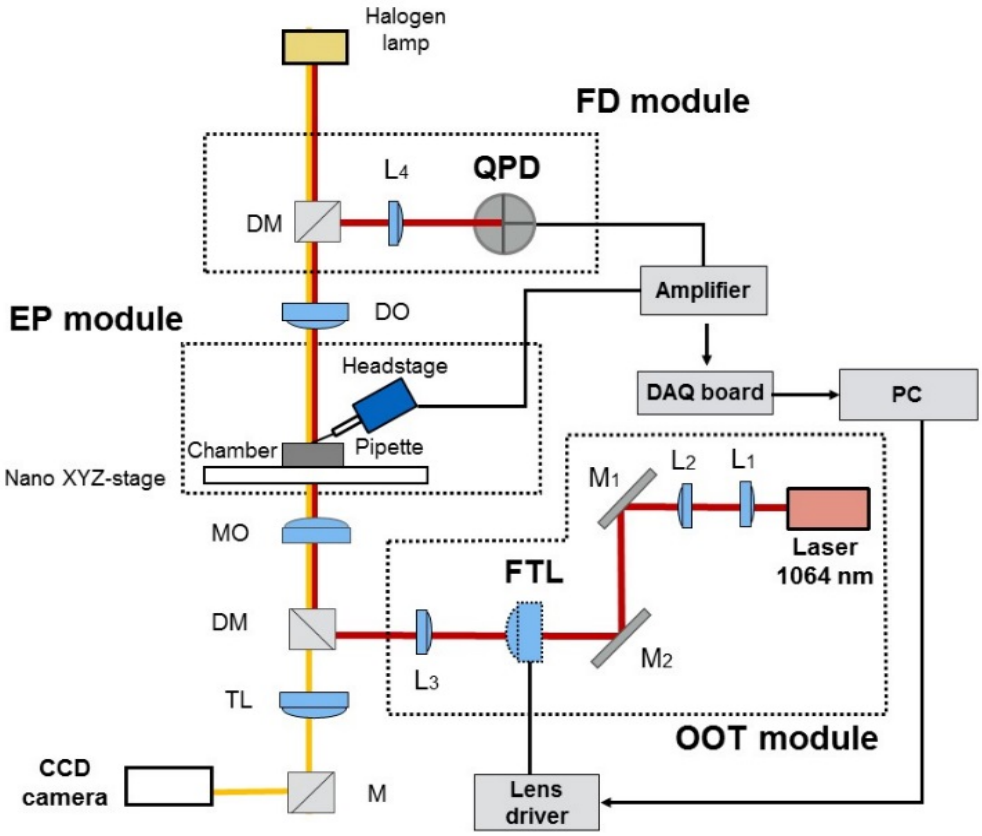

Figure 2. Integrated patch clamp – optical tweezers cell stimulation and force detection setup. The cell is imaged in brightfield on the CCD camera (yellow optical path).
OOT: Oscillatory Optical Tweezers; FTL: Focus Tunable Lens. **FD**: Force Detection; QPD: Quadrant Photo Diode. **EP**: Electrophysiology patch-clamp.
L_1, L_2, L_3, L_4: convergent Lenses; DM: Dichroic Mirrors; MO: Microscope Objective lens; DO: detection objective lens; TL: Tube Lens; M_1, M_2: mirrors

The position of the trap above the coverslip of the sample chamber is is determined by the focal lengths of the four lenses (f1, f2, fFTL and f3) used for collimation, the focal length of the microscope lens, fMO and the relative distances between these components. We designed the configuration to obtain a trap shift of 12 um up from the initial position (2-3 um above the coverslip), linearly with a variation of the fFTL from 55 to 90 mm.

Details on the design and calibration (trap shift vs driver current FTL) of the system are given in[6]. The driver current and hence the focal length of the FTL are

computer controlled by a custom LabView code. With the laser operating at 250 mW, the average power at the sample plane is 25 mW, allowing an axial trap stiffness K_{ot} ~ 0.03 pN/nm. The trap stiffness can be strengthened up to K_{ot} ~ 0.06 pN/nm increasing the laser power by a factor of two (500 mW).

The wavelength of the laser and the output power were chosen to minimize heating and photodamage of the sample. In our previous article[6] we demonstrated the absence of damaging effects of the 1064 nm infrared laser on calcium dynamics in the NG108-15. Measurement of the force of interaction between the bead and the cell membrane and the indentation of the cell membrane are enabled by the force detection (FD) module, using the principle of BFP interferometry.

The laser light scattered by the bead and sample is captured by detection objective lens (Olympus, 10X NA 0.3) and the interference pattern formed in the BFP is projected by the convergent lens L4 (f4= 40 mm) onto the QPD, (PDQ80A, Thorlabs). The electric signals coming from the QPD are amplified and then digitized by an analog-to-digital data acquisition (DAQ card, PCI-4462, National Instrument). The FD module allows to measure axial forces in the range: [0 - 20] pN.

The Electrophysiology setup (EP module) was composed by a patch clamp head stage (PH, CV 201, Axon Instruments) that was mounted onto a manual micromanipulator. Then the signal from the EP module were amplified (Axopatch 200, Axon instruments Inc.) and converted to differential outputs digitized at 10 kHz through a Digidata converter card (Digidata 1440, Molecular Device).

Experimental results and discussion

The mechanical stimulation was performed applying a sinusoidal waveform to FTL to produce an axial indentation on the cell membrane. In all experiments we applied a sinusoidal signal with amplitude A= 2 μm and frequency f= 1 Hz. Preliminary experiments on hippocampal neurons and Ng108-15 cells revealed that the application of mechanical stress in the range of 5-20 pN induced detectable currents.

Testing the protocol on primary neurons, such hippocampal neurons, was fundamental in order to understand if also these cells, obtained from the central

nervous system of a mouse, were mechanosensitive. These hippocampal neurons displayed mechano-responses based on the increase of intracellular Ca^{2+} right after the stimulation, as evidenced in our previous work in which we used Fluo-4 AM calcium dye. Figure 3 display an example of a hippocampal neuron during the application of a mechanical stimulus of about 14 pN. In this case, we detected a current subsequent to the stimulus with an amplitude of approximately 65 pA. In this case the onset of the current corresponds to the beginning of the mechanical stimulus. Using the same protocol, we tested the

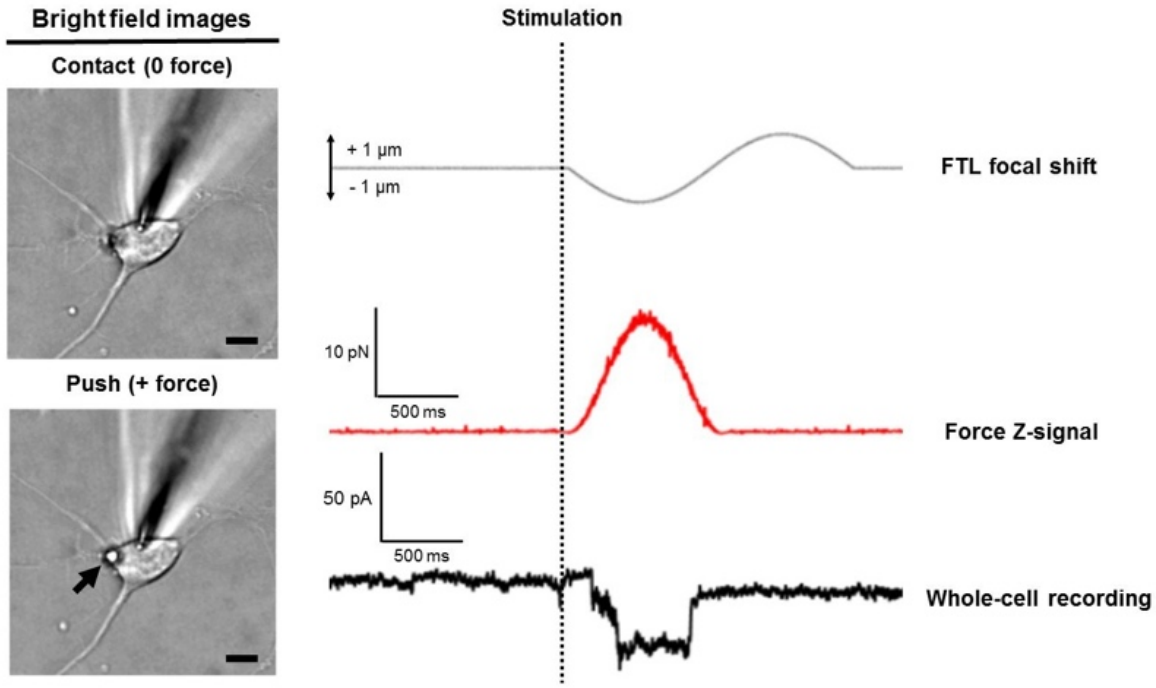

Figure 3. Force and current recordings during the application of a mechanical stimulus to a hippocampal neuron. The two bright field images display the position of the bead. The first one is in the contact position **(0 force)** during which no force was applied to the cell. The second one shows a gentle push **(+ force)** during which a force of approximately 12 pN was applied to the cell membrane. The force applied in this case was approximately of 14 pN. The amplitude of the recorded current was 65 pA. **FTL focal shift** gray trace indicates the variation of the focal length; **Force Z-signal** red trace indicates the strength applied through the bead to the cell membrane; **Whole-cell recording** black trace indicates the current variation due to the mechanical stimulus. Scale bar 10 µm.

possible effect on NG108-15 cells, as displayed in Figure 4 . Here the mechanical stimulation induces a current with a mean amplitude of ~27 pA. In this experiment, the peak of force (force z-signal in red) of the mechanical stimulus corresponds to the onset of the current.

The variability of the delay between the beginning of the mechanical stimulation (contact bead-cell) and the current is probably do to the nature of the stimulus, which in our case is a very gentle pressure, approximately 0.020 mmHg, applied to the cell membrane [6]. Indeed, the opening of very few channels may be more stochastic with these range of forces, if compared to the responses obtained with higher forces stimuli applied with different setups[11,12]. Therefore, we need to perform more experiments in order to have a clearer view of the dependence between our type of stimuli and the elicited currents.

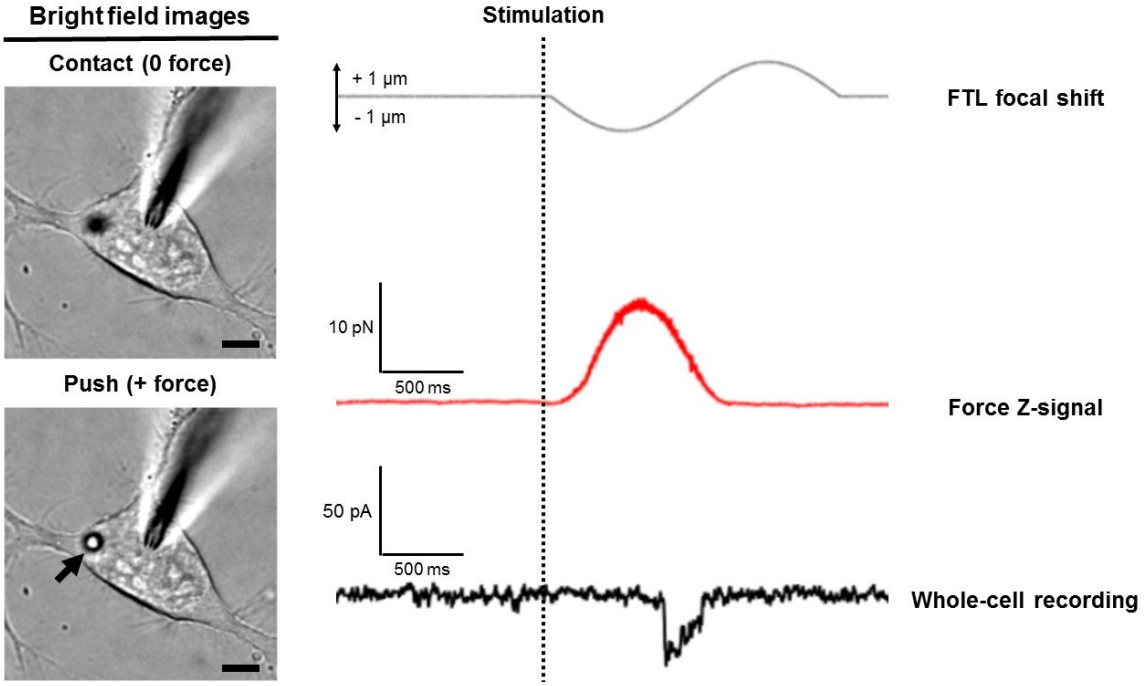

Figure 4. Force and current recordings during the application of a mechanical stimulus to a NG108-15 cell. As in **Figure 3**, the two bright field images display the position of the bead. The amplitude of the recorded current was 38 pA. **FTL focal shift** gray trace indicates the variation of the focal length; **Force Z-signal** red trace indicates the strength applied through the bead to the cell membrane; **Whole-cell recording** black trace indicates the current variation due to the mechanical stimulus. Scale bar 10 µm.

Conclusion

We presented a new method to apply weak forces in the 5-20 pN range vertically to cell membrane, by using an FTL, while simultaneously monitoring the electrophysiological response. The FTL allow us to change the focus of the trapping plane axially. To our knowledge, this is the first application of focus

(electrically) tunable lens (FTL) in optical trapping and manipulation. Its integration with patch-clamp electrophysiology opens new opportunities to study mechanotransduction in neuronal cells. Previous applications of the FTL included laser material processing, high speed microscopy and imaging for laparoscopic fluorescence-guided surgery [13-15]. As a proof of principle, the whole-cell mechano-response was studied on the NG108-15 cells and Hippocampal neurons. These preliminary experiments suggest that pN forces may induce detectable currents across the plasma membrane in whole cell PC configuration. The future experiments will be performed to characterize quantitatively the response of the neuronal cells. Indeed, further investigations are needed to confirm and understand the nature of these currents, using specific ionic concentrations in the bath and in the pipet solution, as well as specific blockers for the mechanosensitive channels.

References

1) Marshall, Kara L., and Ellen A. Lumpkin. “The Molecular Basis of Mechanosensory Transduction.” *Sensing in Nature*, edited by Carlos López-Larrea, vol. 739, Springer US, 2012, pp. 142–55. *Crossref*, doi:10.1007/978-1-4614-1704-0_9.
2) Orr, A. Wayne, et al. “Mechanisms of Mechanotransduction.” *Developmental Cell*, vol. 10, no. 1, Jan. 2006, pp. 11–20. *Crossref*, doi:10.1016/j.devcel.2005.12.006.
3) Sukharev, Sergei, and Frederick Sachs. “Molecular Force Transduction by Ion Channels – Diversity and Unifying Principles.” *Journal of Cell Science*, vol. 125, no. 13, July 2012, pp. 3075–83. *Crossref*, doi:10.1242/jcs.092353.
4) Sakmann, B., and E. Neher. “Patch Clamp Techniques for Studying Ionic Channels in Excitable Membranes.” *Annual Review of Physiology*, vol. 46, no. 1, Oct. 1984, pp. 455–72. *Crossref*, doi:10.1146/annurev.ph.46.030184.002323.
5) Hamill, O. P., et al. “Improved Patch-Clamp Techniques for High-Resolution Current Recording from Cells and Cell-Free Membrane Patches.” *Pflugers Archiv: European Journal of Physiology*, vol. 391, no. 2, Aug. 1981, pp. 85–100.
6) Falleroni, Fabio, et al. “Cell Mechanotransduction With Piconewton Forces Applied by Optical Tweezers.” *Frontiers in Cellular Neuroscience*, vol. 12, May 2018. *Crossref*, doi:10.3389/fncel.2018.00130.
7) Brownell, William E., et al. “Cell Membrane Tethers Generate Mechanical Force in Response to Electrical Stimulation.” *Biophysical Journal*, vol. 99, no. 3, Aug. 2010, pp. 845–52. *PubMed*, doi:10.1016/j.bpj.2010.05.025.
8) K. Hayakawa, H. Tatsumi, and M. Sokabe, "Actin stress fibers transmit and focus force to activate mechanosensitive channels," J Cell Sci **121**, 496-503 (2008).

9) Neuman, Keir C., and Steven M. Block. “Optical Trapping.” *The Review of Scientific Instruments*, vol. 75, no. 9, Sept. 2004, pp. 2787–809. *PubMed*, doi:10.1063/1.1785844.

10) B. Coste, S. E. Murthy, J. Mathur, M. Schmidt, Y. Mechioukhi, P. Delmas, and A. Patapoutian, "Piezo1 ion channel pore properties are dictated by C-terminal region," Nat Commun **6**, 7223 (2015).

11) B. Coste, J. Mathur, M. Schmidt, T. J. Earley, S. Ranade, M. J. Petrus, A. E. Dubin, and A. Patapoutian, "Piezo1 and Piezo2 are essential components of distinct mechanically activated cation channels," Science **330**, 55-60 (2010).

12) Eberle, G., et al. “Simulation and Realization of a Focus Shifting Unit Using a Tunable Lens for 3D Laser Material Processing.” *Physics Procedia*, vol. 41, 2013, pp. 441–47. *Crossref*, doi:10.1016/j.phpro.2013.03.100.

13) Jiang, Jun, et al. “Fast 3-D Temporal Focusing Microscopy Using an Electrically Tunable Lens.” *Optics Express*, vol. 23, no. 19, Sept. 2015, p. 24362. *Crossref*, doi:10.1364/OE.23.024362.

14) Nakai, Yuichiro, et al. “High-Speed Microscopy with an Electrically Tunable Lens to Image the Dynamics of *in Vivo* Molecular Complexes.” *Review of Scientific Instruments*, vol. 86, no. 1, Jan. 2015, p. 013707. *Crossref*, doi:10.1063/1.4905330.

15) Volpi, Davide, et al. “Electrically Tunable Fluidic Lens Imaging System for Laparoscopic Fluorescence-Guided Surgery.” *Biomedical Optics Express*, vol. 8, no. 7, July 2017, pp. 3232–47. *PubMed*, doi:10.1364/BOE.8.003232.

DISCUSSION

Despite recent studies, the way mechanical input is translated into an intracellular biochemical response is currently not well defined. It is well known that mechanical stimulation can affect the activity of ion channels on a milliseconds time scale. A rapid rise in intracellular ion concentrations can depolarize the membrane, open-voltage gate-dependent channels, and the ions themselves can function as secondary messengers, giving to MSCs the ability to convert local mechanical events into global cellular events.

Even though several methods were implemented to study the cellular mechanotransduction during the past years, they do not provide a precise measurement of the applied force; furthermore, they apply forces mainly in the range from nN to mN. The goal of this thesis is to study the effect of weak mechanical stimulation in the range of 5-20 pN, a physical level that cells experience *in vivo*[1,2], applied by optical tweezers on the neuronal physiology. In order to exert controlled mechanical stimulations in the pN range, we established a new method using an optical tweezers with a polystyrene microbead in an oscillatory optical trap. In this way it is possible to touch the cells in the vertical direction and analyze the morphological and biochemical responses to forces[3].

We first explored the possible mechanical-activated calcium response in neuroblastoma cell NG108-15. These cells are an excellent model of neuron since they have morphological, electrophysiological and pharmacological neuronal properties[4,5]. Our results demonstrate that the mechanical stimulation produces an early and local rapid rise in intracellular Ca^{2+} concentration, followed by larger calcium wave, likely due to the release of calcium from internal store and/or delayed opening of additional calcium permeable ionic channels. These results agree with studies showing that mechanical stress opens different mechanically gated machinery, through which Ca^{2+} enters and is critical for triggering intracellular Ca^{2+} release[6]. In fact, an interesting aspect of mechanotransduction, that contrasts with other canonical biochemical signal transduction pathways, is the various responses that can be achieved with a seemingly uniform stimulus: force. This is possible partly because cells experience force of great range in magnitude and time scale or frequency[7]. The calcium pathway and its modulation may be a fine transducer of forces at different magnitude scales. Our study demonstrates that the mechanically activated Ca^{2+}

oscillations in the Ng108-15 cells are dependent on the stimulus strength and number of pulses.

Furthermore, we have found a negative cell adaptation to the repetitive mechanical stimulation at low frequency. This is likely due to a failure in opening of calcium ion channels, both in the plasma membrane and internal stores, due to inactivation mechanism; but this also suggests that there may be an appropriate frequency towards which mechanical stimulations need to be applied to induce an effective mechanotransduction response[8].

In order to verify whether the fast and initial calcium increase is caused by the opening of MSCs in the plasma membrane or is produced by other pathways, we analyzed the effect of the mechanosensitive channels inhibitor GSMTX-4. This is known to modify the gate of MSCs, penetrating inside the membrane at the interface between the MSC and the lipid membrane[9].

Indeed, it is clear that in the mechanotransduction there is not only singer master able to induce the response. At the molecular level the list of cellular components that can be affected by mechanical forces includes, beyond the MSCs, different kinds of element, such as cell adhesion molecules (integrins and cadherins), G-protein coupled receptors, focal adhesion kinase and the nucleus itself[10-14]. For instance, applied tension trough intergrin-bound magnetic particle has been observed to induce Ca^{2+} spikes[15].

We found that intracellular Ca^{2+} increase was significantly diminished and often abolished, suggesting an involvement of the MCSs. The effective presence has been confirmed by immunohistochemistry techniques, showing a relative high native expression of Piezo1 in the NG108-15 cells.

In the second study, we analyzed in detail the mechanotransduction pathway at the level of central nervous system, using hippocampal neurons. The response of nervous cells to mechanical stimuli is particularly interesting, considering their environment. Adult brain is mechanically in-homogeneous with stiffness region-dependent and development-stage-dependent and the mechanics could effectively influence the neuronal development and physiology[16,17]. As a confirmation of that, neuronal stem cells (NSCs), isolated from the SVZ, preferably differentiate into neurons on soft substrate (0.1-1kPa), whereas cells on substrate of increased stiffness favor the differentiation into glia lineage, downregulating neuronal markers[18]. These results highlight that mechanical

cues, such as substrate stiffness, can act as driving force for neuronal differentiation. Therefore, many aspects of axonal growth have been examined in the context of mechanical force. For instance, it has been showed that in addition to biochemical cues, Growth cones (GCs) are susceptible to mechanical stimuli[19,20]. We found that weak mechanical forces in the range of 5-20 pN applied to growth cones of hippocampal neurons induce a repulsive turning. In particular, the mechanical stress seems to act as repulsive molecules, such as the Sema3A and ephrin-A2, inducing a rapid collapse of GC, followed by axon retraction and eventually steering. In line with these observations it has been demonstrated that local mechanical stress application applied by AFM to GC caused a Ca^{2+} influx through MSCs, with subsequent neurite retraction and direction-changing. The calcium ion flux triggers growth cone collapse and neurite retraction by increasing its contractility and/or by destabilizing its focal adhesions[20]. We found also that the same forces applied to the soma evoke its shrinkage.

Following the actin dynamics, by using live cell imaging, we observed that the mechanical stress in the pN range induces a rapid and localized disruption of the F-actin cytoskeletal network. Considering the time-scale, we suggest that this disruption could be related directly to a physical event without any molecular pathways. Interestingly, it has been shown that the average force, at which the single actin filaments broke up *in vitro*, is about 25 pN[21]. Then, this physical perturbation is followed by a retraction and re-modelling of the actin cytoskeleton, both at the level of GC and soma, in which the mechanotransduction pathway could play a key role.

Interestingly, after mechanical indentation, in some cases we observed that the retraction is followed by a retrograde flow of the actin in the adjacent cortical pathway, suggesting a feedback mechanism through which the actin can modulate both the retraction and the mechanotransduction pathway[22].

To explore the molecular mechanotransduction pathway activated by pN forces, we investigated changes in the intracellular Ca^{2+} concentration, using the calcium dye Fluo-4. Our results demonstrate that the OT stress application to the hippocampal plasma membrane causes a rapid rise of the Ca^{2+} within the neurons. In particular, the application of a single mechanical indentation results

in a calcium elevation, which reaches a maximum mean DF/F value of 0.3% within 15 s, and then the concentration returns to the baseline in 20 s (n=4).
However, when we applied three consecutive mechanical pulses at frequency of 1Hz, we observed a relative higher and more prolonged increase of the intracellular Ca^{2+} concentration with a mean DF/F peak of about 0.7%, which returned to baseline within 30-50 s. Here, the intracellular Ca^{2+} elevation is composed by a fast and localized increase near the site of stimulation and a second component that spread toward the entire neurons. These results suggest how the hippocampal neurons can be highly sensitive to the different mechanical stimulations, such as the number of pulses, activating Ca^{2+} responses, which varies in amplitude.
In order to investigate the mechanism coupling mechanical stress and Ca^{2+} to the cytoskeleton contractility that we had observed, we transfected hippocampal neurons with the RhoA GTPase intramolecular FRET sensor. Indeed, as previously reported the Ca^{2+}-mechano activated signal may regulate the cytoskeleton dynamics via activation of Rho GTPase signaling[23]. The Ca^{2+} can regulate cytoskeletal reorganization and contractility by activating Rho signaling trough the calcium sensor-proteins, such as the CAMKII and the tyrosine kinase pyk2[24]. In the mechanotransduction context, recent data suggest that RhoA is a central downstream effector that mediates the actin contraction[25]. For instance, it appears that stiffer tissue inhibits neurogenesis through a calcium mediated pathway with increased activity of RhoA and contractility, as dominant-negative RhoA prevents stiffness-induced neurogenic suppression, both *in vitro* and *in vivo*[26]. RhoA primarily acts upon the regulatory protein Rho-associated, the protein kinase ROCK[27]. The ROCK activation promotes myosin II activity by elevating the phosphorylation of the regulatory myosin light chain MLC that promotes assembly of myosin II into bipolar filaments and enhances the ATPase activity of myosin II, increasing the contractile force generated by myosin II on actin filaments. ROCK also phosphorylates and activates another kinase, the LIM kinase, which in turn phosphorylates and inhibits the actin-severing protein cofilin, increasing the stability of actin filaments. Together, these effects highlight the RhoA GTPase as a central regulator of cytoskeleton contractility.
We found that the mechanical stimulation allows the activation of RhoA, suggesting a key role for the RhoA in the coupling between the Ca^{2+} signal and

the actin cytoskeletal contraction that we observed, due to the pN range mechanical stimulation. Immunochemistry shows that Piezo1 channels are distributed over the entire membrane of hippocampal neurons. These results altogether, suggest that the MSCs, such as the Piezo 1 channel, can potentially regulate the RhoA GTPase as well as the actin cytoskeletal network through a Ca^{2+} pathway, in response to mechanical stress (Figure 1).

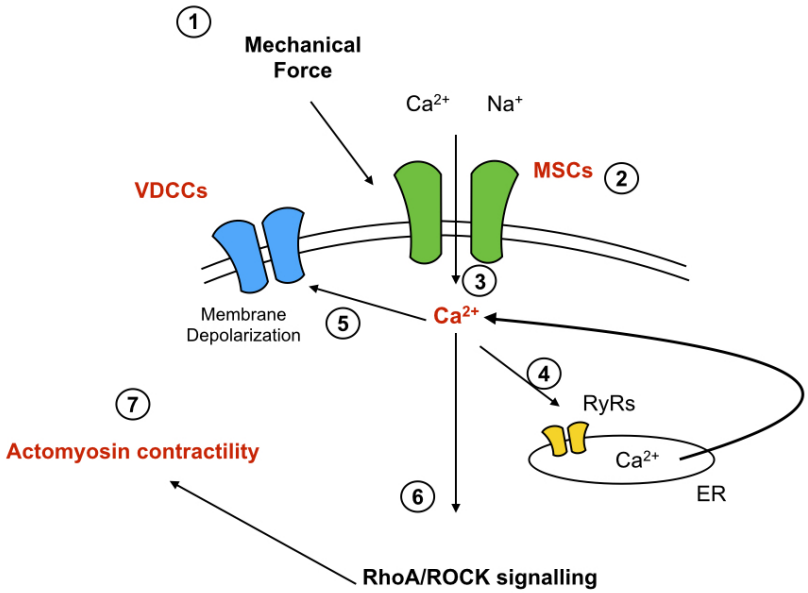

Figure 1. Hypothesis of force-dependent mechanotransduction pathway. The mechanical stress (1) induces changes in plasma membrane tension opening the MSCs (2) with an ion flux, mainly composed by Ca^{2+} (3). The intracellular Ca^{2+} elevation can trigger a subsequent release of Ca^{2+} from the intracellular store (4), membrane depolarization (5) and the calcium transduction pathway. The calcium-dependent pathways can regulate the RhoA GTPase (6) as well as the actomyosin network (7) through various second messengers.

In third study, functional changes in the activity of MSCs on the plasma membrane were addressed by electrophysiology. We demonstrate, for primary hippocampal cells and NG108-15 cells, that stimulation with piconewton forces is enough to regulate the ion currents through the cell membrane. These are preliminary results and future experiments will be performed to characterize quantitatively the response of the neuronal cells. In fact, further investigations are needed to understand the nature of these currents, using specific ionic

concentrations in the bath and in the pipet solution, as well as specific blockers for the mechanosensitive channels.

In conclusion, we have showed how mechanical inputs are translated into biochemical signaling, explaining neuronal mechano-responsiveness, providing an insight into a f ormerly unknown branch pruning mechanism. This clearly strengthens the idea that mechanical cues are involved in neuronal physiology.

References

1) Orr, A. Wayne, et al. “Mechanisms of Mechanotransduction.” *Developmental Cell*, vol. 10, no. 1, Jan. 2006, pp. 11–20. *Crossref*, doi:10.1016/j.devcel.2005.12.006.
2) Finer, Jeffrey T., et al. “Single Myosin Molecule Mechanics: Piconewton Forces and Nanometre Steps.” *Nature*, vol. 368, no. 6467, Mar. 1994, pp. 113–19. *Crossref*, doi:10.1038/368113a0.
3) Falleroni, Fabio, et al. “Cell Mechanotransduction With Piconewton Forces Applied by Optical Tweezers.” *Frontiers in Cellular Neuroscience*, vol. 12, May 2018. *Crossref*, doi:10.3389/fncel.2018.00130.
4) Han, Hui-Quan, et al. “Induction of Formation of Presynaptic Terminals in Neuroblastoma Cells by Synapsin IIb.” *Nature*, vol. 349, no. 6311, Feb. 1991, pp. 697–700. *Crossref*, doi:10.1038/349697a0.
5) Kowtha, V. C., et al. “Comparative Electrophysiological Properties of NG108-15 Cells in Serum-Containing and Serum-Free Media.” *Neuroscience Letters*, vol. 164, no. 1–2, Dec. 1993, pp. 129–33. *Crossref*, doi:10.1016/0304-3940(93)90874-K.
6) Liu, Bo, et al. “Two Distinct Phases of Calcium Signalling under Flow.” *Cardiovascular Research*, vol. 91, no. 1, July 2011, pp. 124–33. *Crossref*, doi:10.1093/cvr/cvr033.
7) Sukharev, Sergei, and Frederick Sachs. “Molecular Force Transduction by Ion Channels – Diversity and Unifying Principles.” *Journal of Cell Science*, vol. 125, no. 13, July 2012, pp. 3075–83. *Crossref*, doi:10.1242/jcs.092353.
8) Sniadecki, Nathan J. “Minireview: A Tiny Touch: Activation of Cell Signaling Pathways with Magnetic Nanoparticles.” *Endocrinology*, vol. 151, no. 2, Feb. 2010, pp. 451–57. *Crossref*, doi:10.1210/en.2009-0932.
9) Bowman, Charles L., et al. “Mechanosensitive Ion Channels and the Peptide Inhibitor GsMTx-4: History, Properties, Mechanisms and Pharmacology.” *Toxicon*, vol. 49, no. 2, Feb. 2007, pp. 249–70. *Crossref*, doi:10.1016/j.toxicon.2006.09.030.

10) Orr, A. Wayne, et al. “Mechanisms of Mechanotransduction.” *Developmental Cell*, vol. 10, no. 1, Jan. 2006, pp. 11–20. *Crossref*, doi:10.1016/j.devcel.2005.12.006.

11) Ross, Tyler D., et al. “Integrins in Mechanotransduction.” *Current Opinion in Cell Biology*, vol. 25, no. 5, Oct. 2013, pp. 613–18. *Crossref*, doi:10.1016/j.ceb.2013.05.006.

12) Leckband, D. E., and J. de Rooij. “Cadherin Adhesion and Mechanotransduction.” *Annual Review of Cell and Developmental Biology*, vol. 30, no. 1, Oct. 2014, pp. 291–315. *Crossref*, doi:10.1146/annurev-cellbio-100913-013212.

13) Chachisvilis, M., et al. “G Protein-Coupled Receptors Sense Fluid Shear Stress in Endothelial Cells.” *Proceedings of the National Academy of Sciences*, vol. 103, no. 42, Oct. 2006, pp. 15463–68. *Crossref*, doi:10.1073/pnas.0607224103.

14) Zebda, Noureddine, et al. “Focal Adhesion Kinase Regulation of Mechanotransduction and Its Impact on Endothelial Cell Functions.” *Microvascular Research*, vol. 83, no. 1, Jan. 2012, pp. 71–81. *Crossref*, doi:10.1016/j.mvr.2011.06.007.

15) Glogauer, M., et al. “Magnetic Fields Applied to Collagen-Coated Ferric Oxide Beads Induce Stretch-Activated Ca2+ Flux in Fibroblasts.” *American Journal of Physiology-Cell Physiology*, vol. 269, no. 5, Nov. 1995, pp. C1093–104. *Crossref*, doi:10.1152/ajpcell.1995.269.5.C1093.

16) Gefen, Amit, and Susan S. Margulies. “Are in Vivo and in Situ Brain Tissues Mechanically Similar?” *Journal of Biomechanics*, vol. 37, no. 9, Sept. 2004, pp. 1339–52. *Crossref*, doi:10.1016/j.jbiomech.2003.12.032.

17) Iwashita, M., et al. “Systematic Profiling of Spatiotemporal Tissue and Cellular Stiffness in the Developing Brain.” *Development*, vol. 141, no. 19, Oct. 2014, pp. 3793–98. *Crossref*, doi:10.1242/dev.109637.

18) Saha, Krishanu, et al. “Substrate Modulus Directs Neural Stem Cell Behavior.” *Biophysical Journal*, vol. 95, no. 9, Nov. 2008, pp. 4426–38. *Crossref*, doi:10.1529/biophysj.108.132217.

19) Koser, David E., et al. “Mechanosensing Is Critical for Axon Growth in the Developing Brain.” *Nature Neuroscience*, vol. 19, no. 12, Dec. 2016, pp. 1592–98. *Crossref*, doi:10.1038/nn.4394.

20) Franze, Kristian, et al. “Neurite Branch Retraction Is Caused by a Threshold-Dependent Mechanical Impact.” *Biophysical Journal*, vol. 97, no. 7, Oct. 2009, pp. 1883–90. *Crossref*, doi:10.1016/j.bpj.2009.07.033.

21) Shimozawa, Togo, and Shin’ichi Ishiwata. “Mechanical Distortion of Single Actin Filaments Induced by External Force: Detection by Fluorescence Imaging.” *Biophysical Journal*, vol. 96, no. 3, Feb. 2009, pp. 1036–44. *Crossref*, doi:10.1016/j.bpj.2008.09.056.

22) Hayakawa, Kimihide, et al. “Actin Stress Fibers Transmit and Focus Force to Activate Mechanosensitive Channels.” *Journal of Cell Science*, vol. 121, no. 4, Feb. 2008, pp. 496–503. *Crossref*, doi:10.1242/jcs.022053.

23) Pardo-Pastor, Carlos, et al. “Piezo2 Channel Regulates RhoA and Actin Cytoskeleton to Promote Cell Mechanobiological Responses.” *Proceedings of the National Academy of Sciences*, vol. 115, no. 8, Feb. 2018, pp. 1925–30. *Crossref*, doi:10.1073/pnas.1718177115.

24) Ying, Zhekang, et al. “PYK2/PDZ-RhoGEF Links Ca^{2+} Signaling to RhoA.” *Arteriosclerosis, Thrombosis, and Vascular Biology*, vol. 29, no. 10, Oct. 2009, pp. 1657–63. *Crossref*, doi:10.1161/ATVBAHA.109.190892.

25) McBeath, Rowena, et al. “Cell Shape, Cytoskeletal Tension, and RhoA Regulate Stem Cell Lineage Commitment.” *Developmental Cell*, vol. 6, no. 4, Apr. 2004, pp. 483–95. *Crossref*, doi:10.1016/S1534-5807(04)00075-9.

26) Keung, Albert J., et al. “Rho GTPases Mediate the Mechanosensitive Lineage Commitment of Neural Stem Cells.” *STEM CELLS*, vol. 29, no. 11, Nov. 2011, pp. 1886–97. *Crossref*, doi:10.1002/stem.746.

27) Xu, Baiyao, et al. “RhoA/ROCK, Cytoskeletal Dynamics, and Focal Adhesion Kinase Are Required for Mechanical Stretch-Induced Tenogenic Differentiation of Human Mesenchymal Stem Cells.” *Journal of Cellular Physiology*, vol. 227, no. 6, June 2012, pp. 2722–29. *Crossref*, doi:10.1002/jcp.23016.